FACULTY OF SCIENCES

The Neuro-Invasive Potential of Human Herpesvirus Type 7

Rianne Verbeek
Student number: 01700125

Supervisor: Dr. Jolien Van Cleemput
Scientific tutor: Dr. Jolien Van Cleemput

Master's dissertation submitted to Ghent University to obtain the degree of Master of Science in Biochemistry and Biotechnology. Major Microbial Biotechnology (MIB)

Academic year: 2022-2023

UNIVERSITEIT GENT

Ghent University

UZ Ghent – Department of internal medicine

Research Group: HIV Cure Research Center

UZ GENT

Acknowledgements

I would like to thank my supervisor, dr. Jolien Van Cleemput, for guiding me during my Master's thesis, as well as all my colleagues with whom I have had the pleasure to work.

Furthermore, I would like to thank my parents for their support during my research and throughout my academic career.

Table of contents

List of Abbreviations

(q)PCR	(Quantitative) Polymerase Chain Reaction
ACD4	Activated $CD4^+$ primary T-cells
BAC	Bacterial Artificial Chromosome
CMV	Cytomegalovirus
CNS	Central Nervous System
CPE	Cytopathic Effect
Cq	Threshold cycle value
CSF	Cerebrospinal Fluid
DIHS	Drug-Induced Hypersensitivity Syndrome
DRESS	Drug Reaction with Eosinophilia and Systemic Symptoms
EBV	Epstein-Barr virus
EIA	Enzyme Immunoassay
ELISA	Enzyme-Linked Immuno Sorbent Assay
FBS	Fetal Bovine Serum
HDR	Homology-Directed Repair
HH	Hemiconvulsion-Hemiplegia
HHV	Human Herpesvirus
HIV	Human Immunodeficiency Virus
HSPG	Heparan Sulphate Proteoglycan
HSV	Herpes Simplex Virus
IB	Immunoblot
IFA	Immunofluorescence assay
LAMP	Loop-Mediated Isothermal Amplification
MACS	Magnetic-Activated Cell Sorting
MCMV	Murine Cytomegalovirus
MCP	Major Capsid Protein
MRV	Murine Roseolovirus
ND4	Non-activated $CD4^+$ primary T-cells
NK	Natural Killer
PAM	Protospacer Adjacent Motif

PBMCs	Peripheral Blood Mononuclear Cells
PNS	Peripheral Nervous System
RA	Retinoic Acid
SCP	Small Capsid Protein
SJS	Stevens–Johnson Syndrome
TCID	Tissue Culture Infectious Dose
TEN	Toxic Epidermal Necrolysis
TP	Triplex Protein
UL	Long unique region
US	Short unique region
VZV	Varicella-zoster virus

Abstract

Human Herpesvirus Type 7 (HHV-7) is a member of the *Herpesviridae* family that has been associated with multiple diseases, ranging from dermatological afflictions such as exanthem subitem, to severe neurological defects such as encephalitis or meningitis. Nevertheless, little is known about its life cycle, and even less about its pathogenic potential. Despite the occurrence of encephalitis as a severe complication of HHV-7 infection in immunocompromised individuals, it is not known whether and how HHV-7 invades the central nervous system (CNS). Therefore, we here hypothesized that HHV-7 possesses the potential to invade neurons.

To explore this hypothesis, viral infection in the SH-SY5Y neuronal cell line was explored in different ways.

For the characterization of viral entry and replication in the SH-SY5Y cells, we produced mutants expressing fluorophore-tagged viral proteins. The chosen viral proteins were different structural proteins, being U31 (major tegument protein), U32 (minor capsid protein) and U14 (minor tegument protein). HEK293T cells were successfully transduced to express Cas9 and sgRNAs targeting specific viral protein-encoding genes, as shown by Cas9-specific ELISA. These cells were then transfected with an *mRFP1* donor plasmid and subsequently infected with HHV-7. As such, fluorophore-tagged viral particles can be produced, where the fluorophore is attached to 3 different proteins respectively. In the purification of these mutant viruses, we managed to obtain a 59% purity for the U32-mRFP1 HHV-7 mutant. We managed to obtain HHV-7-infected HEK293T cell cultures that express a fluorescent signal. Subsequent inoculation of SupT1 cells with the fluorescent cell content resulted in CPE. When HEK293T cells were co-cultured with the infected SupT1 cells, fluorescent plaque formation was observed. This indicated the production of fluorescent HHV-7 viral particles. Nonetheless, a low yield of fluorescent cells, as well as loss of fluorescence in the purification of the viral particles, indicates a problem in this production method. Either the HEK293T cell type used does not stimulate HHV-7 replication or the method of HEK293T HHV-7 inoculation results in a decrease in viral entry. SupT1 cells co-cultured with the HHV-7 mutant-producing HEK293T cells retain fluorescence after separation from the culture and also seem to exhibit CPE, although fluorescence does not seem to occur in all cells that show CPE.

In parallel with the mutant HHV-7, the non-mutated viral strain was used to characterize viral infection in the SH-SY5Y cell line, together with multiple cell types of which infection with HHV-7 is already known and characterized in some cases, like the HEK293T embryonic kidney cell line, the T cell line SupT1 and primary $CD4^+$ T cells. The SH-SY5Y cells showed no intracellular and extracellular replication competent virus when subjected to a viral titration assay. qPCRs were performed as an alternative to quantify intracellular and extracellular virus, for which multiple primer pairs were used and designed. However, all qPCR trials failed due to primer-specific off-target effects.

With this research, we can conclude that no infectious viral particles are formed when SH-SY5Y cells are inoculated with free HHV-7. Whether SH-SY5Y cells can be infected with HHV-7 through cell-cell contact with infected SupT1 cells, remains contested, although this mechanism seems promising in other cell types. When a clearly fluorescent culture of HHV-7 mutants is obtained, it can be determined whether a lack of viral entry, replication, or release is the cause of the low viral titer in SH-SY5Y cells. In future research, regardless of potential infection in SH-SY5Y cells, we would like to extend our study to include primary neurons, other brain-derived cell lines, and glial cells, in order to further investigate the neuro-invasive potential of HHV-7 in humans.

Part 1: Introduction

Human herpesvirus 7 (HHV-7) is a member of the *Herpesviridae* family, which also includes herpes simplex virus (HSV), varicella-zoster virus (VZV), cytomegalovirus (CMV), and Epstein-Barr virus (EBV), and is closely related to HHV-6. HHV-7 was first isolated from peripheral blood lymphocytes in 1990 (Frenkel *et al*, 1990), and since then, it has been identified as a ubiquitous virus that infects nearly all individuals by the age of three years. Despite the discovery of HHV-7 in 1990 and many epidemiological studies published during the last 30 years, little is known about the viral pathogenesis and host-virus interactions. In addition, there are no vaccines or treatments to date. Therefore, only supportive treatment can be provided in severe cases of HHV-7 associated diseases.

1.1. Virus structure

HHV-7 is a double-stranded DNA virus that belongs to the Herpesviridae family, which has a tropism for multiple host species, including humans, pigs, bovines, and birds, and is a member of the subfamily Betaherpesvirinae (Cohen, 2015). The Betaherpesvirinae have a tropism for mammals, and the presence HHV-7 itself has only been described in humans (McGeoch *et al*, 1995). It is very closely linked to HHV-6A, HHV-6B, and CMV. Together with HHV-6, HHV-7 forms the genus Roseolovirus (Gompels, 2014). The genome of HHV-7 shows a high degree of similarity to that of HHV-6. Still, there are a number of key differences between the genome of HHV-7 and that of HHV-6, strongly suggesting that HHV-7 is different enough from HHV-6 to be considered its own species. HHV-6 has two major variants, HHV-6A and HHV-6B, which share approximately 90% genetic homology (Flamand *et al*, 2014). In contrast, HHV-7 has a single variant. The genomes of both viruses consist of linear double-stranded DNA, but they differ in gene organization and content (Davison, 2007). Little variation among HHV-7 strains exists (about 0.1%), and no HHV-7 variant groups have been identified (Caserta, 2018).

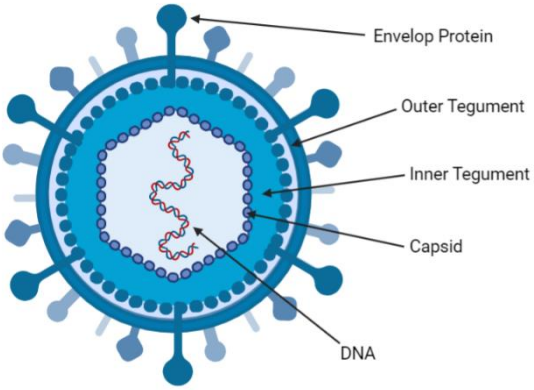

Figure 1. **Structural overview of Human Herpesvirus 7**. Figure made using Biorender

The virus particle, i.e., virion, has a complex molecular structure that includes a lipid envelope, an icosahedral capsid of about 90 to 95 nm, and a central core containing the viral genome of ± 145,000 bp and associated proteins (Fig. 1) (Hudnall *et al*, 2011). The nucleocapsid is surrounded by a tegument of approximately 30 nm, which is enclosed within the envelope (Klussmann *et al*, 1997a). The envelope, a polymorphic lipid bilayer, of HHV-7 is derived from the host cell membrane and is studded with glycoproteins that play important roles in viral attachment, entry, and immune evasion (Cohen, 2015). The envelope surrounds the icosahedral capsid, which is made up of 162 capsomers arranged in a symmetrical pattern. The capsid is composed of three major structural proteins: the major capsid protein, the triplex protein, and the minor capsid protein. Inside the capsid is the central core, which contains the viral genome and associated proteins.

The HHV-7 genome encodes around 90 genes, some of which appear to be unique to β-herpesviruses (Fig. 2) (Staheli *et al*, 2016). The genome is organized into two unique regions, the long unique region (UL) and the short unique region (US), that are flanked by inverted repeat sequences. The UL region encodes most of the genes involved in viral replication and assembly, while the US region contains genes involved in immune evasion and modulation of host cell function. The viral genome is packaged with several viral and cellular proteins to form a complex structure known as the nucleocapsid (Klussmann *et al*, 1997a). The nucleocapsid is composed of the viral DNA, the capsid proteins, and several viral proteins that play important roles in viral replication and gene expression. These proteins include the viral polymerase, the helicase-primase complex, and the DNA-binding protein (Mori & Yamanishi, 2007).

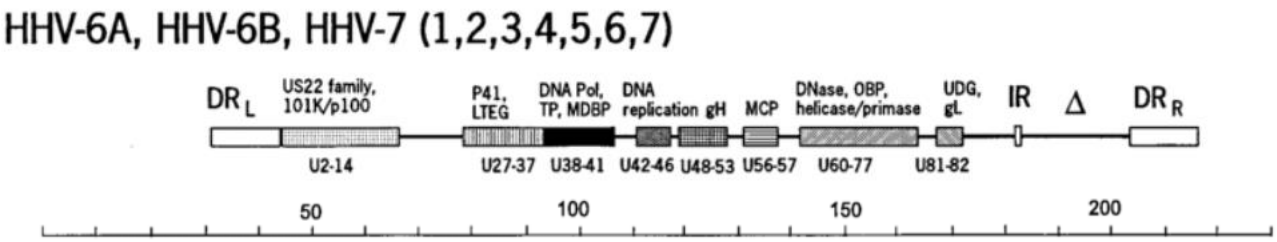

Figure 2**. Conserved herpesvirus gene blocks**. DRL (left) and DRR (right) denote direct repeats. IR denotes an internal repeat. TRL, IRL, IRS, and TRS denote inverted repeats flanking the long or L component and the short or S component, respectively. TR are direct terminal repeats. Some of the gene products found in these sequence blocks are indicated above the HHV-6/7 genome. The 7-kb segment that is present in HHV-6A and HHV-6B and absent in HHV-7 is indicated by Δ. Abbreviations: 101K/p100, virion structural protein; P41, polymerase-associated factor; LTEG, large tegument protein; DNA Pol, DNA polymerase; TP, transport/capsid assembly protein; gH, glycoprotein H; MCP, major capsid protein; UDG, uracil-DNA glycosylase; gL, glycoprotein L. Figure Courtesy of Braun et al. (1997)

1.2. Pathogenesis and clinical manifestations

1.2.1. ***Host Cell tropism***

The cell tropism of HHV-7 has been the subject of recent research. For a time, it was thought that HHV-7 had a narrow tropism for $CD4^+$ T cells (Lusso et al, 1994). And while the virus does primarily target cells of the immune system, such as T lymphocytes, natural killer (NK) cells, and macrophages, it can also infect other cell types, including epithelial and endothelial cells, $CD34^+$ hematopoietic progenitor cells, and $CD68^+$ monocytes and macrophages in lesions of Kaposi sarcoma, giving it a broader cell tropism than HHV-6 (Cohen, 2015; Kempf et al, 1997; Ablashi et al, 1995; Bortolotti et al, 2020; Caserta, 2018). Its presence has also been detected in astrocytes (Skuja *et al*, 2021). *In vitro* studies have shown that HHV-7 can infect and replicate in a variety of human cell lines, including T cell lines and B-cell lines (Cermelli *et al*, 1997). HHV-7 also infects but does not replicate in monocytes and macrophages *in vitro* (Caserta, 2018). However, in an older study, productive replication of HHV-7 in macrophages was observed (Zhang *et al*, 2001). The replication was lost after 2 weeks, but HHV-7 DNA was detected up to 1 month after infection, possibly indicating a viral reservoir. This contradiction in reporting is not uncommon in HHV-7 research and will be highlighted throughout this study. Due to its close relation to HHV-6 and HHV-8, it is also possible that HHV-7 can infect monocyte-derived dendritic cells and human umbilical vein endothelial cells (Wang & Pellett, 2007; Sakurada *et al*, 2001).

The mechanism of HHV-7 entry into host cells is not fully understood, but it is believed to involve several viral glycoproteins that bind to cellular receptors on the surface of target cells. Contrary to HHV-6, HHV-7 uses the CD4 molecule, a known co-receptor for the human immunodeficiency virus (HIV), as a receptor for entry into T cells (Lusso *et al*, 1994; Yasukawa *et al*, 1997). The virus also binds to the heparan sulphate proteoglycan (HSPG) receptor on the surface of epithelial and endothelial cells (Secchiero *et al*, 1997b). Once inside the host cell, HHV-7 undergoes a complex replication cycle that involves viral gene expression, DNA replication, and assembly of viral particles. The virus can establish both lytic and latent infections in host cells, and the mechanisms underlying these different modes of infection are not fully understood (Kondo & Yamanishi, 2007). CMV, HHV-6, and HHV-7 are maintained as episomes in the nucleus of latently infected cells and subsequently express proteins for attaching the viral episome to the host chromosome during cell division (Cohen, 2020). In some infected individuals, HHV-6 is integrated into host chromosomes and the virus is inherited in the germ line (Ward *et al*, 2006). Chromosomal integration of HHV-7 is not known to occur.

HHV-7, like HHV-6, induces a cytopathic effect (CPE) in infected cells which is characterized by ballooning degeneration, a form of apoptosis (Fig. 3) (Mori & Yamanishi, 2007). This form of apoptosis can be attributed to CPE. CPE, or cytopathogenic effect, refers to structural alterations brought on by viral invasion in host cells (Agol, 2012). It results when the infecting virus causes lysis of the host cell or when the cell dies without lysis due to an inability to replicate (Heaton, 2017). A virus is said to be cytopathogenic if it alters the host cell's morphology in this way. Typical signs of the CPE are rounding of the infected cell, joining with neighboring cells to create syncytia, and the formation of nuclear or cytoplasmic inclusion bodies (Laurent-Crawford *et al*, 1991). In the case of HHV-7, multinucleated giant cells occur by the mechanism of polyploidization (Secchiero *et al*, 1997a). This induction of T cell death may be an important immune evasion mechanism of HHV-7, helping the virus to persist in the host organism throughout its lifetime (Secchiero *et al*, 1997a; Mori & Yamanishi, 2007).

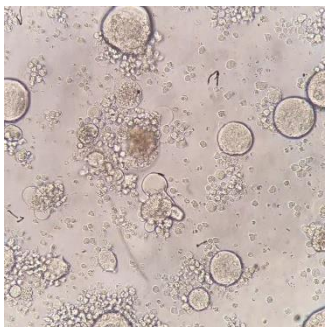

Figure 3. **Cytopathic effect**: Ballooning degeneration of SupT1 cells after infection with HHV-7.

1.2.2. Dermatological diseases

HHV-7 has been linked to a number of dermatological diseases, although its role in the pathophysiology of these illnesses is not fully understood (Table 1).

Both HHV-6 and HHV-7 have a proven association with roseola infantum, also known as exanthem subitem or sixth disease (Yamanishi *et al*, 1988). Exanthem subitum is a common childhood illness which mostly develops before the age of three and is non-discriminatory in gender and location. Symptoms vary from absent to a fever and/or a rash that lasts less than three days. Common complications include febrile seizures, although serious complications are rare (Asano *et al*, 1989). Even though the causality of roseola by HHV-6 has been proven, the direct causality HHV-7 has been under scrutiny, with the involvement of HHV-7

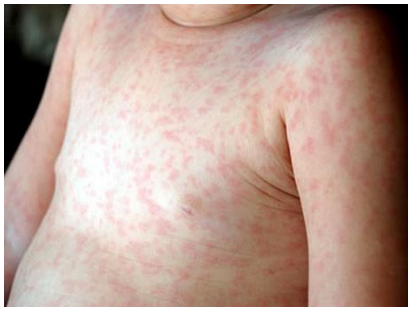

Figure 4. **Child portraying common symptoms of roseola infantum**. Photo courtesy of dr. Jan R. Mekkes.

being linked to its ability to reactivate latent HHV-6 (Wolz *et al*, 2012; Stone *et al*, 2014; Van Den Berg *et al*, 1999). Most cases of roseola infantum improve on their own.

A more debated association of both HHV-7 and HHV-6 is pityriasis rosea, a common skin rash that typically occurs in young adults and usually lasts less than three months and disappears without treatment (Eisman & Sinclair, 2015). The condition often starts with a single, slightly raised, scaly patch called the "herald patch" on the torso, followed by the appearance of smaller similar patches on the torso and extremities (Aoshima *et al*, 1981). According to estimates, men and women in the United States have a combined prevalence of 0.13% and 0.14%, respectively (Schwartz et al, 2022). The most common age range in which pityriasis rosea occurs is between 10 and 35 and it tends to occur more frequently in spring and autumn (Browning, 2009). HHV-7 has been detected in some cases of pityriasis rosea, but its role in the pathogenesis of the disease is still up for debate (Drago *et al*, 1997; Watanabe *et al*, 2002; Broccolo *et al*, 2005; Drago *et al*, 2009). For now, an association seems likely, but the underlying mechanism remains unknown.

Erythema multiforme is a skin condition that causes a rash characterized by reddish or purplish patches, often in a target or bullseye shape, and is occasionally accompanied by fever and malaise (de Risi-Pugliese *et al*, 2019). It typically develops after an infection or drug exposure and may be caused by the deposition of immune complexes, primarily IgM-bound complexes, in the superficial microvasculature of the skin and oral mucous membrane (Imamura *et al*, 1980). Overall, it is a rare condition with a high occurrence in the second and third decades of life. The disease has multiple manifestations or forms, as the name implies. Family members of HHV-7, including HSV, EBV, and CMV are a common trigger for erythema multiforme (Mtiri *et al*, 2021). HHV-7 has been detected in some cases of erythema multiforme (Relhan *et al*, 2013; Wolz *et al*, 2012). However, no clear causality has been proven yet.

The presence of HHV-7 has also been established in some cases of Gianotti-Crosti syndrome, a rare childhood rash that is typically accompanied by fever and enlarged lymph nodes (Chuh *et al*, 2002). The manifestations are a reaction of the skin to a viral infection. The most frequently reported pathogens are Hepatitis B virus and EBV, although other pathogens like hepatitis A virus, hepatitis C virus, CMV, coxsackievirus, adenovirus, enterovirus, rotavirus, rubella virus, HIV, and parainfluenza virus, have also been reported causative agents, while HHV-7 may be implicated as well (Caputo *et al*, 1992; Haki *et al*, 1997; Boeck *et al*, 1998). However, the underlying interaction between the virus and the disease is not well understood and the correlation might even be caused by an HHV-7 based activation of HHV-6 (Wolz *et al*, 2012).

HHV-7 has been detected in some cases of drug-induced hypersensitivity syndrome (DIHS) (Yagami *et al*, 2006; Flamand, 2014). DIHS, also known as drug reaction with eosinophilia and systemic symptoms (DRESS), is a severe and potentially life-threatening drug reaction (Shiohara *et al*, 2006). It is a rare but serious adverse reaction to certain medications, which can result in a variety of symptoms, including a rash, fever, lymphadenopathy, and multiple organ involvement, like that of the kidney, liver, lung, and heart (Seishima *et al*, 2006). Treatment usually involves discontinuation of the offending drug and supportive care, including management of organ dysfunction and symptomatic relief (Shiohara *et al*, 2006). The presence of HHV-7 in some cases of DIHS suggests that the virus may play a role in the pathogenesis of this condition.

HHV-7, but not HHV-6, is currently also a candidate for the cause of lichen planus, a chronic inflammatory and immune-mediated disease that affects the skin, nails, hair, and mucous membranes (de Vries et al, 2006). In addition, multiple case reports link HHV-6 and HHV-7 to other

dermatological disorders, including Stevens-Johnson syndrome, thrombocytopenic purpura, purpura fulminans, papular-purpuric gloves and socks syndrome (Cohen, 2015; Mori & Yamanishi, 2007; Chanas *et al*, 2021).

Table 1. **Overview of dermatological diseases associated or directly caused by HHV-7 infection**. Most common clinical manifestations are provided. DIHS: Drug-induced hypersensitivity syndrome,

Disease	Clinical Manifestations
Roseola Infantum	Fever; rash on torso, face, neck, and extremities
Pityriasis Rosea	herald patch on torso, followed by similar patches on torso and extremities.
Erythema multiforme	Burning or itching rash, primarily on extremities
Gianotti-Crosti syndrome	Papules on cheeks, buttocks, and extremities; lymphadenopathy; mild fever
DIHS	Rash; erythroderma; fever; lymphadenopathy

1.2.3. Encephalitis

Encephalitis is a condition that refers to inflammation of the brain, which is usually caused by an infection or an autoimmune reaction (Roos, 1999). The inflammation can damage brain cells and lead to a range of symptoms, from mild flu-like symptoms to severe neurological dysfunction and even death (Venkatesan *et al*, 2013). Viral encephalitis is a type of encephalitis that is caused by a viral infection (Whitley, 2010). The viruses can enter the brain through several routes, including hematogenous spread through the bloodstream or direct invasion from a nearby site of infection, for example the respiratory tract (Whitley & Gnann, 2002). Just like other types of encephalitis, viral encephalitis causes inflammation of the brain, leading to a range of neurological symptoms, that usually develop within a few days to a week after infection and can vary widely. In addition to common symptoms like fever, headache, vomiting and confusion, patients may also experience seizures, as well as weakness or paralysis in one or more limbs (Venkatesan & Murphy, 2018). In severe cases, patients may even fall into a coma or pass away.

The diagnosis of viral encephalitis typically involves a combination of clinical examination, blood tests, imaging studies such as CT or MRI scans (Fig. 5), and analysis of cerebrospinal fluid (CSF). The CSF analysis can help identify the specific virus causing the infection and determine the appropriate treatment. There are many different viruses that can cause encephalitis, including HSV, West Nile virus, Japanese encephalitis virus, and Zika virus (Roos, 1999). Some of these viruses are typically spread through the bite of infected mosquitoes or ticks, or through contact with infected animals or humans.

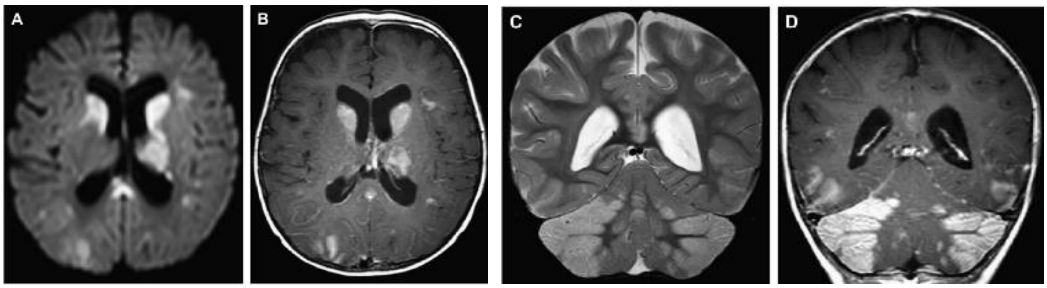

Figure 5. **HHV-7–related encephalitis in 2-year-old girl with febrile convulsions**. Axial DW image (A) shows multiple, patchy high signal lesions with prominent enhancement on contrast-enhanced T1W images (B) in lentiform nuclei and left thalamus and in gray and subcortical white matters and meninges. Coronal T2W (C) and contrast- enhanced T1W (D) images reveal diffuse, cortical engorgement with marked parenchymal and meningeal enhancement in cerebellar and cerebral hemispheres. Photo courtesy of Bulakbasi et al. (2008)

The other member of the genus *Roseolovirus*, HHV-6, has been associated with CNS diseases such as focal encephalitis, Alzheimer's disease, multiple sclerosis, and other pathologies such as tumorigenesis and mood disorders (Yao *et al*, 2010; Opsahl & Kennedy, 2005; Donati *et al*, 2003; Fotheringham *et al*, 2007; Houshmandi *et al*, 2015). More specifically, cutaneous diseases like roseola and the cutaneous eruptions associated with primary HHV-6 infection have been connected to a specific type of viral encephalopathy (Wolz *et al*, 2012). In addition, HHV-6 neuro-invasion has been reported and the virus shows *in vitro* tropism for different CNS cells (Opsahl & Kennedy, 2005; Albright *et al*, 1998; Ahlqvist *et al*, 2005). Samples taken from patients with neurological illnesses have frequently been reported to have higher rates of HHV-6 DNA detection (Yao *et al*, 2009, 2010). Children with primary HHV-7 infection are more likely than those with primary HHV-6 infection to have febrile seizures and clinical manifestations associated with HHV-7 viremia are often similar between primary and reactivated infections, with the exception of seizures (Hall *et al*, 2006). There seems to be some discourse on the frequency of occurrence of seizures in primary and reactivated infections, where one study states that seizures occur more in primary infections (Coserta *et al*, 1998), while another study stated the opposite, with a higher occurrence in reactivated infections (Hall *et al*, 2006). The reported evidence for the neuro-invasive potential of HHV-6 and its role in CNS diseases, combined with the closeness of relation, provide indirect evidence for a neuropathological role of HHV-7 (Helmke *et al*, 2001).

Even though there has been no proven causality of HHV-7 infection in encephalitis, reported synthesis of intrathecal antibodies against HHV-7 suggests that HHV-7 can invade the brain (Torigoe *et al*, 1996). The CNS manifestations caused by HHV-7 may be the result of viral invasion of the brain or focal impairment of blood flow brought on by viral vasculitis (van den Berg et al, 1999). The presence of HHV-7 has been shown in astrocytes, a type of glial cell in the brain, which can induce the production of cytokines and chemokines that promote inflammation (Skuja *et al*, 2021). However, no viral replication could be determined in these glial cells.

It is important to note that the association of HHV-7 with encephalitis has been exclusively reported by case studies, where HHV-7 DNA was detected in the cerebrospinal fluid and serum and supported by serological studies (Aburakawa *et al*, 2017a; Parra *et al*, 2017; Riva *et al*, 2017; Van Den Berg *et al*, 1999; Yang *et al*, 2022; Schwartz *et al*, 2014; Aburakawa *et al*, 2017b). In one case of fatal encephalitis, the presence of HHV-7 DNA was shown in cerebrospinal fluid and brain stem tissue samples (Chan *et al*, 2002). Cases of encephalitis have been reported both during primary infection of HHV-7, as well as reinfection, the latter often occurring in immunocompromised patients (Holden & Vas, 2007; Parra *et al*, 2017; Christou *et al*, 2022; Chan *et al*, 2002). However, in

cases of delayed primary infection with HHV-7 in healthy individuals, with the primary infection occurring later in life, serious neurological pathologies like encephalitis and paralysis might also occur (Ward *et al*, 2002a). Severe manifestations of encephalitis, like hemorrhagic brainstem encephalitis, have also been associated with HHV-7 in a previously healthy individual (Fay *et al*, 2015).

These cases suggest, but do not prove, a neurotropic and neuropathogenic potential of HHV-7. However, HHV-7 is not a common cause of encephalitis, and the development of the disease is likely multifactorial. Factors that may contribute to the development of HHV-7-associated encephalitis include the ability of the virus to infect brain cells and its ability to disrupt the homeostasis of the blood-brain barrier and induce an inflammatory response.

1.2.4. Meningitis

In one case study of a patient presenting with aseptic meningitis, the antibody titer of HHV-7 was increased significantly (Yoshikawa *et al*, 2003). Meningitis is a condition that occurs when the protective membranes surrounding the brain and spinal cord become inflamed (Putz *et al*, 2013). The inflammation can be caused by a viral or bacterial infection, as well as other types of infections, medications, or autoimmune disorders. Symptoms of meningitis can include severe headache, fever, nausea and vomiting, sensitivity to light, a stiff neck and, in some cases, a rash (Swanson, 2015). Different causes for meningitis might present with different symptoms. Bacterial meningitis is a medical emergency and can be life-threatening if not treated promptly (Heckenberg *et al*, 2014). Treatment for bacterial meningitis typically involves antibiotics and supportive care, such as IV fluids and pain relief medications. Viral meningitis is typically less severe and can often be treated with supportive care, such as rest and fluids (Lee & Davies, 2007). However, in the case of immunocompromised patients, symptoms may be severe, for example in the case of a transplantation patients who suffered from meningitis (Yoshikawa *et al*, 2003). This patient showed the presence of HHV-7 DNA in their CSF. In a Canadian study, 8 children who showed HHV-7 DNA in their CSF, were also diagnosed with meningitis. (Schwartz *et al*, 2014). The presence of HHV-7 DNA in CSF of meningitis patients was also detected in other case studies (Pohl-Koppe *et al*, 2001; Marcelo Miranda *et al*, 2011; Grose, 2022; Wada *et al*, 2009). Given the fact that closely related herpesviruses, like HSV-2 and VZV, are already known to cause aseptic menigitis, it might be reasonable to suppose that HHV-7 might share that same potential (Chapenko *et al*, 2016).

HHV-7 is also associated with meningoencephalitis, a very similar encephalopathy to meningitis, characterized by infection of both the meninges and the brain, where blood-brain barrier damage and high CSF/blood viral copies ratio were correlated with a more severe presentation (Pohl-Koppe *et al*, 2001; Foiadelli *et al*, 2022). HHV-7 was also considered as a pathogen in a case report of a meningoradiculopathy, the pinching of a nerve, with long-term motor neurologic sequelae of a young girl (Rangel *et al*, 2017).

To diagnose meningitis, a doctor may perform a physical exam, review medical history, and order diagnostic tests such as a lumbar puncture to analyze the CSF for signs of infection or inflammation (Swanson, 2015). Vaccines exist for certain types of bacterial meningitis, however no such preventative measure exists for HHV-7 associated meningitis (Schwartz *et al*, 2014).

1.2.5. ***Complications in transplantations***

Complications in transplantations have also been associated with HHV-7 infection (Pellett Madan & Hand, 2019). Active infection with both HHV-6 and HHV-7 is common following bone marrow or solid organ transplantation, most likely due to reactivation of the recipient's virus or re-infection (Clark, 2002). Reactivation of dormant viruses during an immune-deficiency period, can result in rashes, cytopenia, pneumonitis, hepatitis, and encephalitis in transplant recipients, as well as colitis and retinitis in HIV-positive individuals (Clark & Griffiths, 2003; Gautheret-Dejean *et al*, 2003; Holden & Vas, 2007). After kidney transplantation, roseoloviruses have also been found in patients with chronic renal disease (Vasques Raposo et al, 2020). In solid organ recipients, such as kidney transplant patients, viral reactivations frequently result in serious illnesses with detrimental implications on outcomes (Pellett Madan & Hand, 2019). Both HHV-6 and HHV-7 were detected in transplant patients who died of acute liver failure with no defined etiology (Mendez *et al*, 2001).

The presence of an HHV-7 infection may be the causal agent of an increase in time to neutrophil engraftment after bone marrow transplantations (Chan *et al*, 1997). One bone marrow transplantation patient that presented with acute myelitis, an inflammation of the spinal cord, showed a reactivated HHV-7 infection in the CSF (Ward *et al*, 2002b). A stem cell receiver also presented with bilateral optic neuritis and aseptic meningitis and showed a significant increase in HHV-7 antibody titer, which decreased as the patient’s condition improved (Yoshikawa *et al*, 2003).

A significant increase in viral replication was observed in the oral fluid of post-renal transplant patients, which resulted in the recognition of the salivary glands as a significant location of viral infection, particularly in individuals who are immunosuppressed (Raposo *et al*, 2020a).

There is also the potential that HHV-7 can also coinfect with or reactivate other viruses in transplant recipients, which can worsen clinical outcomes. HHV-7 has been proven to interact with CMV, which is known to complicate stem cell and organ transplantations (Razonable & Paya, 2002; Ljungman, 2002). HHV-7 can also reactivate or coinfect with HHV-6, a virus that has been linked to a number of clinical conditions in people who have had bone marrow transplants, including encephalopathy, interstitial pneumonitis, early and late graft failure, and bone marrow suppression (Clark, 2002).

Overall, HHV-7 infection can lead to various complications in transplant recipients, and its contribution to clinical outcomes is still not well understood. Monitoring for HHV-7 infection, coinfection with other viruses, and HHV-7 related immune modulation may help to identify patients at risk for complications and guide treatment decisions.

1.2.6. ***Other clinical associations***

Infection with HHV-7 is associated with a number of other symptoms, including acute febrile respiratory disease, optic neuritis, vomiting, diarrhea, and low lymphocyte counts (Mori & Yamanishi, 2007; Clark *et al*, 1997). Furthermore, there are indications that HHV-7 can contribute to the development of hepatitis infection, postinfectious myeloradiculoneuropathy, recurrent myocarditis, and the reactivation of other viruses like HHV-4, HHV-6 and CMV, with their respective complications (Cohen, 2015; Mori & Yamanishi, 2007; Chanas *et al*, 2021; Ljungman, 2002).

As mentioned, febrile seizures can occur as a side-effect of primary infection or reinfection with HHV-7 (Clark *et al*, 1997; Ward *et al*, 2005). Congruent with febrile seizures, HHV-7 has also been associated with status epilepticus (Epstein *et al*, 2012). Status epilepticus describes one prolonged seizure or a series of shorter ones that happen without the child regaining consciousness in between (Loddenkemper, 2014). Feverish status epilepticus refers to febrile seizures lasting at least 30 minutes. An association between the presence of HHV-7 and hippocampal sclerosis was found (Li *et al*, 2014). Hippocampal sclerosis is characterized by loss of neurons and reactive astrocytosis and gliosis of the hippocampus (Prayson, 2018). Hippocampal sclerosis represents the most common neuropathological finding in patients undergoing surgery for intractable temporal lobe epilepsy (Özkara & Aronica, 2012). Intractable epilepsy is defined as a failure of at least two antiepileptic drugs. This type of epilepsy might be mediated by inflammatory factors like TGF-β, that are upregulated in the presence of an HHV-7 infection (Li *et al*, 2014; Cacheaux *et al*, 2009).

Hemiconvulsion-hemiplegia (HH) syndrome, which typically affects children under the age of four, is defined by protracted seizures with a unilateral predominance followed by the onset of hemiplegia (Gastaut et al, 1959). Hemiplegia is, in its most severe form, complete paralysis of muscles on one side of the body (Piña-Garza & James, 2019). Despite the fact that HH syndrome can have a variety of causes, including vascular illness, trauma, or inflammatory disease, its etiology in an individual is not usually clear-cut. There is one case report of HHV-7-induced exanthem subitem, combined with acute infantile hemiplegia (Torigoe *et al*, 1996). In another case study, a suspected primary HHV-7 infection was involved in the development of HH (Kawada *et al*, 2004). However, in that study, peripheral leukocytes also contained HHV-6 DNA, suggesting that HHV-6 reactivation, brought on by HHV-7, may have been the cause of HH.

HHV-7 has also been detected in the CSF of patients suffering from Guillain-Barré syndrome (Schwartz *et al*, 2014). Guillain-Barré syndrome is a rapidly developing muscular weakness brought on by damage to the peripheral nervous system from the immune system (Shahrizaila *et al*, 2021). Changes in sensation or pain, frequently in the back, are the first symptoms, followed by muscle weakness that starts in the hands and feet and frequently spreads to the arms and upper body (Wijdicks & Klein, 2017). About 15-30% of those who experience the disorder's acute phase suffer breathing muscle weakness and require artificial ventilation, making it potentially fatal (Shang *et al*, 2020). Some patients are impacted by changes in the autonomic nervous system's operation, which can result in dangerous deviations in blood pressure and heart rate (Tuck & McLeod, 1981). The underlying mechanism, which is an autoimmune condition in which the body's immune system mistakenly targets the peripheral nerves and destroys their myelin coating, is still unclear (Koike & Katsuno, 2021). This immune dysfunction can occasionally be brought on by an infection, potentially with HHV-7 (Koike *et al*, 2021).

Acute cerebellitis is caused by damage to the cerebellum following a viral infection, often characterized by symptoms such as headaches, vomiting and disturbance of consciousness (Desai & Mitchell, 2012). It can be potentially life threatening due to raised intracranial pressure. In one case of acute cerebellitis, serological tests revealed the presence of HHV-7 (Hacohen *et al*, 2011). Acute cerebillitis was also reported during a case of primary HHV-6 infection, a family member of HHV-7 (Kato *et al*, 2003).

Stevens–Johnson syndrome (SJS)/toxic epidermal necrolysis (TEN) is a life-threatening hypersensitivity reaction, with dry eyes, vision impairment, and psychological issues being long-term consequences (Harr & French, 2010). TEN is primarily brought on by medication. However,

viral infections, including coxsackievirus A6, are recognized causes of this condition (Schwartz *et al*, 2013). In the first reported case study on HHV-7 and SJS/TEN, a causal relationship between was established from a chronological sequence of events, virus-specific antibodies, and RT-PCR (Shen *et al*, 2020).

1.3. Epidemiology

1.3.1. ***Distribution***

HHV-7 is a ubiquitous virus that is widely distributed throughout the world, with over 95% of adults being seropositive for HHV-7, and over three quarters of those having been infected before the age of six. HHV-7 infection is most common in early childhood with about 18% of children infected by one year of age and 53% by two years (Cohen, 2015; Clark *et al*, 1993). Infection rates decrease with age, with lower rates observed in adolescents and adults. This decrease in infection rates may be due to the development of immunity over time. However, a primary HHV-7 infection delayed into adolescence can cause serious neurologic disease (Schwartz *et al*, 2014). For example, a primary HHV-7 infection in an immunocompetent 19-year-old man was associated with encephalitis and flaccid paralysis for which all other suspected causes had been excluded (Ward *et al*, 2002a).

Seroprevalence varies by age and geographic region, with higher rates of infection observed in children and in some developing countries (Agut *et al*, 1996). Additionally, trends of HHV-7 infection exhibit seasonal variation, with higher rates of infection observed in the summer and autumn months in some regions (Yildirim *et al*, 2004). The primary infection of HHV-7 among children generally occurs after primary infection of HHV-6 (Cohen, 2015). Sampling of HHV-7 from healthy adults show its presence predominately in the mouth. Underlying conditions can also influence the prevalence and severity of HHV-7 infections. HHV-7 is more common and more severe in immunocompromised individuals, such as those with HIV/AIDS or undergoing immunosuppressive therapy (Agut *et al*, 2016).

1.3.2. ***Transmission***

The primary mechanism of transmission is through close contact with infected individuals, such as through saliva, respiratory secretions, or blood (Maldonado, 2011). Indeed, HHV-7 is shed from saliva in up to 90% or more of adults (Hall *et al*, 2006). Mother-to-child transmission can also occur during birth or through breast milk (Hall *et al*, 2004; Pass, 2004). HHV-7 DNA, but not HHV-6 DNA, has been detected in breast milk samples (Emery & Clark, 2007). However, antibodies to HHV-7 in breast milk may protect against infection, since breast-feeding has been associated with a lower risk of early acquisition of HHV-7 infection (Fujisaki *et al*, 1998). HHV-7 DNA has been detected in 2.7% of cervical swabs obtained from women in their third trimester of pregnancy, but from none of the swabs of non-pregnant control women, suggesting that pregnancy may be associated with reactivation of HHV-7 (Okuno *et al*, 1995). Perinatal transmission from contact with infected maternal secretions is unknown, and neonatal infections with HHV-7 have not been reported. An estimated 80% to 90% of the population sheds HHV-6 and HHV-7 intermittently in saliva, the prominent medium for viral host transfer (Wolz *et al*, 2012).

1.3.3. ***Diagnosis***

The diagnosis of HHV-7 infection can be challenging, as the virus typically causes mild or asymptomatic infections and may not be routinely tested for in clinical settings. The diagnosis of HHV-7 infection is typically based on serology, polymerase chain reaction (PCR), and viral culture, depending on the presentation of symptoms and available resources in the clinical setting.

Serological testing involves the detection of HHV-7-specific IgM and IgG antibodies in serum or plasma, and it can be used to diagnose acute or past infection (Yoshikawa *et al*, 1989; Ihira *et al*, 2002). However, serological testing may not be useful for diagnosing active infections, as it can take several weeks for antibodies to develop after initial infection. Still, similar to HHV-6, ELISA-based seroconversion is the most popular diagnostic procedure for HHV-7 in children (Cohen, 2015). Since HHV-7 is much less frequently found in serum or plasma than HHV-6, finding HHV-7 DNA in blood in the absence of virus-specific antibodies is more likely to indicate an acute infection (Wang & Pellett, 2007).

Immunofluorescence assay (IFA) is another serological test used to detect HHV-7 antigens in serum, saliva, skin, or other tissue samples, providing a rapid and specific method for diagnosing certain dermatological diseases associated with HHV-7 infection (Ward *et al*, 2001b; Cohen, 2015). IFA is a widely used virological method for detecting antibodies by their specificity in reacting with viral antigens produced in infected cells where bound antibodies are visualized by incubation with fluorescently tagged anti-human antibodies (Simonetti *et al*, 2015). Since antibody avidity gradually rises over time following exposure to an immunogen, primary infections can be identified using antibody avidity testing (Ward *et al*, 2001a). A low antibody avidity indicates that the primary infection was recent, and a high avidity indicates that the primary infection must have occurred in the more distant past (Ward *et al*, 2001b).

Black *et al.* (1996) compared antibodies in human serum using an enzyme immunoassay (EIA), an immunoblot test (IB), and an indirect IFA. The EIA was the most sensitive of the three assays (94%), although the IB was the most specific (94%) (Black *et al*, 1996).

PCR is a highly sensitive and specific method for detecting HHV-7 DNA in blood, saliva, cerebrospinal fluid, or other clinical samples (Ansari *et al*, 2004). Positive results of a PCR test indicate an active infection. However, PCR testing may not be widely available in all clinical settings. Also noteworthy, is that PCR will also detect latent viral DNA, and might not give indication of a primary infection, Quantitative HHV-7 DNA PCR can be used to document the presence of the virus as well as track the course of infection. Extraction of HHV-7 viral DNA from specimen followed by amplification and detection using real-time, quantitative PCR. Multiple PCR-based HHV-7-detection kits are already available on the market. Loop-mediated isothermal amplification (LAMP) is a technique for the amplification of DNA to detect certain diseases (Notomi *et al*, 2000). LAMP can be used for the detection of HHV-7 with high specificity and efficiency for the amplification of viral DNA (Yoshikawa *et al*, 2004).

Viral culturing is another method for diagnosing active HHV-7 infection, but it is rarely used due to the difficulty of culturing the virus (Ablashi *et al*, 1998). HHV-7 can be cultured from blood, saliva, or other body fluids, but this method is less sensitive and specific than PCR and may take several weeks to obtain results (Cermelli *et al*, 1997; Klussmann *et al*, 1997b). The primary phytohemagglutinin-stimulated $CD4^+$ T lymphocytes from cord blood or peripheral blood

mononuclear cells (PMBCs), as well as a continuous $CD4^+$ lymphoblastic cell line called SupT1, are required for HHV-7 isolation (Yasukawa *et al*, 1997).

In some cases, clinical diagnosis may be based on the presentation of characteristic symptoms, such as fever, rash, or encephalitis, along with other laboratory or imaging findings. However, the formal demonstration of the causative role of HHV-7 in many acute and chronic human diseases is difficult due to the ubiquitous nature of the virus, chronicity of infection, similarity to HHV-6, and limitations of current investigational tools.

1.3.4. Treatment

Currently, there is no specific treatment or antiviral medication approved for the treatment of Human herpesvirus 7 (HHV-7) infection. The virus typically causes mild or asymptomatic infections that resolve on their own without medical intervention. However, certain clinical manifestations of HHV-7 infection, such as encephalitis and drug-induced hypersensitivity syndrome, may require supportive care or treatment of associated symptoms, such as intravenous fluids, respiratory support, and management of seizures or other neurological symptoms (Mori & Yamanishi, 2007). Antipyretics, such as acetaminophen, can be used to manage the febrile phase by reducing fever and preventing the temperature spikes that can cause febrile seizures, while anticonvulsants, such as diazepam, can be used to treat occurring febrile seizures (Murata *et al*, 2018).

Although there is no specific antiviral medication approved for the treatment of HHV-7 infection, some studies have suggested that antiviral drugs used for other herpesviruses, such as acyclovir, ganciclovir, and foscarnet, may be effective against HHV-7 *in vitro* (Yang *et al*, 2022; Maltsev, 2022). However, due to inconsistencies in reports on the efficacies of different antiviral drugs used, further studies are needed to determine the clinical efficacy of these drugs against HHV-7 *in vivo* (Brennan *et al*, 2000; De Clercq *et al*, 2001; Li *et al*, 2022). The antiviral susceptibility of HHV-7 has not been well characterized. Although the numbers of patients were too small to demonstrate statistical significance, the trends observed suggest that at full therapeutic dosage, both acyclovir and ganciclovir may suppress HHV-7 activity *in vivo* (De Clercq *et al*, 2001; Maltsev, 2022). However, it is not possible to conclude that HHV-7 disease is treatable with these antiviral agents. In renal transplant recipients, ganciclovir prophylaxis did not influence the prevalence of HHV-7 viremia (Galarraga *et al*, 2005). Antiviral drugs like ganciclovir, foscarnet, and cidofovir may even cause serious side effects including bone marrow suppression and renal dysfunction (Clark *et al*, 2003).

Patients with drug-induced hypersensitivity syndrome or other dermatological diseases associated with HHV-7 infection may require treatment of associated symptoms, such as topical or systemic corticosteroids, antihistamines, or other medications (Wolz *et al*, 2012).

There is a lack of clinical experience in the management of HHV-7 CNS illness. Meningitis, meningoradiculopathy, myelitis, encephalitis, and Guillain-Barré syndrome have all been documented to improve without the need for particular antiviral therapy (Pohl-Koppe *et al*, 2001; Schwartz *et al*, 2014; Fay *et al*, 2015; Rangel *et al*, 2017). This also applied to patients who had HHV-7 amplification and aseptic meningitis. Treatment for viral encephalitis typically involves supportive care to manage symptoms, along with antiviral medications to target the specific virus causing the infection (Kennedy, 2004). High-dose corticosteroids, intravenous immunoglobulins, and plasma exchange helped an 11-year-old patient with brainstem encephalitis get well (Fay *et al*, 2015). Acyclovir has been used in cases of encephalitis (Ward *et al*, 2002b, 2001b) with what appears to be

success despite having little *in vitro* action against HHV-7 (Zhang *et al*, 1999). According to Zhang *et al*., foscarnet has more strong *in vitro* action against HHV-7 than ganciclovir. This is backed up in patients by Corral *et al*. (Corral *et al*, 2018). Early treatment is essential, as it can help prevent complications and improve outcomes. For some cases of viral encephalitis, a preventative measure can be taken, like vaccination against Japanese encephalitis, caused by the mosquito-borne Japanese encephalitis virus. However, no such vaccine is available for HHV-7 (Chen *et al*, 2015).

Overall, treatment of HHV-7 infection is primarily supportive, and antiviral therapy is not routinely recommended unless the patient has severe or life-threatening manifestations of the infection (Flamand, 2014). Patients with HHV-7 infection should be monitored closely for any associated symptoms or complications, and appropriate management should be provided as needed.

Prevention of HHV-7 transmission relies on standard precautions, such as hand hygiene and respiratory etiquette. Blood products should be screened for HHV-7 to prevent transfusion-transmitted infection.

In summary, HHV-7 is a common human virus that is widely distributed throughout the world, with high seroprevalence rates observed in children and in some developing countries. Transmission occurs through close contact with infected individuals, and the virus is usually asymptomatic or causes mild symptoms in young children. While HHV-7 infection is generally not a significant public health concern, it can cause disease in immunocompromised individuals and might pose a problem in certain clinical settings.

Part 2: Aim of Research Project

2.1. HHV-7: a new and understudied pathogen

HHV-7 was discovered in 1990 making it a relatively new virus of interest. Because of its ubiquitous nature, with a seroprevalence over 95% in the adult population, it can be challenging to perform a disease association for HHV-7 based on seroconversion. Severe clinical associations of HHV-7 (e.g., febrile seizures and encephalitis) have been reported, especially in children and immunocompromised patients. Still, the exact neurogenic targets of HHV-7 remain unknown. These case studies only show a sporadic association of HHV-7 with encephalitis, but do not suggest an underlying causality. Because so little is known about the viral pathogenesis and host-virus interactions, the mechanism in which HHV-7 could potentially cause encephalitis is still unknown. The most recent form of therapy consists of antiviral drugs, for example artesunate, valganciclovir, valacyclovir, foscarnet, cidofovir and ganciclovir (Galarraga *et al*, 2005; Zhang *et al*, 1999; De Clercq *et al*, 2001). These drugs have proven successful in cases of HHV-7 associated complications in immunocompromised patients, also other patients recovered without the use of antiviral drugs (Rangel *et al*, 2017).

The lack of knowledge on the neuroinvasive potential of HHV-7 is still a major hurdle in the development of adequate therapies and vaccines. It has been shown that both HHV-6A and HHV-6B can infect different nerve cell types, like glia, neurons and Purkinje cells, and different neurotransmitter phenotypes derived from differentiated human neural stem cells (Bahramian *et al*, 2022). At this moment, HHV-7 has only been studied in infection experiments of human cord blood mononuclear cells, peripheral blood mononuclear cells (PBMC) and a $CD4^+$ lymphoblastic cell line (SupT1), partly due to the substantial lack of tools available to study the infection of neurons (Cermelli *et al*, 1997; Ablashi *et al*, 1998). These combined research questions have led to the goal of our study, in which we want to create the necessary tools to subsequently study HHV-7 infection of other cell types, more specifically neurons. Finally, we want to better characterize the viral proteins involved in the infection process.

2.2. Studying the neuro-invasive potential of HHV-7 using CRISPR/Cas9

In order to better understand and therefore treat herpesvirus-induced encephalitis, the neuro-invasive potential of HHV-7, a previously unexplored tropism of HHV-7, will be studied *in vitro*. First, the CRISPR-Cas9 methodology will be used to construct the tools necessary to track HHV-7 entry. Two components of the HHV-7 virions (i.e., capsid and tegument) are released in the cytoplasm and can traffic in the cytoplasm and nucleus upon viral entry. In order to track these viral components during invasion of different cell types, we will construct HHV-7 mutants with N- or C-terminally tagged mRFP1-U32 (minor capsid protein), U31 (major tegument protein), or U14 (minor tegument protein). These mutants will be constructed using CRISPR-Cas9 technology. CRISPR-Cas9 is one of the most powerful and versatile tools for precise gene editing at this time. It outcompetes the traditional approach to construct herpesvirus mutants which involves homologous recombination of DNA fragments with the viral genome, often introduced as a bacterial artificial chromosome (BAC), which is a slow and laborious process. The cell types that will be used to study invasion of HHV-7 include $CD4^+$ T cells, an embryonic kidney cell line, and neurons. Studies have been done on

propagation of the virus in $CD4^+$ T cells. In our research, the invasion of $CD4^+$ T cells will be used as a control to compare with the invasion of neuronal cells. A neuronal cell line (SH-SY5Y) will be studied for their potential to host viral replication. Different methods of neuronal cell invasion will be studied, including the addition of extracellular virus particles to the medium and the usage of infected $CD4^+$ T cells to transfer the virus to the other cell type through cell-to-cell spread of intracellular virus particles.

2.3. Expected accomplishments

By the end of this research project, we will have created a collection of fluorophore-tagged HHV-7 mutants. These mutants could be useful in further research regarding the infection and replication of HHV-7. Furthermore, we will also have created HEK293T cell lines expressing Cas9 and HHV-7 targeting sgRNAs, which could be used in the production of other HHV-7 mutants.

Furthermore, we will have explored the cell tropism and replication cycle of HHV-7 in different cell types, providing us with a better understanding of the viral pathogenesis.

Contributions by third parties

We would like to thank dr. Jolien Van Cleemput and Elianne Burg for their help in the construction of the LentiV2 plasmids and the pcDNA donor plasmids.

We would also like to thank the Red Cross for providing us with the buffy coats needed for PBMC isolation.

Part 3: Results

3.1. HHV-7 stock production

3.1.1. ***Viral titration***

HHV-7 was propagated and titrated in SupT1 cells. SupT1 cells are derived from a malignant pleural effusion taken from an 8-year-old Caucasian male with T cell lymphoblastic lymphoma. They are CD4 positive, making them suitable for HHV-7 infection (Yasukawa *et al*, 1997). Viral infection and replication were verified visually by the occurrence of CPE. The viral stock was titrated on fresh SupT1 cells, calculated using the Reed-Müench formula, and expressed as $TCID_{50}$/mL (Reed & Müench, 1938). The $TCID_{50}$ (50% tissue culture infectious dose) assay is used to determine an infectious virus titer. This endpoint dilution experiment measures the quantity of virus needed to cause 50% of inoculated tissue culture cells to exhibit a cytopathic impact. The viral titer of the first viral stock according to the standard protocol is $10^{3.80}$ $TCID_{50}$/mL.

Reed-Müench formula: $proportional\ distance = \frac{(\%mortality\ at\ next\ dilution\ above\ 50\%) - 50\%)}{(\%mortality\ at\ next\ dilution\ above\ 50\%) - (\%mortality\ at\ next\ diulution\ below\ 50\%} \ . dilution$

The standard protocol as performed by our research group for the infection of other viruses such as HIV, consists of inoculating SupT1 cells with free HHV-7, followed by spinoculation. During the process of spinoculation, both the viral vector and the cells are centrifuged together to potentially aid the viral uptake by the target cells by influencing both the number of viral particles in the vicinity of a cell, as well as the cellular cytoskeleton, which in turn promotes receptor mobilization, viral entry, and post-entry processes (Guo *et al*, 2011). Spinoculation is also used to increase infection of cells by lentiviruses, including HIV (O'Doherty *et al*, 2000). However, the spinoculation step is time-consuming. For this reason, we wanted to investigate whether the spinoculation step is necessary, as well as investigate the infection of SupT1 cells after trypsin treatment. In the trypsin experiment, the SupT1 cells were subjected to a trypsin treatment after primary inoculation to make the cells more susceptible to viral infection, since a trypsin treatment can influence the infection rate because of the characteristic of proteases to cut viral or cellular proteins and bring them in an activation state where the viral entry rate is higher (Kim *et al*, 2022).

Consequently, two additional protocols were compared to the standard protocol (Table 2). An infection was performed where the spinoculation step of the standard protocol was skipped. Another infection comprised a trypsin treatment after inoculation. We used the initial stock of $10^{3.80}$ $TCID_{50}$/mL stock to generate new stocks in different ways in the above-mentioned experiment.

No improvement was observed in viral infection by including a spinoculation step ($TCID_{50}$/mL of $10^{6.54}$) compared to no spinoculation ($TCID_{50}$/mL of $10^{6.54}$) (Table 3). The trypsin treatment ($TCID_{50}$/mL of $10^{4.80}$) improved the viral infection compared to its respective mock treatment which included washing steps but no trypsin treatment ($TCID_{50}$/mL of $10^{3.80}$). However, the titer was lower compared to the standard protocol. Due to the extensive washing steps in the protocol a major loss of cells was observed, likely causing the lower titer of this stock compared to those of the other protocols. For this reason, the trypsin treatment was not considered effective for SupT1 infection. Based on these results and to save time, we decided to use the standard protocol without spinoculation for future stock productions and virus titrations in SupT1 cells. All HHV-7 stock used in following experiments was thus obtained in this manner, unless otherwise indicated.

Table 2. **Protocols for 3 methods of SupT1 infection with HHV-7**. Standard protocol of the research group contains spinoculation. The modified protocol follows the standard protocol with the exception of spinoculation. In parallel, a trypsin treatment was used to investigate its potential to improve HHV-7 infection.

Method	Protocol
Standard	1. Plate a 96 well flat bottom plates with 50 000 SupT1 cells/well 2. Prepare serial dilutions of the viral stock (0, 10^{-1}, 10^{-2}, 10^{-3}, …, 10^{-7} 3. Transfer 50 µl inoculum to the cells in the 96 well plates 4. Spinoculate cells 2300 rpm, 60 min, 20°C 5. Resuspend the cells and add 100 µl complete RPMI 6. Transfer plate to incubator (37°C, 5% CO2) for 5 days
Trypsin treatment	1. Plate a 96 well flat bottom plates with 50 000 SupT1 cells/well 2. Prepare serial dilutions of the viral stock (0, 10^{-1}, 10^{-2}, 10^{-3}, …, 10^{-7}) 3. Transfer 50 µl inoculum to the cells in the 96 well plates 4. Spinoculate 2300 rpm, 60 min, 20°C 5. Incubate for two hours 6. Transfer the cells to U-bottom plates 7. Centrifuge 7 min 1700 rpm 8. Add 25 µl trypsin to the cells 9. Incubate for 10 minutes at 37°C 10. Add 200 µl RPMI complete to all the wells 11. Centrifuge 7 min 1700 rpm 12. Remove the supernatant 13. Add 200 µl RPMI and transfer to new F bottom plate 14. Incubate 7 days and analyse titer as step 10 above
Modified	1. Plate a 96 well flat bottom plates with 50 000 SupT1 cells/well 2. Prepare serial dilutions of the viral stock (0, 10^{-1}, 10^{-2}, 10^{-3}, …, 10^{-7}) 3. Transfer 50 µl inoculum to the cells in the 96 well plates 4. Incubate for 2h 5. Resuspend the cells and add 100 µl complete RPM 6. Transfer plate to incubator (37°C, 5% CO2) for 5 days

Table 3. **HHV-7 titer in SupT1 cells**. Cells were subjected to three different protocols to optimize HHV-7 stock production in SupT1s cells. Cells were either subjected to a trypsin treatment, a mock treatment without trypsin, spinoculation or plain inoculation and subsequent incubation. Titer was calculated using the Reed-Müench formula "$\text{proportional distance} = \frac{(\%\text{mortality at next dilution above 50\%}) - 50\%)}{(\%\text{mortality at next dilution above 50\%}) - (\%\text{mortality at next diulution below 50\%}} . \text{dilution}$" and expressed in $TCID_{50}$/mL.

Standard protocol	No spinoculation	Trypsin treatment	Mock Trypsin
$10^{6,54}$	$10^{6,54}$	$10^{4,80}$	$10^{3,80}$

3.1.2. qPCR

Viral DNA was purified from different dilutions of HHV-7-infected SupT1 cell pellets and supernatants using the QIAamp MinElute virus spin kit (Qiagen, Hilden, Germany) according to the manufacturer's protocol. This was done to determine the relative amount of HHV-7 genomes for each virus stock by means of quantitative PCR (qPCR).

In the first performed PCR, viral samples were taken from the 0, 10^{-5} and 10^{-7} dilutions of both the infected and mock-infected SupT1 cells obtained by the viral titration experiment (see 3.1.2.). Cell pellets were separated from the supernatant and each assayed individually to reflect the amount of intracellular and extracellular virus respectively. Primers against 5 different glycoprotein-coding regions, being gB, gL, gH, gO, gQ, were used to quantify the presence of HHV-7, while primers for RPP30, the human ribonuclease P protein subunit p30, were chosen as a positive internal control. RPP30 was also used to normalize the differential viral load of the infected cell pellets. However, the glycoprotein primers showed off-target effects and were thus deemed unfit for the detection of HHV-7, as shown by the melting curves (Fig. 6). This correlates with the reported high Cq values, most of which were over 40. The Cq value represents the number of cycles needed to reach a set threshold fluorescence signal level (Ruiz-Villalba *et al*, 2021). The higher the Cq value, the less DNA was present in the original sample. This, combined with a positive signal in SupT1 cells that were not inoculated with HHV-7, led us to the conclusion that the obtained differential viral loads were inaccurate (Table 4).

Table 4. **Differential viral loads of intracellular HHV-7 of infected SupT1s at 0, 10^{-5} and 10^{-7} dilutions obtained by the viral titration experiment, expressed in %.** High Cq values (>40) were reported, as well as potential off-target effects, resulting in an unreliable representation of intracellular HHV-7 DNA.

	gB	gL	gH	gO	gQ
0	-2.04238	-2.04238	-2.04238	-2.04238	58.64831
10^{-5}	2.643401	2.643401	2.643401	2.643401	60.54717
10^{-7}	7.361218	7.361218	-6.56932	7.361218	62.45902

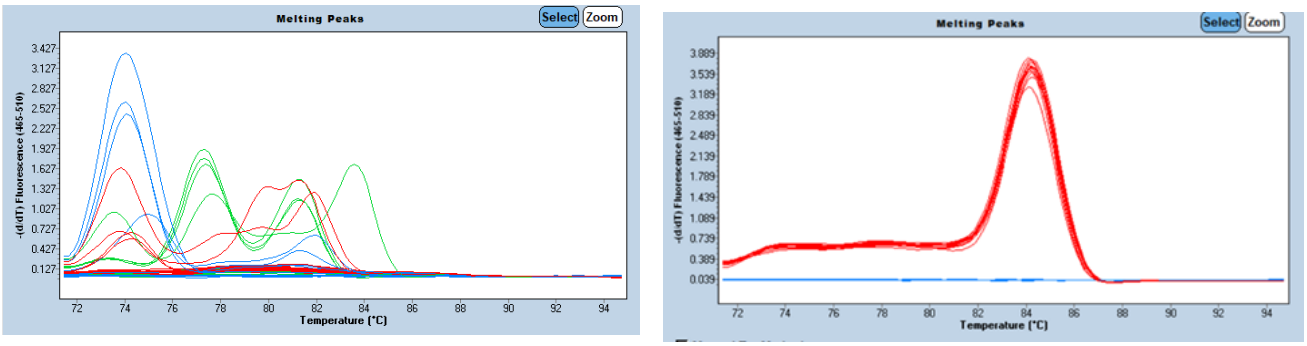

Figure 6. **Melting curves of the gB- (blue), gL- (green), gH- (green), gO- (red) and gQ- (red) amplified products (left) and RPP30-amplified products (right).** The presence of multiple peaks indicates the presence of off-target effects. Primers were thus proven to be unfit for use of HHV-7 detection. RPP30 is a reference gene used for standardization of products in the cell pellet. RPP30 curve is an accurate representation of reference curves obtained in subsequent experiments.

The second performed PCR was done on the cell pellets and supernatants of the 0 and 10^{-4} dilutions of the infected SupT1 cells of the viral titer assay of the spinoculated, non-spinoculated and trypsin-

treated conditions (see 3.1.2.). Primers were chosen based on literature of HHV-7 qPCRs performed in a clinical setting, targeting the U37- and U57-coding regions respectively (Li *et al*, 2021; Raposo *et al*, 2020b; Zheng *et al*, 2021). RPP30 was again included a positive internal control.

The Cq values of both the U57 and U37 primers were relatively high, ranging between 35 and 40. Furthermore, the differential viral load of HHV-7 DNA of the pellet samples was inconsistent, since the higher dilution appeared to have a higher viral load compared to the lower dilution (Table 5). The U57 primers showed a positive result in the viral DNA isolated from the supernatant of the titration experiment, but only in 2 pellet samples. The U37 primer showed positive results in the pellet samples. However, in subsequent experiments (3.3.2 and 3.4.1), the U37 primer showed activity in negative control samples containing cellular DNA but no viral DNA, meaning that this primer pair shows off-target effects, which was backed-up by their melting curves (Fig. 7). Since RPP30 gave a correct signal, the protocol should be correct. The melting temperature of their respective papers was also used. The off-target effects are thus unusual, as these primers seemed to work well in the literature they were taken from. However, in these studies, samples were taken from serum or ocular or oral fluids, which might not have contained the DNA that provided the off-target effects.

Table 5. **qPCR relative quantification of different HHV-7 production protocols in SupT1 cell pellets using the HHV-7 U37 and U57 primers**. RPP30 was chosen as a positive control and used for standardization. Differential viral load was obtained by comparison to the mock treatment (SupT1 cells not inoculated with HHV-7). Differential viral load values were ultimately rejected due to off-target effects of the primers, as well as the high Cq count.

Primer	Condition	Dilution	Differential viral load
U57	Spinoculation	0	-35.02616708
U57	Spinoculation	-4	-65.03216586
U37	Spinoculation	0	-43.00612233
U37	Spinoculation	-4	96.74754068
U37	No spinoculation	0	87.49885182
U37	No spinoculation	-4	72.03655129
U37	Trypsin	0	98.06413662
U37	Trypsin	-4	-35.02616708

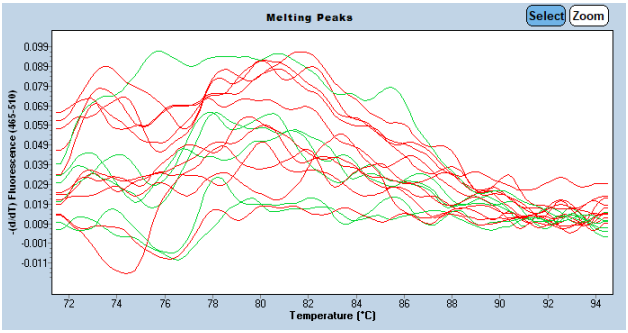

Figure 7. **qPCR melting curves of the U37- and U57-amplified products**. SH-SY5Y cells, SupT1 cells and activated and non-activated $CD4^+$ T cells were inoculated with HHV-7 and DNA was isolated from the pellets and supernatant of those cultures and subjected to qPCR to detect HHV-7 levels. The U57 primer pair showed no signal in most samples, while both primer pairs also showed off target effects, as visualized by the presence of multiple peaks. Green curves represent U37-amplified products, while red curves represent U57-amplified products.

As an alternative, the Benchling qPCR primer design wizard tool was used to develop primers based on the sequence of the HHV-7 Ji strain (Benchling, 2023). Primers were validated on characteristics such as the absence of hairpin formation and the absence of off-target effects using Unafold and UCSC In-Silico PCR, respectively (Markham & Zuker, 2008; Kent *et al*, 2002). Primers were tested on HHV-7- or mock-infected SupT1 cells, primary activated and non-activated $CD4^+$ T cells and SH-SY5Y cells (see 3.3.2, 3.4.1 and 3.4.2). This primer pair also showed off target effects, as observed by the presence of multiple peaks and positive signal in the conditions containing no HHV-7 (Fig. 8).

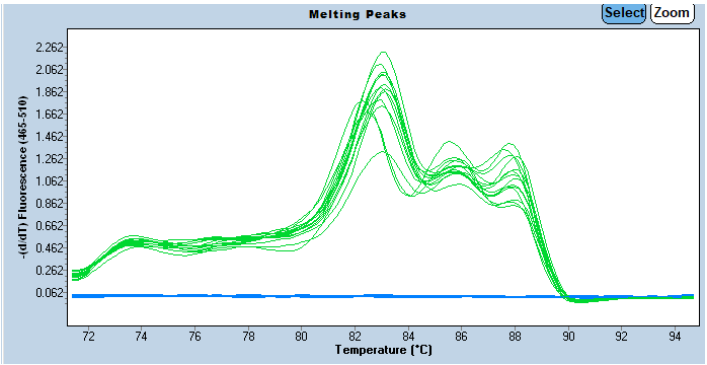

Figure 8. **Melting curve of the HHV-7 primers designed using Benchling (left) or RPP30 primers (right).** The presence of multiple peaks on the left graph shows the occurrence of off-target effects.

Due to the consistent occurrence of off-target effects in the qPCRs, the alternative method of viral titration was chosen to detect the amount of (replication competent) virus in further experiments. Viral titration has the disadvantage of taking a week to complete. However, it has the advantage of showing not only the presence of virus, but the presence of replication-competent virus, something the qPCR does not detect, as qPCR simply detects the presence of viral DNA.

3.2. HHV-7 mutant production

3.2.1. LentiCRISPRv2 transduction of HEK293T cells

Fluorophore-tagged HHV-7 mutants were constructed using CRISPR-Cas9. Using specific sgRNAs, certain proteins in the HHV-7 genome were targeted, after which the mechanism of homology directed repair (HDR) was exploited to insert the coding sequence for mRFP1 up- or downstream of the target protein. The chosen proteins for this experiment were U32 (minor capsid protein), U31 (major tegument protein) and U14 (minor tegument protein). All of these proteins are structural proteins and are built into the virion. This allowed us to monitor both infection and replication in different cell types. Since the position of a fusion protein might have impacted protein function, the fluorescent mRFP1 protein were attached either N- or C-terminally, giving for example mRFP1-U31 and U31-mRFP1 respectively.

The CRISPR-Cas9 system consists of two main components: the CRISPR sgRNA and the Cas9 enzyme. The sgRNA is a short RNA molecule that binds to a specific DNA sequence in the genome, known as the target site. The Cas9 enzyme is a protein that cuts the DNA at the target site upon recognition of the protospacer adjacent motif (PAM). The PAM is a 2–6-base pair DNA sequence that immediately follows the DNA sequence targeted by the sgRNA. After Cas9 cuts the DNA at the target site, the cell's natural DNA repair mechanisms will then repair the DNA sequence. If a donor sequence encoding *mRFP1* flanked by homology arms similar to regions flanking the target site is

provided, reparation can be completed through the process of HDR. In the production of fluorophore-tagged viral particles, the *mRFP1* gene of interest was flanked between 2 homology arms, of which one was homologous to a part of the viral protein of interest and another was homologous to a sequence adjacent to the viral protein of interest. The *mRFP1* gene and the homology arms were offered for use in the HDR by a plasmid, subsequently called the donor plasmid.

First, cells stably expressing Cas9 and a sgRNA against an HHV-7 gene of interest were generated using lentiviral transduction. Lentiviral transduction is a technique used in molecular biology to stably introduce genetic material, such as DNA or RNA molecules, into cells using viral vectors. Lentiviruses are a type of retrovirus that can infect dividing and non-dividing cells, making them useful vectors for delivering genetic material into a wide range of cells, including difficult-to-transfect cell types.

The lentiviral transduction process involves several steps. First, the genetic material of interest is cloned into a lentiviral vector (Fig. 9), which is then packaged into lentiviral particles. The lentiviral particles are then added to the target cells, where they bind to the cell surface and release their genetic cargo into the cell. Once inside the cell, the genetic material can be reverse transcribed and subsequently integrated into the host cell's genome, where it can be expressed and potentially modify the cell's behavior or function. Lentiviral transduction has several advantages over other gene delivery methods, such as high efficiency and stable gene expression. However, it also has some limitations, such as the risk of insertional mutagenesis, which can potentially disrupt normal cellular processes or cause genetic instability. Therefore, careful consideration and optimization of lentiviral transduction protocols is necessary to ensure safe and effective gene delivery.

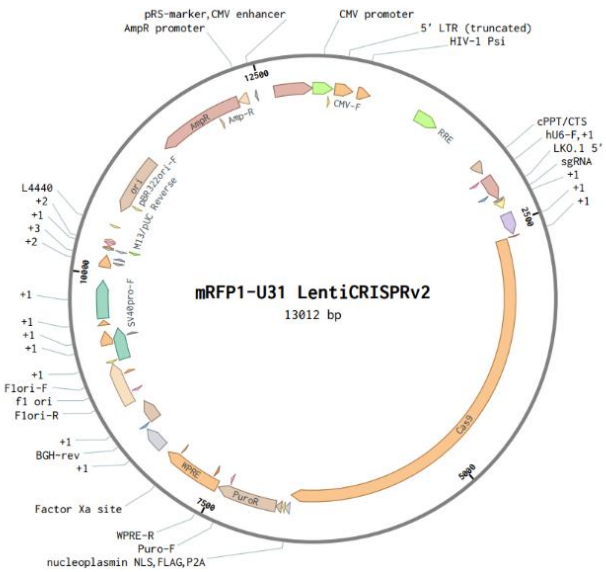

Figure 9. **Lentiviral plasmid containing the coding sequence for Cas9 and sgRNAs against U31.** Plasmid was used to produce LentiCRISPR viruses, which in turn were used to transduce HEK293T cells to obtain Cas9 and sgRNA expressing HEK293T cells.

The transduction with lentiviruses resulted in a mosaic culture of HEK293 T cells expressing no, low-level, or high-level Cas9, since Cas9 is integrated in different parts of the genome within the same culture (Fig. 10). Using puromycin selection, where the puromycin resistance gene was present together with Cas9 and the sgRNAs on the lentiviral vector, only cells expressing enough Cas9 -and thus puromycin resistance- will survive.

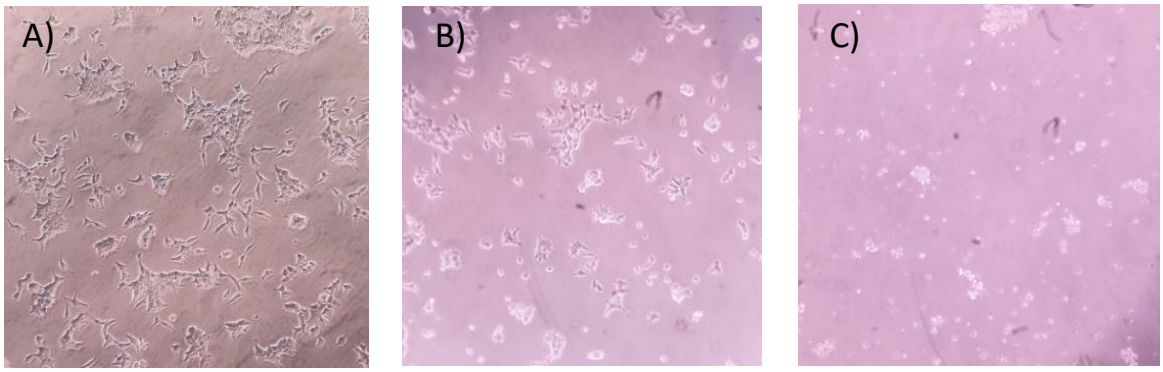

Figure 10. **HEK293T cell transduction.** HEK293T cells after A) LentiCRISPRv2 transduction with Cas9 and sgRNA for mRFP1-U31 and subsequent negative selection with puromycin (the image is representable for all different LentiCRISPRv2-transduced HEK293T cells treated with puromycin); B) no transfection and no selection with puromycin C) no transduction but selection with puromycin.

3.2.2. *Cas9 Western Blot*

To prove the presence of Cas9 in the transduced cells, a Western blot was performed. A Cas9-containing nanoparticle was chosen as a positive control (Mangeot *et al*, 2019). The first Western Blot failed, as neither the sample nor the positive control could be detected. To optimize the protocol, the Western Blot was repeated with a longer transfer time and the extra step of a Ponceau staining, to determine the transfer efficiency (Fig. 11). In the Ponceau staining, the VSV G protein that was part of the nanoparticle that functioned as the positive control, was visible. This suggests that the transfer occurred correctly. However, the Cas9 protein of the positive control, which is larger than VSV G and thus should have been located higher, was not visible.

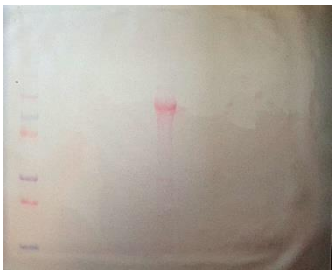

Figure 11. **Ponceau staining of Cas9 containing cell lysates and positive control.** Red stain detects the VSV G protein of the positive control.

After visualization using anti-Cas9 antibodies, there was no signal in either the positive control or the sample, which means that Cas9 could not be detected using Western Blot. The positive control was proven in previous research using a Western Blot to contain Cas9, but only after long exposure (Fig. 12). This indicates that the Western Blot most likely did not fail due to lack of Cas9, but due to the low sensitivity of this technique.

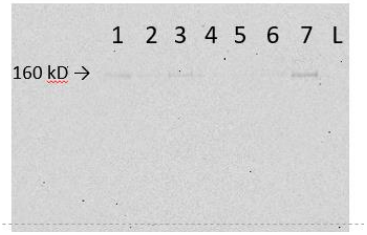

Figure 12. **Western Blot of Cas9 Nanoblades.** Nanoblade 3 was used as a positive control in experiment 3.2.2.

3.2.3. *Cas9 ELISA*

A Cas9 ELISA was performed as an alternative to the Western Blot, with the added advantage of a higher sensitivity. The first Cas9 ELISA gave an oversaturated positive signal in all the HEK293T cell cultures for the presence of Cas9. Since the signal was too strong to accurately quantify Cas9 amounts using the standard curve, the experiment was then repeated using a 1:100 dilution of the samples. Values were normalized using normal HEK293T cells (0.03 Cas9 ng/mL) and blanks. The HEK293T cells containing mRFP1-U14 contained the most Cas9 (2588 ng/mL), followed by mRFP1-U31 (1628 ng/mL), U14-mRFP1 (1395 ng/mL), U31/U32-mRFP1 (833 ng/mL) and lastly mRFP1-U32

(515 ng/mL) (Fig. 13). It is interesting to note that the mRFP1-U14 HEK293T strain had a slower growth rate than the other cell cultures.

The ELISA value of the positive control used in 3.2.2. was 2109 Cas9 ng/mL. This indicated that Cas9 is indeed present but was not abundant enough to be picked up by the Western Blot.

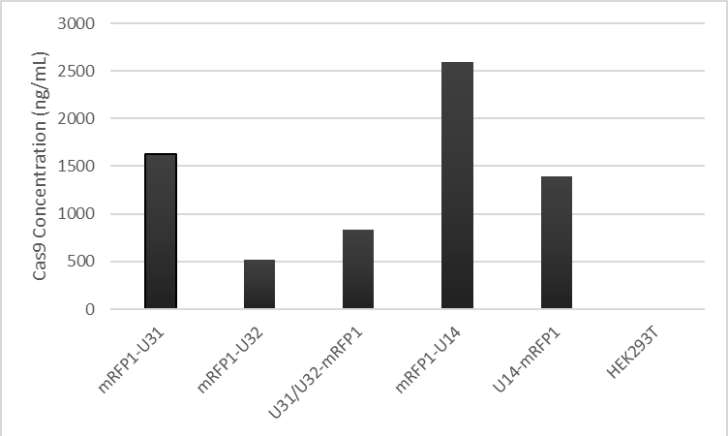

Figure 13. **Cas9 ELISA**. HEK293T cells were lentivirally transduced to express Cas9 in order to produce mutant HHV-7. Cas9 concentration was determined using the Cell Biolabs Cas9 CRISPR ELISA kit.

3.2.4. HHV-7 inoculation and donor plasmid transfection

The transduced and selected HEK293T cells were subsequently used to produce fluorophore-tagged HHV-7 mutants. To do so, the cell cultures were infected by either free HHV-7 virus or addition of HHV-7-infected SupT1 cells and transfected the next day with a pcDNA construct containing *mRFP1* and the homology arms corresponding to the surroundings of the target protein. In this way, *mRFP1* will be integrated after Cas9 cuts at the site indicated by the sgRNA and the site is repaired by homology directed repair, where the homology arms and *mRFP1* on the pcDNA will be used as a template (Fig. 14). This protocol was derived from used for the production of fluorophore-tagged CMV viral particles, a family member of HHV-7, in another study where cells were infected with CMV and subsequently transfected with a *GFP* donor plasmid. (King & Munger, 2019).

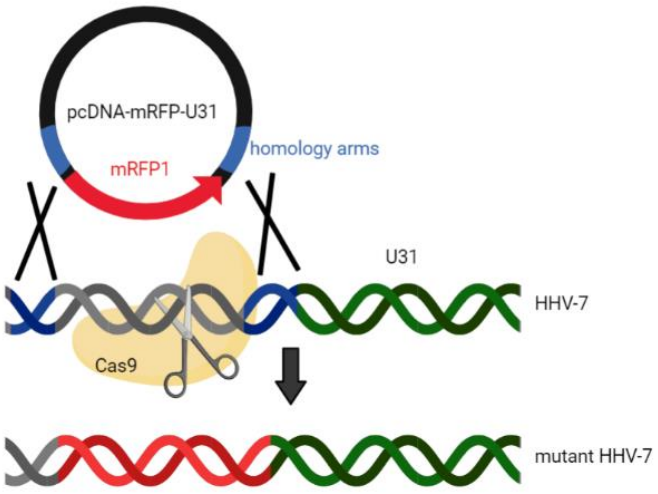

Figure 14. **Schematic representation of homology directed repair that occurs after Cas9 cuts in the HHV-7 viral DNA at the sgRNA target site.** Homology directed repair results in the production of fluorophore-tagged HHV-7 mutants produced by HEK293T cells. Figure made using BioRender.com.

The plasmid containing *mRFP1* is administered by transfection. Transfection is the process of introducing genomic material into cells without the use of a viral vector. The cell culture chosen for this transfection, were HEK293T cells, since they are easily transduced and transfected. HEK293 cells are a specific immortalized cell line derived from human embryonic kidney cells grown in tissue culture taken from a female fetus in 1973. HEK293T cells express a mutant form of the SV40 big T antigen Another option would have been the SupT1 cell culture. However, even though SupT1s are easily transducable, they are hard to transfect without electroporation which causes significant losses in cell viability. Since HEK293T cells are easier to transfect with donor plasmids when compared to SupT1 cells, HEK293T cells were chosen to produce mutant HHV-7 stocks. SupT1 cells are most commonly used to produce HHV-7 viral stocks. However, these cells are hard to transfect with donor plasmids containing the template for HDR as mentioned above. In previous experiments, SupT1 cells have been electroporated with plasmids expressing mRFP1, but no fluorescence was observed. In addition, a major loss in cell viability (up to 50%) was observed.

Interestingly, we previously observed that HHV-7-infected SupT1 cells can transfer HHV-7 infection to HEK293T cells. These HEK293T cells showed plaque formation, as well as the formation of protrusions in response to HHV-7 infection (Fig. 15).

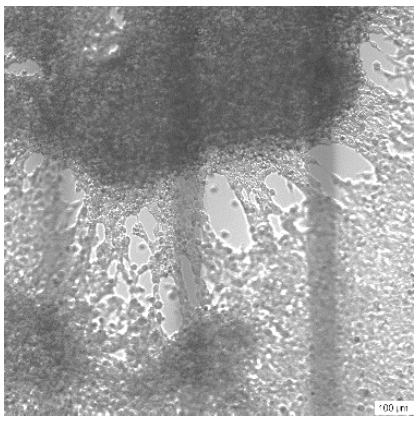

Figure 15. **Microscopic observation of HEK293T cells infected with HHV-7 following cell-to-cell spread from HHV-7-infected SupT1 cells.** Infected HEK293T cells showed plaque formation and occurrence of protrusions stemming from the plaque

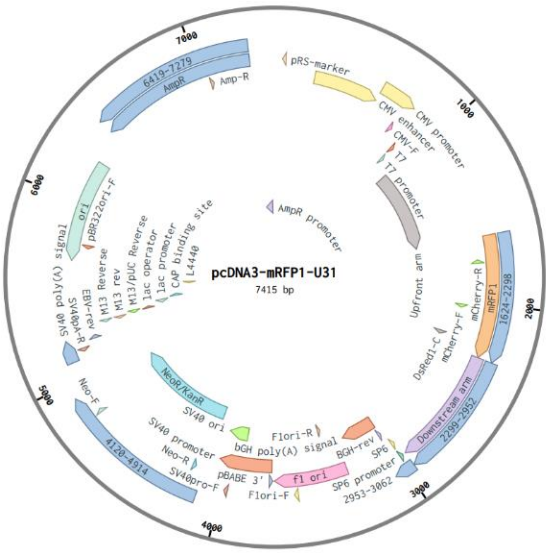

Figure 16. **Donor plasmid containing the coding sequence for mRFP1-U31**. This plasmid was used to obtain fluorophore-tagged HHV-7 viruses after transfection and infection of HEK293T cells.

The donor plasmids were constructed using the HiFi DNA assembly method (NEB). All donor plasmids derive from a pcDNA3-mRFP1 backbone (Fig. 16). The gBlock was synthetically made and contains part of the respective viral gene we want to mutate fused to a fluorophore and flanked by homology arms that match viral genes upstream and downstream of the targeted region. A protein linker is attached if the viral protein precedes mRFP1, but not if it is located downstream of mRFP1, as the C-terminus of mRFP1 may function as a linker. The mutants are modified so the necessary STOP- and START-codons are removed. The PAM sequence is also mutated to avoid cleavage of mutant viral DNA during CRISPR-mediated HDR. Two PCR fragments were generated by PCR of the gBblock and of the plasmid and combined using Hifi DNA assembly. HiFi DNA assembly, also known as high-fidelity DNA assembly, is a molecular biology technique used for the construction of large DNA molecules. It is a method to join multiple DNA fragments together in a specific order to create longer and more complex DNA sequences. The traditional DNA assembly methods, such as restriction enzyme digestion and ligation or overlap extension PCR, often introduce errors and limitations when assembling longer DNA fragments or multiple fragments simultaneously. HiFi DNA assembly, on the other hand, addresses these limitations and offers improved fidelity and efficiency. All plasmid sequences were verified using Sanger sequencing.

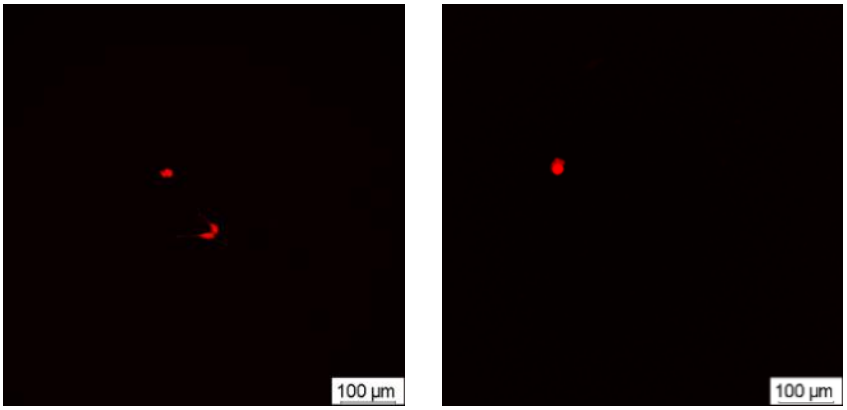

Figure 17. **mRFP1-U31 HHV-7 mutant production in HEK293T cells**. Cas9 expressing HEK293T cells were infected with HHV-7 infected SupT1 cells and subsequently transfected with a donor plasmid containing mRFP1-U31.

HEK293T cells were obtained that produced an mRFP1 signal (Fig. 17). However, this was considered a very low yield of fluorescence since we were only able to obtain 3-6 fluorescent cells. Furthermore, no fluorescent plaques were able to be isolated in subsequent experiments (3.2.5).

Due to the lack of fluorophore-tagged virus production, an alternative mutant production method was performed on the different HHV-7 mutants. In this method, the infection and transfection were switched, where the fluorophore-linked protein plasmid was added to the HEK293T cells before the HHV-7 infected SupT1s were added to the cells. The lack of fluorescence in earlier mutants could possibly have been due to Cas9 cutting the viral DNA, without the plasmid being present to facilitate HDR, thus resulting in a reduction in active virus. In the new protocol, the virus was added when the plasmid was already present and mutant production could begin instantaneously. Different cell cultures were obtained that expressed one of 5 different fluorophore-tagged HHV-7 viruses of the 3 different proteins (being mRFP1-U31, U31-mRFP1, U32-mRFP1, U14-mRFP1 and mRFP1-U14) (Fig. 18). However, mock-infected HEK293T cells transfected with the U32-mRFP1 and U14-mRFP1 donor plasmids also produced a red fluorescent signal since the necessary start- and stopcodons were present on those plasmids, so a part of the fusion protein could be transcribed and expressed. Therefore, we could not conclude that the fluorescent signal originated from mutant virus production. Still, the cells were still used for plaque purification, as described in 3.2.5,

and the formation of fluorescent plaques indicated the possibility that, despite the false positive signal from the donor plasmid, mutant HHV-7 was indeed produced.

It is interestingly to note that the viruses that expressed U31 linked to a fluorophore showed a lot less intensity of the fluorescent signal than those that had U32 linked to a fluorophore. U31 codes for the major tegument protein, while U32 codes for the minor capsid protein. A reason for the difference in fluorescence might be due to the amount of protein copies that is present in the virion and during viral replication in the cell.

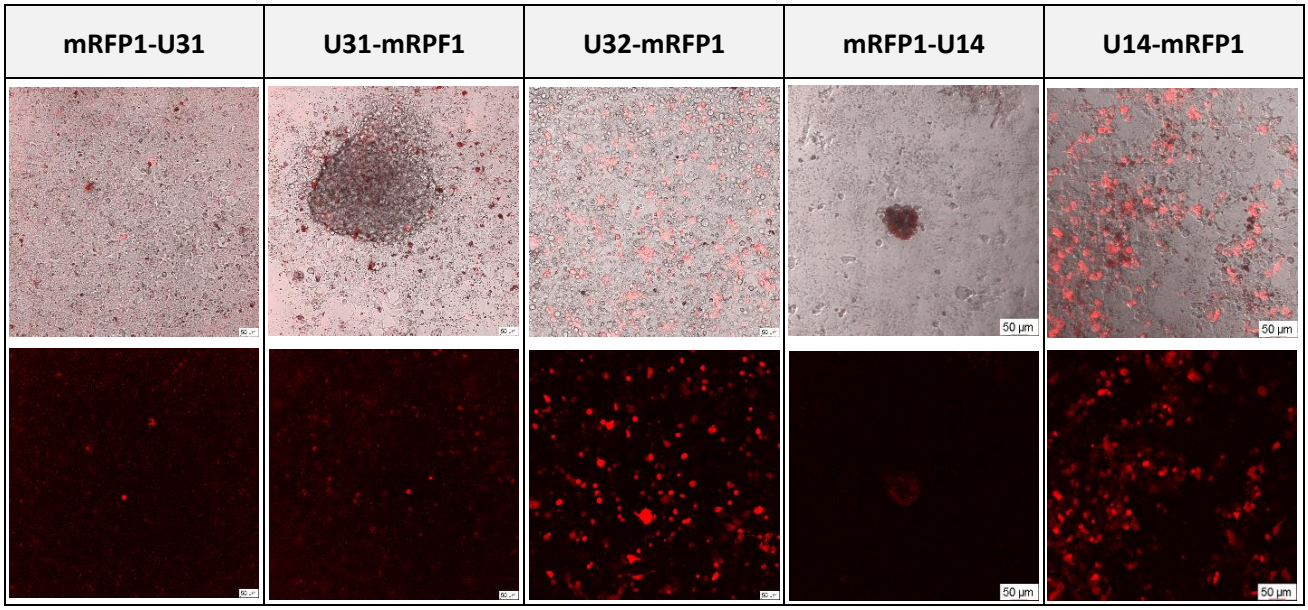

Figure 18. **Fluorescent HHV-7 mutant production in HEK293T cells**. Fluorophore-linked protein plasmid was added to Cas9 and sgRNA expressing HEK293T cells before they were inoculated with HHV-7 infected SupT1s.

3.2.5. Plaque purification

In a first attempt to purify the mutant viruses, a U32-mRFP1 HHV-7-positive plaque (Fig. 19) was picked and subjected to a new round of plaque purification on HEK293T cells, where cells were inoculated with free virus from the picked plaque. However, no fluorescent plaques were observed, meaning this one mutant viral plaque was lost during the purification process. It is unlikely that this fluorescent signal originated from leftover donor plasmid that was harvested from the cells.

To determine if the plaque purification failed due to low viral levels of mutant HHV-7, a qPCR was performed on the collected HEK293T cells. However, due to primer-specific off target effects, no conclusions could be made on the presence of infectious virus. Therefore, in a following trial to produce mRFP1-U31 mutant viruses in HEK293T cells, a titration experiment was performed on the harvested material. No CPE was observed, indicating that there was an inadequate level of viral particle production in HEK293T cells alone.

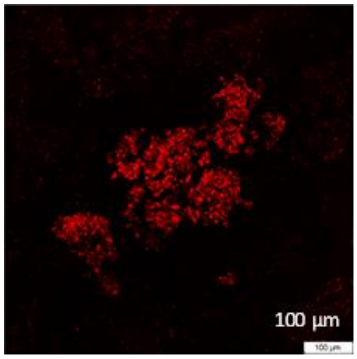

Figure 19. **Plaque containing U32-mRFP1 HHV-7 mutant infected HEK293T cells.** HEK293T cells were inoculated with U32-mRFP1 containing HHV-7 mutants in plaque assay medium. Cells of one plaque are infected with the progeny of one virus.

Therefore, HHV-7 mutants obtained from the new protocol as described in 3.2.4 were first used to infect SupT1 cells in a viral propagation step. This propagation was done to obtain higher levels of mutant virus, as well as to facilitate transfer to the HEK293T cells, as the use of infected SupT1s proved to be efficient to transfer HHV-7 to HEK293T cells in preceding experiments. The viral progeny was harvested and subjected to plaque purification. For this, HEK293T cells were inoculated with either free mutant virus or with SupT1 cells infected with mutant virus. Plaque formation was observed after 3 days in HEK293T cells inoculated with infected SupT1 cells (Fig. 20). In HEK293T cells inoculated with free mutant virus, plaque formation was observed after 4 days, however 6-fold lower levels compared to the HHV-7-infected SupT1s inoculated cells. Still, the most notable observation about these plaques, is the significant reduction in fluorescence compared to fluorescence observed during mutant production in the Cas9-expressing HEK293T cells (Fig. 18). Indeed, we could only observe one clearly fluorescent plaque in the cell layer inoculated with the U32-mRFP1 mutant stock, but not for the U31-mRFP1 nor mRFP1-U31 mutants.

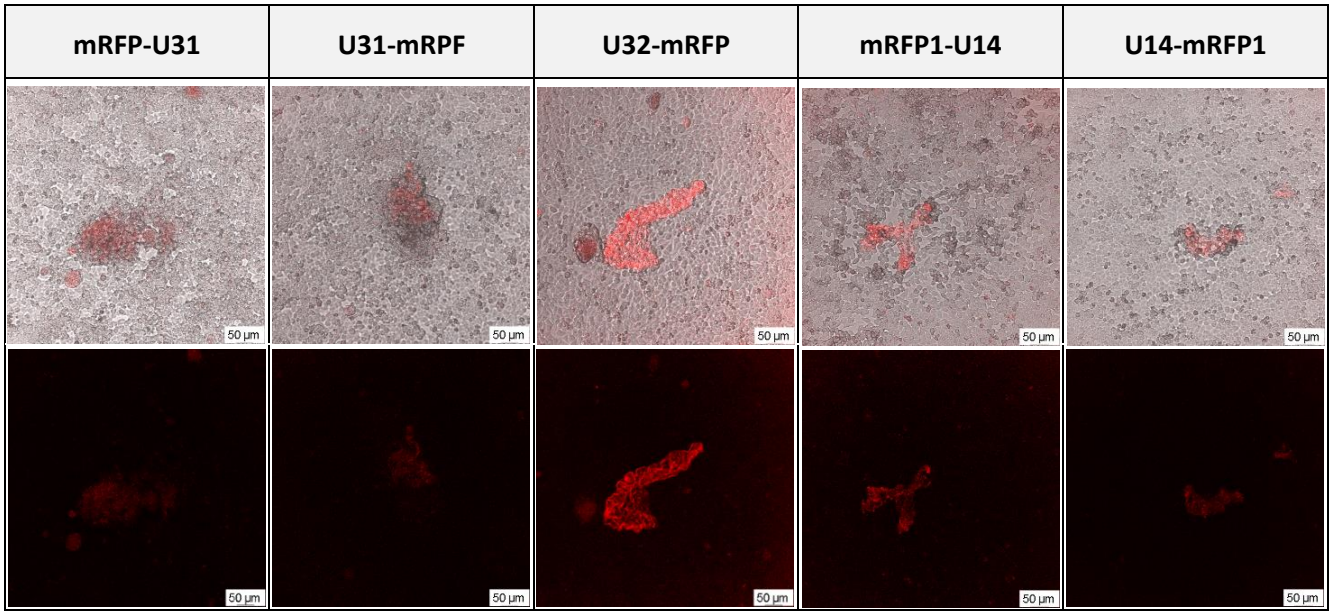

Figure 20. **Plaques containing fluorescent HHV-7 mutant infected HEK293T cells.** HEK293T cells were inoculated with fluorophore-tagged HHV-7 mutants, as obtained by the new protocol consisting of a transfection followed by and HHV-7 infection, in plaque assay medium. Cells of one plaque are infected with the progeny of one virus.

Fluorescent plaques were used for further purification, according to the same protocol. SupT1 cells were inoculated with the viral plaque and HEK293T cells were inoculated with the infected SupT1 cells. Following a second round of purification of a U32-mRPF HHV-7-positive plaque, we observed a higher amount of fluorescent plaques (up to 58.8% of total viral plaques), indicating successful isolation of the mutant. Due to the lack of time for further purification, we used two of those fluorescent plaques for the live-cell imaging experiment of U32-mRFP1 infection in SH-SY5 cells and SupT1 cells.

In the meantime, the difficult process of plaque purification on HEK293T cells lead to the search of alternative methods to harvest HHV-7 fluorophore tagged mutants. In the production of the mutants in Cas9 containing HEK293T cells by infecting them with HHV-7 infected SupT1 cells, the presence of fluorescence was observed in the remaining SupT1 cells, thus indicating the possibility that the fluorescent HHV-7 has the capacity to infect SupT1 cells (Fig. 21). To explore this possibility, U32-mRFP1 and U14-mRFP1 HHV-7 mutants were produced according to the previously mentioned

protocol. After the observation of fluorescence in the Cas9 containing HEK293T cells, these cells were co-cultured with fresh SupT1s to propagate mutant viruses.

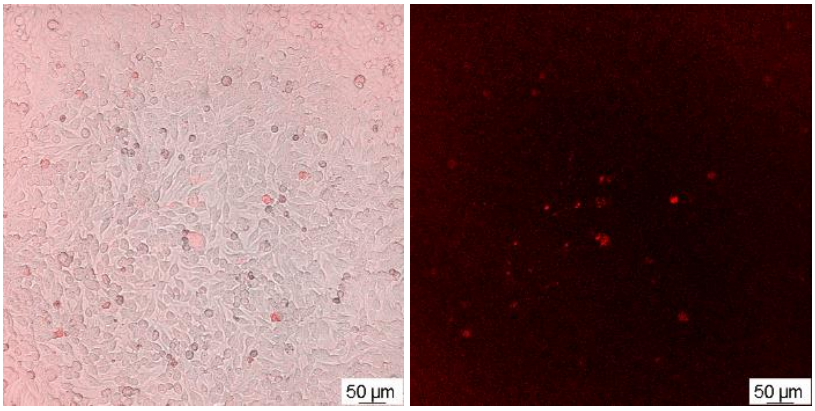

Figure 21. **SupT1 cells showing fluorescence in the vicinity of U32-mRFP1 HHV-7 mutant producing HEK293T cells.** In a coculture of fluorophore-tagged HHV-7 producing HEK293T cells and SupT1 cells, there seems to occur an infection of remnant SupT1 cells with mutant HHV-7 virus.

Interestingly, these fresh SupT1 cells also showed fluorescence after separation from the HEK293T cell culture (Fig. 22). These fluorescent SupT1s also showed CPE in many cases, indicating active mutant HHV-7 replication. The existence of these fluorescent SupT1 cells suggests that, even though a false positive signal was obtained from the donor plasmid, there still is formation of mutant HHV-7. The donor plasmid was removed from the HEK293T cells before the infected SupT1s were added and SupT1 are hard to transfect, making it practically impossible for remaining donor plasmids to enter the SupT1 cells and give a false positive signal.

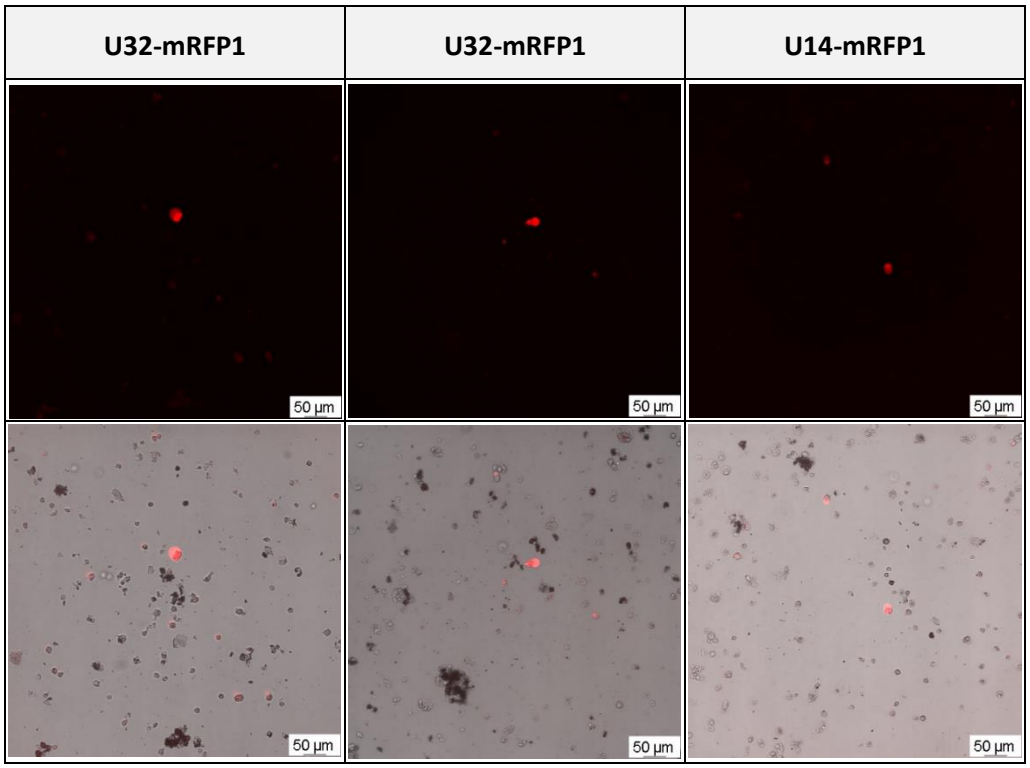

Figure 22. **SupT1s isolated from the U32-mRFP1 and U14-mRFP1 HHV-7 producing HEK293T cells**. HEK293T cells containing Cas9 and sgRNAs against U32 and U14 respectively were transfected with a mRFP1 donor plasmid and subsequently infected with HHV-7 infected SupT1 cells. Fluorescence was observed in both HEK293T cells and SupT1 cells after 7 days. SupT1 cells were separated from HEK293T cells and examined for fluorescence. Fluorescent signal and CPE were observed in several SupT1s, indicating mutant HHV-7 infection.

Fresh SupT1s were added to these fluorescent cells to see if they would transfer these supposedly fluorescent HHV-7 particles to other cells. Fluorescence and CPE was observed in the SupT1 cells after several days, however the amount of fluorescence did not seem to increase in a visible way (Fig. 23).

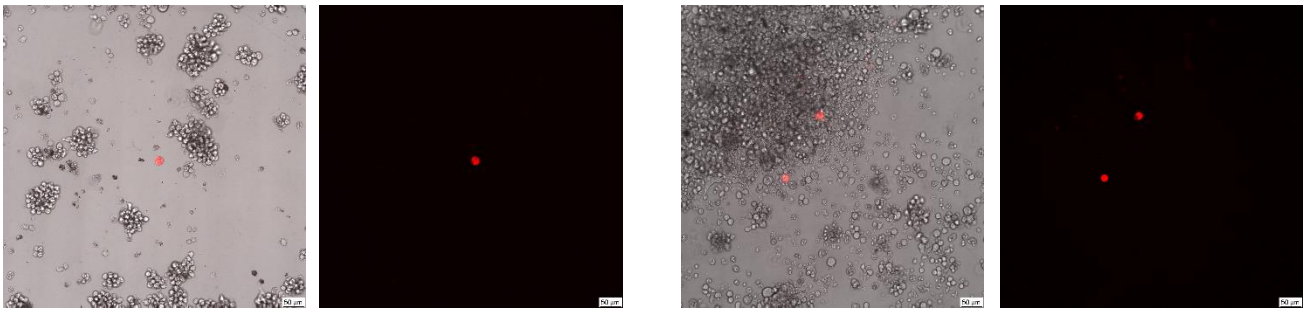

Figure 23. **SupT1s after coculture with U32-mRFP1 HHV-7 producing HEK293T cells and subsequent isolation for 5 days.** Cells were still shown to be fluorescent and express CPE but did not seem to spread this fluorescence to other cells in high quantities. Cells were harvested and frozen for future experiments.

Interestingly, a high level of CPE was observed in the SupT1 cells that were isolated from the U32-mRFP1 HHV-7 producing HEK293T cells, yet these ballooning cells did not show any fluorescence (Fig. 24). The fluorescence occurred almost exclusively in single cells.

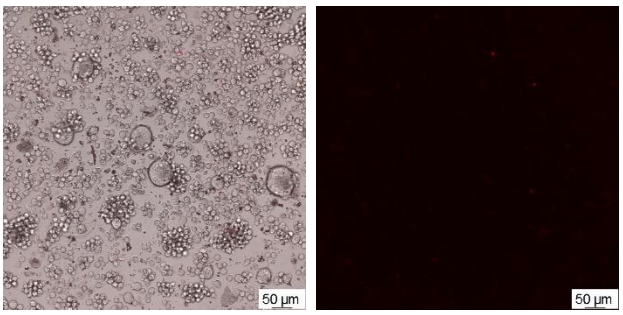

Figure 24. **SupT1s after coculture with U32-mRFP1 HHV-7 producing HEK293T cells and subsequent isolation for 5 days showing CPE and fluorescence.** A prominent level of CPE occurred, indicating viral replication. However, fluorescence occurred primarily in cells showing no or limited amounts of CPE (swelling, but no formation of syncytia).

3.3. Neuronal cell infection

3.3.1. Neuronal differentiation of SH-SY5Y cells

The SH-SY5Y cell line is a human-derived cell line and was subcloned from the original SK-N-SH cell line, which was obtained from a bone marrow biopsy of a four-year-old girl with neuroblastoma. *In vitro* models of neuronal function and differentiation frequently employ SH-SY5Y cells. They exhibit dopaminergic markers in addition to having an adrenergic phenotype, and as a result, have been utilized to research Parkinson's disease, neurogenesis, and other features of brain cells. Undifferentiated SH-SY5Y cells can gather into mounds that disperse differentiated cells into the surrounding tissue (Fig. 25) (Shipley *et al*, 2016).

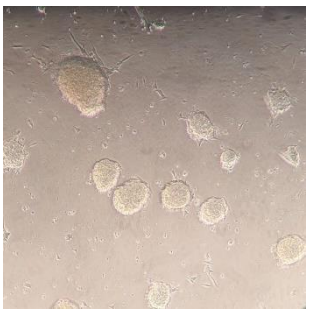

Figure 25. **Undifferentiated SH-SY5Y cells.** SH-SY5Y cells form mounds from which neurite-like processes migrate out.

Based on literature, SH-SY5Y cells are differentiated by adding retinoic acid (RA) to the medium. By performing a concentration-range experiment of

different RA concentrations ranging from 1000 µM to 0.01 µM in a 96-well plate and following up over time using an Incucyte incubator, an optimal concentration of 10 µM was decided upon based on the differentiation level after 5 days (Fig. 26). This concentration is congruent with literature, in which 10 µM RA is often used in the differentiation of SH-SY5Y cells. The concentration-range experiment was performed with two different media, DMEM/F12 and Neurobasal medium supplemented with growth factors. The DMEM/F12 medium seemed to support the differentiation of SH-SY5Y cells the best.

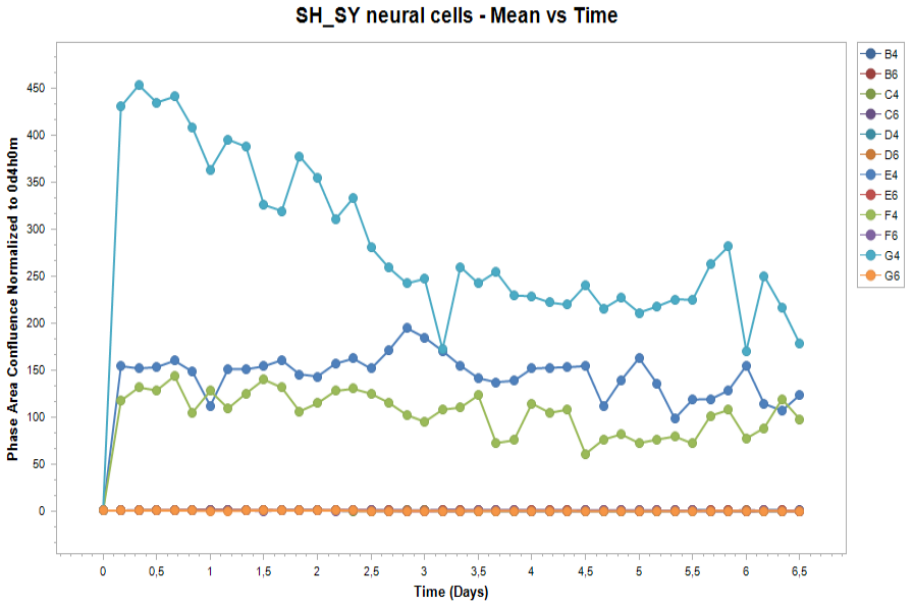

Figure 26. **SH-SY5Y cell differentiation in DMEM/F12 at different concentrations of retinoic acid (RA).** The different concentrations consisted of 1000 µM, 100 µM, 10 µM, 1 µM, 0.1 µM and 0.01 µM respectively. Cells were differentiated in duplicate. Shown is the confluence of the neuronal cells in function of time. For SH-SY5Y cells, confluence represents level of differentiation, since this cell type spreads out over a larger surface area when differentiated. D4: 10 µM; E4: 1 µM, F4: 0.1 µM.

Another important factor that was observed in the differentiation of SH-SY5Y cells, is cell density upon addition of the RA. The first attempt at differentiation failed due to a low cell count at seeding (50 000 cells/cm^2) (Fig. 27). SH-SY5Y cells grow and differentiate better when they experience cell-to-cell contact (Kovalevich & Langford, 2013). For this reason, the experiment was repeated with a higher cell count per well, as described below, and a much better differentiation was observed.

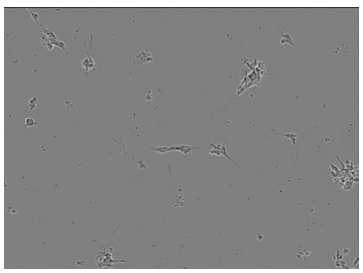

Figure 27. **Neuronal differentiation of SH-SY5Y cells**. Cells were cultured in DMEM/12 medium supplemented with retinoic acid for 7 days.

A monolayer of cells showing axon and dendritic-like protrusions can be observed after incubation with 10 µM RA for 5 days in DMEM/F12 medium (Fig. 28). In absence of RA, the SH-SY5Y cells still heavily form their undifferentiated cell clusters. The Neurobasal medium, even when supplemented with growth factors, seemed to fail to sustain SH-SY5Y cell differentiation. Indeed, analysis of the cell confluency shows that cells in the presence of DMEM/F12 with RA reach confluence in a shorter time span (Fig. 29). This represents the tendency of the differentiated cells to spread out instead of forming clusters, and matched the visual phenotype observed.

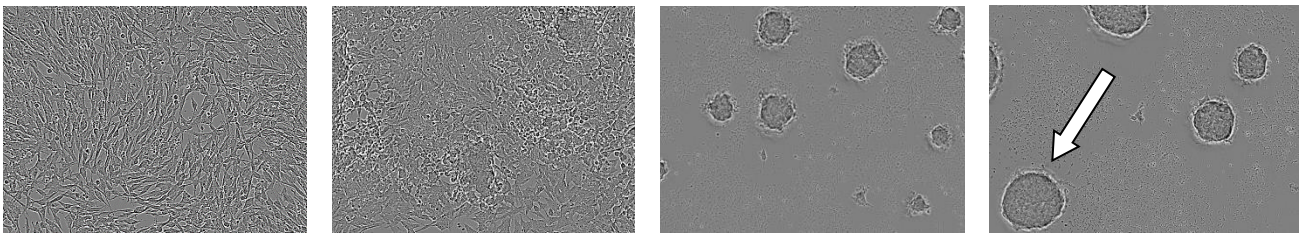

Figure 28. **Neuronal differentiation of SH-SY5Y cells in presence or absence of retinoic acid (RA) different media**. From left to right: SH-SY5Y cells cultured with DMEM/F12 + 10 µM (RA), DMEM/F12, Neurobasal medium + 10 µM RA, Neurobasal medium after 5 days. Undifferentiated cell clusters of SH-SY5Y cells are indicated by an arrow.

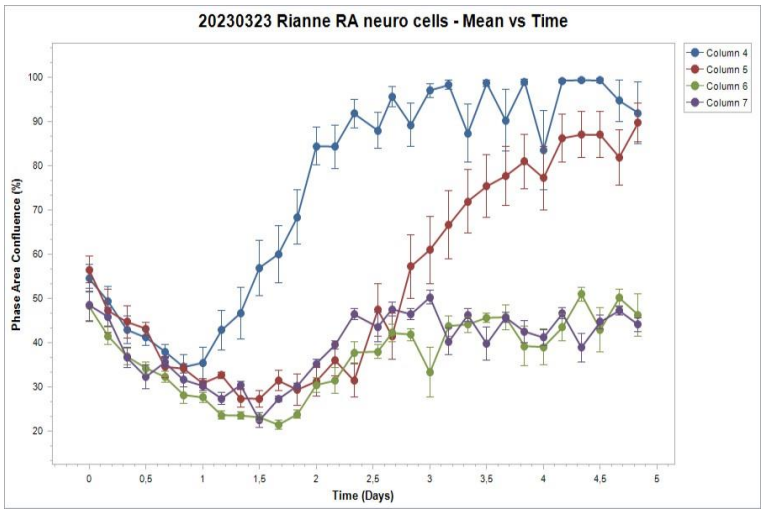

Figure 29. **Confluence graph of SH-SY5Y cells**. Cells were grown in DMEM/F12 medium supplemented with retinoic acid (Column 4), DMEM/F12 alone (Column 5), Neurobasal medium supplemented with retinoic acid (Column 6) and Neurobasal medium alone (Column 7). For SH-SY5Y cells, confluence represents level of differentiation, since this cell type spreads out over a larger surface area when differentiated.

To determine the optimal density of SH-SY5Y cells for HHV-7 infection, multiple concentrations (1.10^6/mL, 2.10^6/mL, 4.10^6/mL, 8.10^6/mL, 16.10^6/mL and 20.10^6/mL) were grown in a 24-well plate and differentiated with 10 µM RA. Based on visual evidence after 5 days, a density of 250 000 cells/cm^2 at seeding was decided as the optimal cell density (Fig. 30), as all other conditions resulted in cell cultures that were overgrown.

Figure 30. **Optimalisation of differentiation**. SH-SY5Y cells seeded at a density of 250 000 cells/cm^2 and differentiated with 10 µM RA after 5 days.

A parallel experiment was conducted after witnessing that the undifferentiated SH-SY5Y cells have the propensity to always have a fraction of the cell culture remaining present in the supernatant, instead of adhering to the flask. The SH-SY5Y cultures include both adherent and floating cells, both types of which are viable. Few studies address the biological significance of the adherent versus floating phenotypes, and their conclusions are inconsistent, as most reported studies only utilize adherent populations and discard the floating cells during media changes (Kovalevich & Langford, 2013). When the floating cells are transferred to a new flask, they do not adhere to the bottom, even after several days. This led to the hypothesis that non-adherend cells always tend to stay in the supernatant, while those that adhere, will always prefer to adhere. In literature, both types of SH-SY5Y cells (those adhered and those non-adhered) are used for differentiation. Undifferentiated, non-adherend SH-SY5Y cells were cultured with 10 µM RA, to see if they lose their preference for

staying non-adherend after differentiation. Indeed, the floating cells become entirely adherent and differentiated after 5 days (Fig. 31). In following experiments, both the adherent and non-adherent cells were used for differentiation.

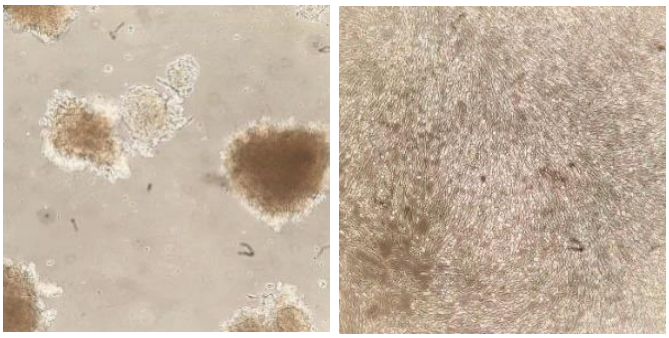

Figure 31. **Non-adherent SH-SY5Y cells after differentiation.** Pictured are SH-SY5Y cells without (left) or with (right) 10 µM retinoic acid. Despite their floating nature, cells showed complete adherence and differentiation in the presence of retinoic acid.

3.3.2. SH-SY5Y infection with HHV-7

Undifferentiated SH-SY5Y cells were inoculated with 0.5 mL undiluted HHV-7 virus stock containing $10^{5.05}$ $TCID_{50}$/mL. No phenotypic differences were observed 7 days after inoculation (Fig. 32). Cell pellets and supernatant were collected to determine the presence of the intracellular and extracellular viral presence and titer.

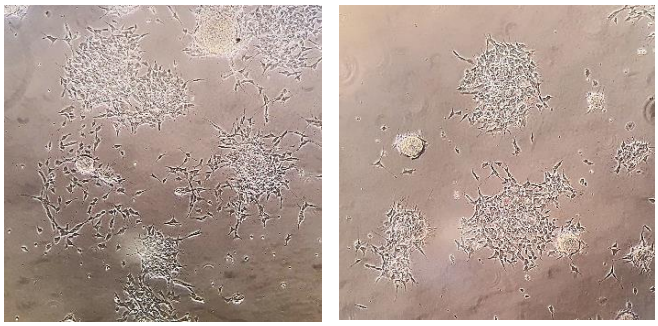

Figure 32. **HHV-7 on SH-SY5Y cells**. SH-SY5Y cells were inoculated with free HHV-7 (left) or treated as mock (no HHV-7) (right)

Since the qPCR could not be validated due to non-specific reactions, it was decided to check the viral titer in the cell pellets and supernatants of the inoculated SH-SY5Y cells with the use of a virus titration experiment. However, no CPE was observed in the SupT1 cells that were inoculated with the supernatant and intracellular content of the SH-SY5Y cells (Fig. 33). This might suggest that free HHV-7 virus is unable to infect undifferentiated SH-SY5Y cells.

The differentiated SH-SY5Y cells were then infected with free HHV-7 and HHV-7 infected SupT1 to see if differentiated SH-SY5Y showed a visible consequence of this infection, like for example the CPE observed in SupT1 cells. No CPE or any other visible sign of infection was observed (Fig. 33)

Figure 33. **Differentiated SH-SY5Y cells after addition of HHV-7 infected SupT1 cells and incubation for 7 days**. SH-SY5Y were differentiated using 10 µM retinoic acid.

3.3.3. *SH-SY5Y infection with mutated HHV-7*

To follow the viral entry and replication with the use of fluorophore-tagged HHV-7 virions, SH-SY5Y cells were seeded and differentiated. These cells were then, together with SupT1 cells, inoculated with either U32-mRFP1 infected SupT1s or free U32-mRFP1 mutant HHV-7, as obtained through plaque purification. Inoculation was performed by addition of either mutant HHV-7 infected SupT1 cells or free HHV-7 mutant virus. The infected SupT1 cells that were added, were tagged with FITC, to discern between old infected SupT1 cells and new infected SupT1 cells. DAPI was used to color the cell nuclei in order to obtain relative spatial information of the position of the fluorescent viral particle. Fluorescence was checked using confocal microscopy after 2 days, but no red fluorescent viral particles could be observed (Fig. 34).

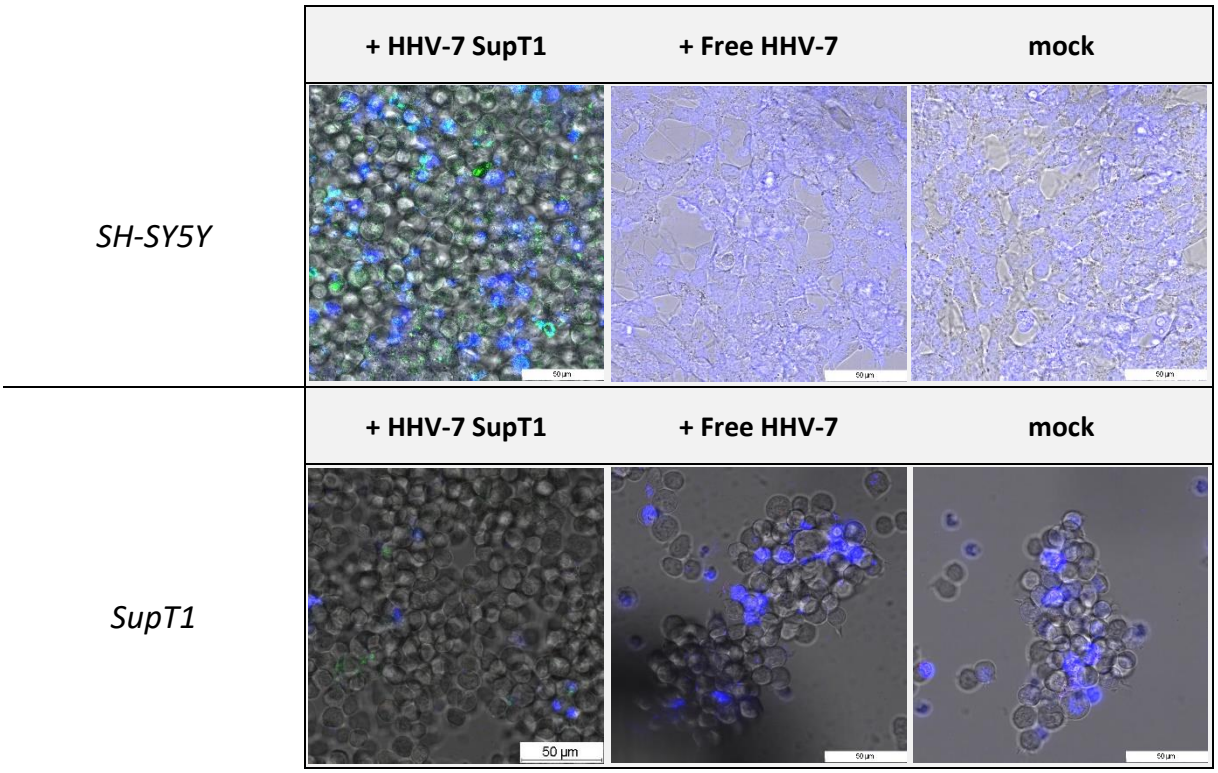

Figure 34. **SH-SY5Y and SupT1 cells inoculated with U32-mRFP1 mutant HHV-7 after 2 days**. HHV-7 was added to the respective cell types either through free virus (obtained by a freeze-thaw cycle) or though infected SupT1s. Infected SupT1s were stained with FITC (green) before addition and cell nuclei were colored with DAPI (blue)

3.4. CD4$^+$ cell infection

3.4.1. *Activated CD4$^+$ T cells*

Primary T cells were derived from buffy coats using MACS separation and activated via CD3- and CD28-binding by using T cell TransAct^{TM}. These activated CD4$^+$ T cells were then infected with free HHV-7. A phenotype similar to the CPE in SupT1 cells, was observed (Fig. 35).

Cell pellets and supernatant were collected after 7 days. A viral titration experiment was performed on to derive the presence of HHV-7 in the cell pellet (intracellular virus) and the supernatant (extracellular virus) of

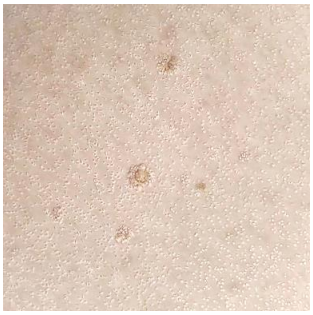

Figure 35. **Primary activated CD4$^+$T cells after infection with free HHV-7.** A cytopathic effect was observed, indicating infection and replication

activated CD4+ T cells by the CPE as observed in infected SupT1 cells (Fig. 36). CPE was observed in SupT1 cells that were infected with the CD4+ T cell content, as well as those infected with the CD4+ T cell supernatant. The titer for the intracellular virus was $10^{2.54}$ $TCID_{50}$/mL, while the titer for the extracellular virus was $10^{2.05}$ $TCID_{50}$/mL, thus indicating the potential for HHV-7 to replicate in primary activated CD4+ T cells.

3.4.2. Non-activated CD4+ T cells

Primary T cells were derived from buffy coats using MACS separation. Without the addition of TransAct™, resting CD4+ T cells were then infected with free HHV-7. A very low level of CPE - when compared to the activated CD4+ T cells - was observed after 7 days. A viral titration experiment was performed on SupT1 cells to derive the presence of HHV-7 in the cell pellet and the supernatant of non-activated CD4+ T cells by the CPE as observed in infected SupT1 cells. A CPE was observed in SupT1 cells that were infected with the CD4+ T cell intracellular virus, and in those infected with the extracellular virus (Fig. 36). Interestingly, a decrease in viral titer was observed between the intracellular virus and the extracellular virus in both the activated and non-activated CD4+ T cells. This effect was outspoken in the non-activated CD4+ T cells, where the titer of the extracellular virus was 32-fold lower. This might indicate a block in viral replication in stages such as assembly or release of HHV-7 progeny in non-activated CD4+ T cells.

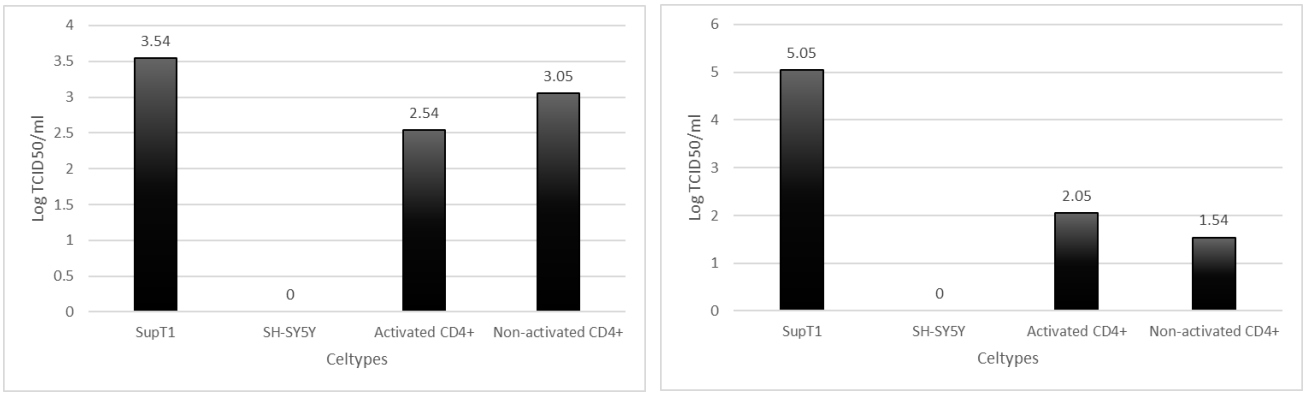

Figure 36. **Titers of HHV-7 in SupT1 cells after replication in different cell types.** SupT1 cells, SH-SY5Y cells, and primary activated and non-activated CD4+ T cells were inoculated with HHV-7, and the supernatant and pellet of those cells was collected after 7 days. SupT1 cells were subsequently inoculated with either the contents of the pellet (left) or the supernatant (right), and the titer of HHV-7 present in those samples was derived from the occurrence of a cytopathic effect.

3.5. Inoculation of different cell types with HHV-7: a time- course experiment

To explore and compare the infection and replication capacity of HHV-7 in different cell types, a time-course experiment was set up where different cell types, being the differentiated SH-SY5Y neuronal cells line, the SupT1 cell line and primary activated and non-activated CD4+ T cells, were inoculated with free HHV-7 particles. Cells were monitored visually for 7 days to track CPE (Fig. 37). In addition, cell supernatant and cell pellets were harvested at different time points (1 day, 2 days, 4 days, and 7 days post inoculation) and titrated onto SupT1 cells.

The infection and replication of HHV-7 in certain cells could be seen with the occurrence of the CPE. For the SupT1 cells, as well as the activated CD4+ T cells, CPE was observed after 4 days. This

indicated the presence of replication competent virus in these cell types. Interestingly, a massive amount of cell death was observed in SupT1 cells after 7 days, while the amount of CPE stayed approximately the same in the activated $CD4^+$ T cells.

In the non-activated $CD4^+$ T cells, CPE was observed after 7 days, thus indicating the potential of HHV-7 to infect and replicate in non-activated $CD4^+$ T cells. However, the rate of infection and replication seemed lower when compared to the activated $CD4^+$ T cells. In the SH-SY5Y cells, no phenotypic difference was observed at the different time points.

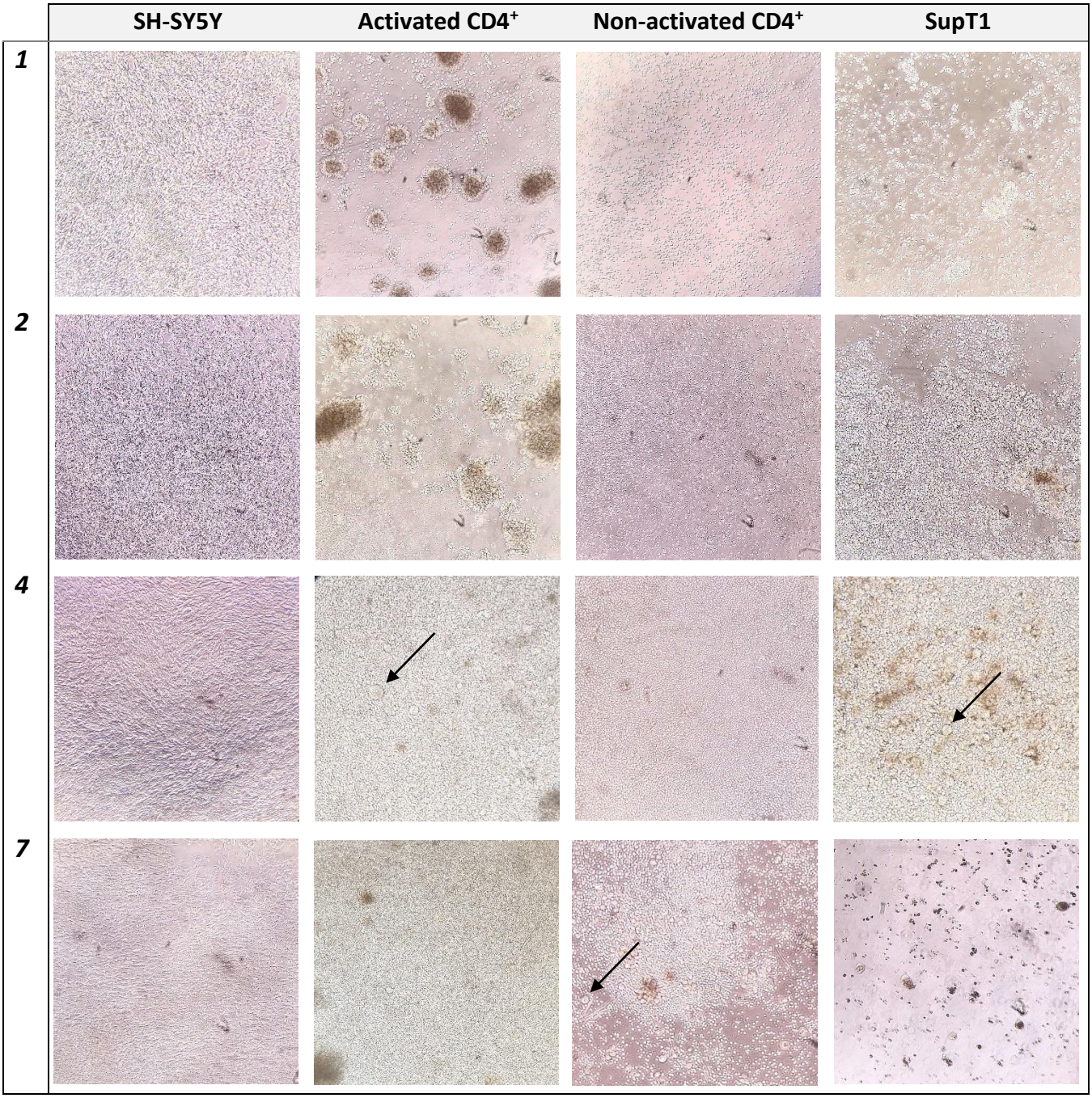

Figure 37. **SH-SY5Y cells, SupT1 cells, and primary activated and non-activated $CD4^+$ T cells after inoculation with HHV-7**. Cells were inoculated with HHV-7 and followed up over 4 timepoints (1 day, 2 days, 4 days, and 7 days). CPE (marked with an arrow) occurred in SupT1 cells and primary activated $CD4^+$ T cells after 4 days, while CPE occurred in non-activated $CD4^+$ T cells after 7 days. No phenotypic difference was observed in the differentiated SH-SY5Y cells after inoculation.

Supernatant and cell pellets were collected from the inoculated cells at different time points. These pellets and supernatant were then titered on SupT1 cells and $TCID_{50}$/mL was calculated according to the observed CPE (Fig. 38). Based on this growth curve, the titer of HHV-7 was seen to double in SupT1 cells in 1.75 days when in the exponential phase.

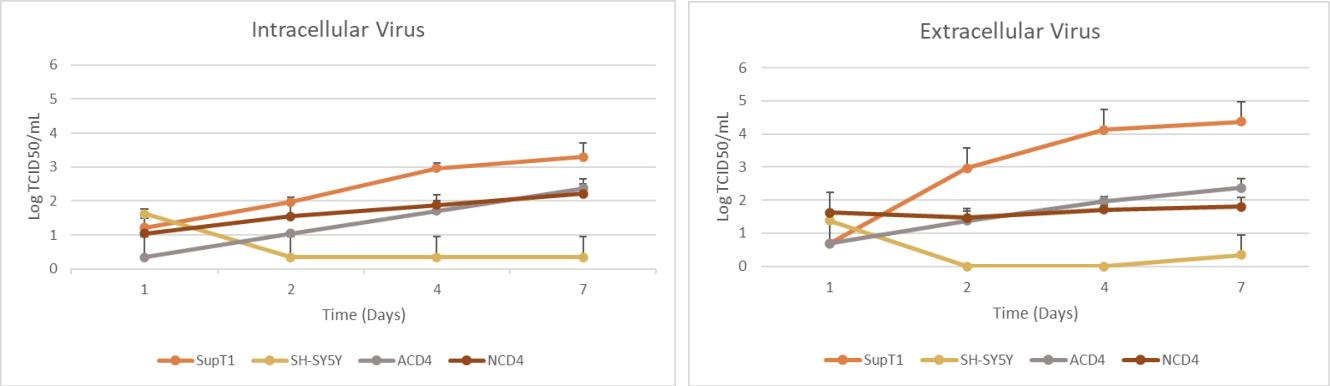

Figure 38. **Growth curve of intracellular and extracellular virus in SupT1 cells, activated $CD4^+$ (ACD4) and non-activated $CD4^+$ (NCD4) and SH-SY5Y cells after inoculation with free HHV-7.** Titer is expressed as log TCID50/mL and represents the dilution of a virus required to infect 50% of a given cell culture.

The titers for the intracellular virus were compared using the Kruskal-Wallis test for independent samples for each cell type per time point. There was a significant difference between the titers of the cells at all timepoints (p=0.035; p=0.036; p=0.020; p=0.020). Upon closer inspection, the significant difference was between the SupT1 cells and the SH-SY5Y cell line (p=0.025; p=0.038; p=0.011; p=0.011). There was no statistical difference between the other cell types.

The titers for the extracellular virus were compared in the same way as the intracellular virus. The titers for the extracellular virus were compared in the same way as the intracellular virus. There was a significant difference between the titers of the cells at all timepoints (p=0.045; p=0.021; p=0.016; p=0.014). After 1 day, there was a trend in difference in the comparison of the non-activated $CD4^+$ cells and the activated $CD4^+$ cells (p=0.116) and SupT1 cells (p=0.116) respectively. At the other time points, the statistical difference occurred between the SupT1 cells and the SH-SY5Y cells (p=0.011; p=0.011; p=0.011). There was no statistical difference in the other cell comparisons at any other time point.

3.6. Inoculation with HHV-7 through cell-cell contact: a time-course experiment

After witnessing a difference in infection efficiency of HEK293T cells when using HHV-7 infected SupT1 cells, a hypothesis was formed that HHV-7 can only directly infect cells expressing certain proteins (like $CD4^+$ T cells) and indirectly infect cells that do not express those proteins through cell-cell contact. To test this hypothesis, a time-experiment similar to 3.5.1 was set up, in which HEK293T cells and differentiated SH-SY5Y cells were inoculated with either HHV7-infected SupT1 cells (TCID50/mL of $10^{5.05}$) or free virus particles (TCID50/mL of $10^{5.05}$) (Fig. 39). Simultaneously, SupT1 cells were infected with HHV-7 (TCID50/mL of $10^{5.05}$) and used as a control for HHV-7 replication after 7 days. At three different time points (day 1, day 2 and day 7), the cell pellets and supernatants were harvested and subjected to a titration experiment to determine the presence of intracellular and extracellular HHV-7 in the different cell types.

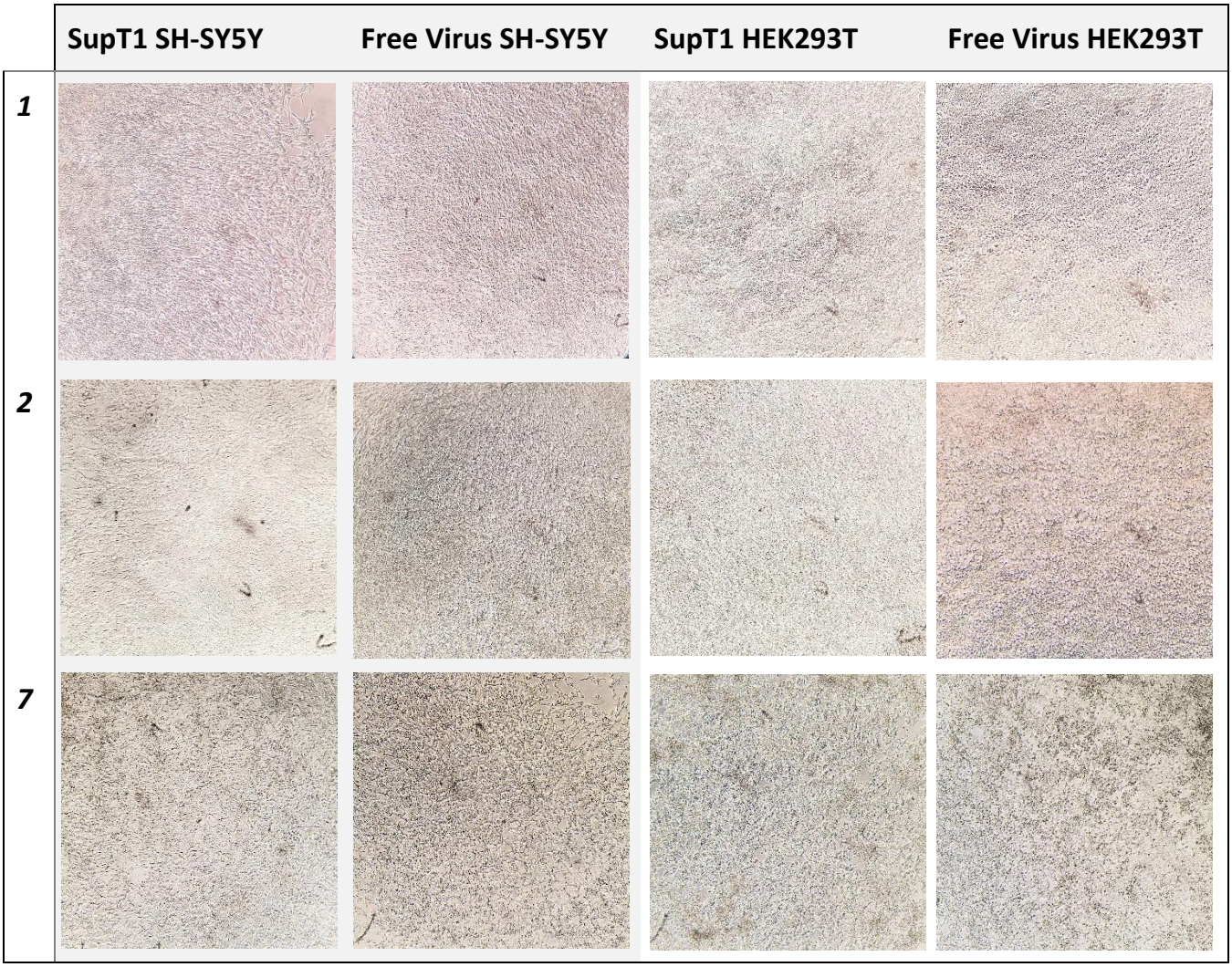

Figure 39. **SH-SY5Y cells and HEK293T cells after inoculation with either free HHV-7 or HHV-7 infected SupT1 cells**. Cells were inoculated with HHV-7 and followed up over 4 timepoints (1 day, 2 days, 4 days, and 7 days).

No clear formation of a CPE was observed in either the HEK293T cells or the SH-SY5Y cells. However, the HEK293T cells had a higher tendency to detach from the well, as opposed to the HEK293T cells that were not inoculated with HHV-7 (Fig. 40). This might be a response to infection that would be interesting to investigate further.

Figure 40**. HEK293T cells after a week without HHV-7 inoculation.** Cells were seeded simultaneously with HEK293T cells in fig. 28. and incubated for a week.

Supernatant and cell pellets were collected from the inoculated cells at different time points. These pellets and supernatant were then titered on SupT1 cells and $TCID_{50}$/mL was calculated according to the observed CPE (Fig. 41). Since the SupT1s were co-incubated with the SH-SY5Y and HEK293T cells during the course of the experiment, a well with only infected SupT1 cells was incubated for 7 days as internal control. If HHV-7 propagates on fresh HEK293T or SH-SY5Y cells following transfer infection from infected SupT1 cells, a higher titer was expected in those wells when compared to wells with the infected SupT1 cells alone. Titration of the supernatant of infected SupT1 cells after 7 days was performed. There seemed to be a gradual decrease in titer of intracellular and extracellular virus in both the SupT1 inoculated and free virus inoculated

conditions in both cell types. The SupT1 cells had a $TCID_{50}$/mL of $10^{5.05}$ after 7 days, which is in comparison much higher than those for the extracellular virus on the HEK293T cells ($TCID_{50}$/mL of $10^{2.63}$) and the SH-SY5Y cells ($TCID_{50}$/mL of $10^{1.63}$).

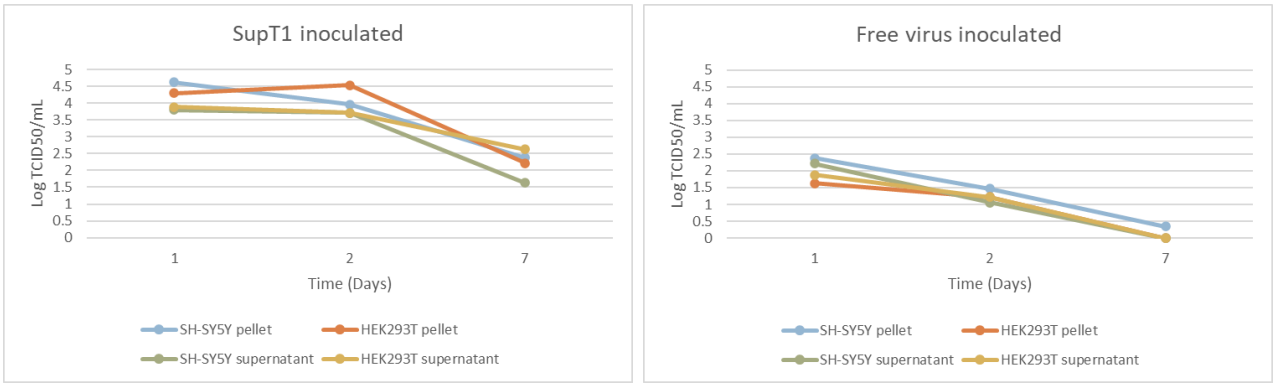

Figure 41. **Growth curve of intracellular (pellet) and extracellular (supernatant) virus in HEK293T and SH-SY5Y cells after inoculation with either HHV-7 infected SUpT1 cells or free HHV-7.** Titer is expressed as log TCID50/mL and represents the dilution of a virus required to infect 50% of a given cell culture.

For the intracellular virus of the SupT1 inoculated cells, a trend was observed in the difference between the titer in the HEK293T cells and SH-SY5Y cells after 1 day (p=0.096). After 2 days, a significant difference in titer was observed (p=0.024). After 7 days, no significant difference in titer was observed. For the extracellular virus of the SupT1 inoculated cells, only a significant difference in titer was observed between the cell types on day 7 (p=0.043).

For the intracellular virus of the free virus inoculated cells, only a significant difference in titer was observed between the cell types on day 7 (p=0.043). For the extracellular virus of the free virus inoculated cells, no significant difference in titer was observed between the cell types.

Part 4: Discussion

Since its discovery in 1990, the Human Herpesvirus type 7 (HHV-7) has been associated with multiple cases of a variety of illnesses, including roseola infantum, pityriasis rosea, Guillain-Barré syndrome and encephalitis. However, despite its association with these diseases and ubiquitous nature, with over 95% of adults having been infected with HHV-7, little is known about its processes of infection and replication. In this study, we attempted to uncover the infective and replicative potential of HHV-7 in different cell types, more specifically in neuron-derived cells, in order to explore the neuro-invasive potential of HHV-7.

4.1. Free HHV-7 is able to infect and replicate in SupT1 cells, HEK293T cells, activated and non- activated primary $CD4^+$ T cells, but not SH-SY5Y cells

A known cell type susceptible to HHV-7 infection, is the SupT1 cell line. These cells contain the $CD4^+$ surface marker that HHV-7 uses for its entry in cells (Lusso *et al*, 1994). After infection and replication, SupT1 cells undergo a form of apoptosis, called ballooning degeneration or the cytopathic effect (CPE). This phenomenon indicates the presence of replication competent HHV-7.

To optimize the production of HHV-7 stock, different protocols were used for the infection of SupT1 cells, and the efficacy was determined through titration on SupT1 cells. It was observed that the process of spinoculation, where the virus and the cells are centrifuged together to aid viral binding to the target cells, did not improve the infection and replication of HHV-7 in SupT1 cells in the analyzed conditions. Free HHV-7 can thus easily bind SupT1 cells in its vicinity and has a high infectious potential for this specific cell line. Spinoculation influences the amount of viral particles in the vicinity of a cell, as well as the cellular cytoskeleton, which in turn promotes receptor mobilization, viral entry, and post-entry processes (Guo *et al*, 2011), and is often used to increase infection of cells by lentiviruses, including HIV (O'Doherty *et al*, 2000). By comparing the respective titers, it was concluded that these cellular changes are unnecessary for an efficient infection of SupT1 cells by HHV-7.

In subsequent experiments, when cell cultures such as the SH-SY5Y cell line and the HEK293T cell line were inoculated with HHV-7 infected SupT1 cells, there did seem to be an improvement in infection with the use of spinoculation. In those co-cultures, spinoculation concentrates the HHV-7-infected SupT1 cells onto the surface of adherent cell cultures. However, this effect needs to be compared and quantified accurately in future experiments. Remarkably, for the production of fluorophore-tagged HHV-7 mutants, infection of the HEK293T cell line seemed to improve 6-fold with the use of infected SupT1 cells, as opposed to solely using free HHV-7 particles. The combination of this observation with the improved efficiency with spinoculation, lead to the hypothesis that HHV-7 infects certain cell types through cell-cell contact.

We tried to confirm this hypothesis by performing an experiment where HEK293T cells and SH-SY5Y cells were inoculated with either infected SupT1 cells or free HHV-7 virus. In the infection of HEK293T cells and SH-SY5Y with free HHV-7, no replicative viral particles were observed after 7 days. Whether HEK293T cells and SH-SY5Y cells can be infected with HHV-7 through cell-cell contact with infected SupT1 cells, remains contested, since there is possibility that the observed titer is the

result of remaining infected SupT1 cells. However, we can conclude that there was a decrease in HHV-7 replication in both cell times, since the viral titer decreased in both conditions, especially when compared to the titer in SupT1 cells. This might be due to a lack of infection or a lack of replication in these particular cell types. It is known that HHV-7 establishes latency in both replicating and non-replicating cells. It is thus possible that HHV-7 establishes latency in HEK293T cells and SH-SY5Y cells, which explains the lack of infectious viral particles as quantified by the titration experiment. Another explanation might be disruptions in viral entry. HEK293T cells endogenously express HSPGs receptors, which are used by HHV-7 during entry of epithelial cells (Dela Paz *et al*, 2014). However, it is entirely possible that the expression of these receptors is diminished due to the cell line used, experimental condition, and passage number. This could explain a decrease in viral entry when free virus is used. To investigate whether the decrease in titer was due to an inability of the virus to enter the cell, our mutant HHV-7 fluorescent viral particles could be used to track entry. If entry is confirmed, a qPCR might then be helpful to discern the presence of intracellular viral DNA. Both of these techniques would still have to be optimized for HHV-7 before any conclusion can be made.

In primary $CD4^+$ T cells, a similar phenotype as the SupT1 cell line was observed after inoculation with HHV-7. It is important to note, however, that the occurrence of CPE happened earlier and at higher levels in primary $CD4^+$ T cells that were activated, as opposed to non-activated primary $CD4^+$ T cells. After activation, T cells undergo clonal expansion and differentiation. It is perhaps this clonal expansion and/or differentiation that increases HHV-7 infection and replication. Activated $CD4^+$ T cells have a higher capacity of endocytosis (Charpentier & King, 2021). However, no endocytic pathway has been described for HHV-7 yet (Tognarelli *et al*, 2021). HHV-7 possesses a protein, U24, that downregulates the T cell receptor complex and endocytic recycling after infection, suppressing activation of $CD4^+$ T cells (Sullivan & Coscoy, 2010). This might be because HHV-7 prefers to establish a latent infection and a high amount of replication, as represented by CPE, may activate the immune system. This could explain why less CPE was observed in non-activated $CD4^+$ T cells, since these cells would be perfect for establishing a latent infection.

When comparing the extracellular virus to the intracellular virus of non-activated primary $CD4^+$ T cells, the low levels of extracellular virus compared to the intracellular virus could indicate that HHV-7 has the potential to infect non-activated primary $CD4^+$ T cells, but is less able to replicate, assemble, and/or release new virions in this cell type. This could be investigated further using the U32 fluorescent mutants, since the fluorescent capsid protein could then be followed intracellularly through the life cycle of the virus.

A trend was observed in the difference between the intracellular and extracellular virus coming from SupT1 cells and activated $CD4^+$ T cells. This might be due to the limited growth of the activated $CD4^+$ T cells compared to the SupT1 cells. There are, however, other possible explanations, such as the expression of certain proteins. SupT1 cells do not express viperin. Viperin is an interferon-stimulated gene that has broad antiviral activity against both RNA and DNA viruses including some herpesviruses, flaviviruses, retroviruses, orthomyxoviruses, paramyxoviruses, togaviruses, and rhabdoviruses (Payne, 2017). Viperin is expressed by activated $CD4^+$ T cells, where it inhibits the release of some viruses but may also have other means of inhibiting virus replication. But CMV induces viperin expression to enhance viral infectivity (Chin & Cresswell, 2001), a characteristic that HHV-7 might share, which would explain its potential to infect and replicate in activated $CD4^+$ T cells. A similar protein is tetherin, which is known to block many different types of enveloped viruses by tethering the budding virus like particles and inhibiting them from leaving the cell surface

(Le Tortorec *et al*, 2011). Tetherin has been known to inhibit HSV-1 and HHV-8, which in response encode proteins that antagonize tetherin (Giese *et al*, 2016). It is possible that HHV-7 also encodes similar tetherine-antagonizing proteins, which might be interesting for future research regarding the release of HHV-7 virions.

In the process of the production of fluorophore-tagged HHV-7 viral particles, Cas9 and sgRNA expressing HEK293T cells were used. Since the production of fluorescent viral particles was successful, it can be concluded that HHV-7 has the capacity to infect the HEK293T cell line, albeit more effectively through the use of infected SupT1 cells. This also indicates that HHV-7 can replicate in other cell types, like for example embryonic kidney cells. The presence of HHV-7 in kidney cells could explain its association with CMV disease, as well as perhaps the increase in HHV-7 viral replication, in renal transplant patients (Tong *et al*, 2000; Raposo *et al*, 2020a).

It was also observed during the mutant production, that fluorescent particles showed a connection between neighboring HEK293T cells. Cell-to-cell spread is typical for herpesviruses (ἕρπειν (herpein) 'to creep'). HSV-1 uses cell-to-cell spread to move from the primary site of infection, often mucosal epithelial cells, right into the adjacent sensory neurons, where it creates a latent infection (Carmichael *et al*, 2018). This cell contact could be a way for the mutant viral particles to spread and infect other cells, thus backing up the argument of cell-cell contact being important in the spread of HHV-7 to other cells and an interesting mechanism to explore in future experiments.

4.2. Fluorescent mutant production: obstacles, alternatives, and solutions

During the production of fluorescent HHV-7 mutants, we first used a protocol that was also utilized for the production of fluorophore-tagged CMV particles (King & Munger, 2019). Our initial reasoning for this was the longer replication cycle for beta-herpesviruses compared to alpha-herpesviruses. Since CMV is, like HHV-7, a beta-herpesvirus, we expected the same protocol to work just as efficiently. However, following the same protocol as used for the PRV, an alpha-herpesvirus, yielded a much higher amount of fluorescent viral particles (Cleemput *et al*, 2021). The main difference between the two protocols is the order in which the cells are transfected and infected, being first transfected with the *mRFP1* donor plasmid and subsequently infected with HHV-7 in the CMV protocol, and vice versa in the PRV protocol. The lower yield of HHV-7 with the CMV protocol can be explained by the presence of Cas9, which cleaves the genomic material of the incoming virus and thus rendering it unable to replicate, something that did not seem to happen in the study regarding CMV. In another study regarding fluorophore-tagged CMV, the cells were first infected and only transfected 2 days later (Sampaio *et al*, 2005). However, it should be noted that this study did not use the CRISPR/Cas9 methodology. Nevertheless, it is interesting to observe that fluorophore-tagged CMV can be produced both ways, while this has not been explored yet in HHV-7. This information could help in understanding more about the replication cycle of HHV-7 and the differences with CMV.

In the production of the mutant HHV-7 viruses, we observed a remarkable loss of fluorescence. This might be because of several reasons, some intrinsic to the HHV-7 itself. Either the HEK293T cell type used does not stimulate HHV-7 replication or the method of HEK293T HHV-7 inoculation results in a decrease in viral entry. Another explanation might be that replication in HEK293T switches the cell tropism of HHV-7, making it less inclined to subsequently replicate in SupT1 cells

or other HEK293T cells. Indeed, a family member of HHV-7, the EBV, switches cell tropism based on its host cell of origin (Borza & Hutt-Fletcher, 2002). It might also be the above-mentioned preference for latency that potentially decreases viral replication in HEK293T cells, leading to a decrease in mutant production and plaque formation. This might be solved with the use of other cell type for the propagation of HHV-7 mutants. In previous research, SupT1 cells were ruled out for HHV-7 mutant production. HHV-7 has been shown to replicate in different cell lines, like for example the Jurkat T lymphocyte cell line or the U937 monocyte cell line-derived, when these have been transduced to express high levels of $CD4^+$. Another alternative is the monocytic THP-1 cell line, which endogenously expressed CD4. The THP-1 cell culture has already been used to study human CMV, HHV-6 and HHV-8 infection (Sanchez *et al*, 2012; LI *et al*, 2003; Kerur *et al*, 2010). One study, however, claims that THP-1 were not infected with HHV-7 (Zhang *et al*, 2001), but due to the close homology of HHV-7 to HHV-6, HHV-8 and CMV, it might be worth reevaluating this infection potential. If THP-1 is proven to be permissive for HHV-7 infection, this can be exploited in the production of fluorophore-tagged HHV-7 mutants.

When SupT1 cells co-cultured with the HHV-7 mutant producing HEK293T cells were separated from the HEK293T culture, they retained fluorescence for several days. Oftentimes, cells exhibiting fluorescence, also showed CPE. However, this CPE was phenotypically different from CPE observed in HHV-7 infected SupT1 cells, as it only involved the swelling of one cell and no syncytia were formed. In the meantime, the “normal” form of CPE occurred in the same culture of SupT1 cells, but these ballooning cells did not show any fluorescence. The spread of fluorescence to other SupT1 cells in the culture was also limited. This complicated the propagation of mutant HHV-7 in SupT1 cells. A possible solution could be the use of fluorescence-activated cell sorting to sort out the fluorescent cells and obtain a pure culture of mutant virus that way. These cells could then be used to inoculate SupT1s or other cell types with mutant HHV-7 infected SupT1 cells or free mutant HHV-7 obtained after a freeze-thaw cycle. It might be possible that the attachment of mRFP1 to the capsid or tegument protein renders the virus incapable of efficiently spreading. This could be further investigated after inoculation with these mutants using confocal microscopy at a high magnification.

To investigate the infectious potential of HHV-7 in a more quantifiable manner, we would like to optimize our qPCR. In order to do this, we will create a matrix of reactions for different primer pairs at different concentrations. We will simultaneously test different annealing temperatures, as well as consider the use of probes to increase the specificity. Since the primers we designed gave off-target effects even though they were validated using a sequence alignment tool, primers will likely have to be tested experimentally for off-target effects in the cell types we are interested in using. In cell types shown to have little replication of HHV-7, we will determine the limit of detection of the qPCR by using high amounts of cell material and preparing serial dilutions of the target DNA. In this way, we can look for the intracellular presence of HHV-7 in the case that the fluorescent mutant production has not been able to provide us with that information.

4.3. The future of HHV-7 and its potential in medicine

In future research, we would like to extend our study to include primary neurons, other brain-derived cell lines, and perhaps even organoids, in order to further investigate the neuro-invasive potential of HHV-7 in humans. Not only neurons could be investigated this way, but also glial cells.

To explore the associations with CNS diseases, HHV-7 infection and replication could be further explored in glial cells such as astrocytes, oligodendrocytes, and ependymal cells. Furthermore, the infection of neuronal cells in the peripheral nervous system (PNS) by HHV-7 could be further explored to discern the mechanisms of primary infection, as well as latency in neurons, Schwann cells, and satellite cells. Understanding the infection pathway in the PNS could explain how the infection spreads to the CNS and can cause diseases in immunocompromised patients. Combining this research into the neuro-invasive potential of HHV-7 with its potential to infect and affect immune cells, could also help to resolve the additional dangers that occur with a late primary infection, as opposed to a primary infection early in childhood.

The different fluorescently labelled proteins could uncover more about the life cycle of HHV-7 and its potential to infect, replicate, and assemble in different cell types. As mentioned, the U32 capsid mutant could indicate the occurrence of viral assembly and the release of new virions. HHV-7 is described as a latent virus in multiple cell types, and a good working qPCR could confirm this latency and expand on the cell types and conditions in which this latency occurs. The U32-mRFP1 mutant could also decipher the process of viral penetration into the host's nucleus, since herpesviruses usually dock their capsid on the nucleopore complex and release the genomic material into the nucleus from there. The U31 and U14 mutants could tell us more about the structure of the virion, as well as the process of uncoating and releasing of the capsid. Neurotropic viruses that enter via axons may have to move in retrograde direction over the full length of axons, which can be over a meter in length, to reach the nucleus. This could be visualized perfectly over time using these fluorophore-tagged mutants.

Animal models, such as mice, can be used to study the neuro-invasive potential of HHV-7 in a more complex biological system. Intranasal or intracranial inoculation can be performed to mimic natural routes of viral entry into the CNS. Behavioral testing, histopathological analysis, and viral load quantification in the brain and other neural tissues can provide valuable information about the virus's ability to invade the nervous system and induce neurological symptoms. When this inoculation is done with our fluorescent HHV-7, blood can be drawn to look for the presence of viral particles with the use of flow cytometry or microscopy. Tissues can also be taken from the brain to investigate the invasive potential of HHV-7. As an alternative, our mutants can be modified to contain luciferase, in which bioluminescence can provide a full-body overview of the distribution of HHV7. Unfortunately, in vivo studies are complicated by the fact that HHV-7 is a human-specific virus and is not known to naturally infect or cause disease in animals or other non-human species. But there are solutions and alternatives to further explore HHV-7 pathogenesis in animal models. Firstly, a mouse model already exists that mimics HHV-6B pathogenesis, and this model is based on humanized mice in which human immune cells were engrafted and maintained (Wang *et al*, 2020). Secondly, there exists a murine roseolovirus, which is a betaherpesvirus more closely related to the roseoloviruses, HHV-6A, HHV-6B, and HHV-7, than to another murine betaherpesvirus, mouse cytomegalovirus (MCMV) (Patel *et al*, 2017). Given the high degree of homology in both genome sequence and physiological effects, this MRV might be an interesting substitute to explore immune effects in mice and extrapolate them to humans. Another such virus that closely resembles HHV-7, is the pigtailed macaque roseolovirus, or *Macaca nemestrina* herpesvirus 7 (MneHV7). Detailed genomic analysis has revealed the presence of gene homologs to all 84 known HHV-7 open reading frames, and phylogenetic analysis confirmed that MneHV7 is a macaque homolog of HHV-7 (Staheli *et al*, 2016). This homologue could also be used in further research regarding HHV-7. Even though there are many differences between animal models and humans, it is undeniable that an animal

model mimics the complex interplay between the different cell types that are susceptible to HHV-7 infection, like the interplay between T cells and neurons or glial cells and neurons, which cannot be accurately replicated *in vitro*. These models could aid in assessing the immune response and inflammatory processes triggered by HHV-7 in the CNS with the use of cytokine and chemokine profiles, immune cell infiltration, and activation markers in infected brain tissues or cerebrospinal fluid.

Furthermore, the creation method of these fluorescent mutants could be adapted to create other HHV-7 mutants using CRISPR-Cas9. These mutants could carry proteins attached to a cleavable linker instead of mRFP1. This could turn HHV-7 into a vector that could carry proteins or other encapsulated molecules to specific target cells, like $CD4^+$ T cells or neurons. These vectors could play important roles in the fight against certain $CD4^+$ T cell related autoimmune diseases like inflammatory bowel diseases, systemic lupus erythematosus, and rheumatoid arthritis.

These vectors could also aid in delivering drugs to neurons in patients suffering from neuropathologies like Alzheimer's disease. An example is Aducanumab, an antibody a that breaks down the amyloid plaques. Currently, it is administered intravenously via a 45- to 60-minute infusion every 4 weeks. However, a specific vector encapsulating a drug like this, could result in a higher efficiency of delivery to the right target cells, as well as an increase in half-life.

We have only recently begun to understand the significance of memory helper T cells in the development of vaccines. Many more recent vaccinations and vaccines under development are frequently created to stimulate T cell responses that may aid the antibody response, serve as direct effectors themselves, or stimulate innate effector cells like neutrophils and macrophages. Some of those vaccines include conjugate vaccines, recombinant antigens with adjuvants, viruses that encode recombinant antigens, nucleic acids, nanoparticles, and virus-like particles. Since HHV-7 infects $CD4^+$ T cells, this cell tropism could be exploited to obtain the wanted T helper cell response in a given vaccine. This could be done by delivery of certain antigens or adjuvants to these cells.

There are some caveats to the use of HHV-7 vectors, however. The existence of an immunity against these viruses in most people is very likely, since it has a seroprevalence of 95% in the population. This could be remedied by making some alterations to certain antigens on the surface of the virus, but this has to be extensively researched and evaluated. Furthermore, since HHV-7 has the potential of infecting multiple cell types, the vector has to be adapted to only infect one cell type, which would take more research into its surface proteins and mechanisms of infection. If the vector is not adapted to its target cell type, it has to be made sure that the drug delivered does not cause negative off-target side-effects. It also has to be made sure that the HHV-7 virus is made replication-incompetent when used as a vector, to avoid cell death and undesired side-effects.

Alternatively, the broad cell tropism could prove useful in diseases that affect multiple cell types, like HIV infection. There is an overlap in cell tropism between HIV and HHV-7, which could be exploited in the fight against AIDS.

If, however, the use of HHV-7 derived vectors is deemed unfit for the clinic, it might still prove a useful vector in the transduction of multiple cell types, including the commonly used Supt1 cell line.

Part 5: Materials and Methods

5.1. Cells

SupT1 cells (CRL-1942; ATCC, Manassas, VA, USA) were used to produce and titer HHV-7. The cells were maintained in RPMI-1640 medium supplemented with 10% fetal bovine serum (FBS) and 1% antibiotics (penicillin/streptomycin) at 37°C.

HEK293T cells (CRL-3216; ATCC, Manassas, VA, USA) were used to produce the LentiCRISPR v2 lentiviruses and produce HHV-7 mutants. These cells were maintained in Dulbecco's modified Eagle medium (DMEM) supplemented with 10% fetal bovine serum (FBS) and 1% antibiotics (penicillin/streptomycin) at 37°C.

Primary CD4$^+$ T cells were isolated from buffy coats obtained through the Red Cross using peripheral blood mononuclear cell isolation followed by positive selection using magnetic-activated cell sorting (MACS) separation. The cells were maintained in TexMACS Medium supplemented with 5% human serum, 20 ng/mL IL2, and 1% antibiotics (penicillin/streptomycin) at 37°C. Primary CD4$^+$ T cells were activated using TransAct^{TM} (Miltenyi Biotec). T Cell TransAct^{TM} consists of a colloidal polymeric nanomatrix conjugated to humanized CD3 and CD28 agonists providing primary and co-stimulatory signals for an optimized and efficient T cell activation and expansion.

Using magnetic nanoparticles coated with antibodies against a specific surface antigen, the MACS technique can separate cells (Fig. 42). The magnetic nanoparticles attach to the cells that are expressing the antigen of interest. Once the beads and cells have been incubated, the solution is then transferred to a column in a high magnetic field. In this step, cells that are linked to the nanoparticles and that are express the antigen stay on the column whereas cells that are not expressing antigen pass through. The cells can be sorted either positively or negatively, according to their specific antigen(s). This technique was invented and patented by Miltenyi Biotec (EP1207961B1).

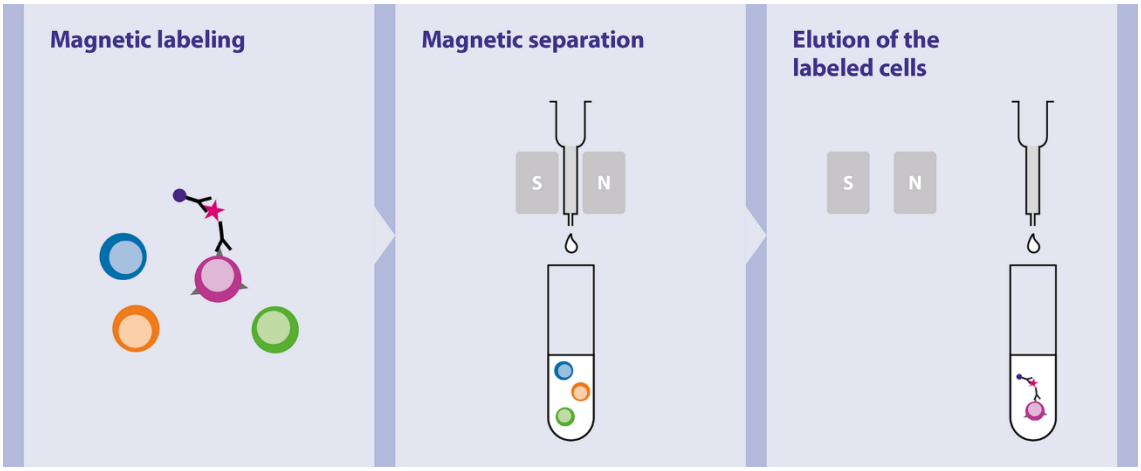

Figure 42. **The process of MACS separation**. Figure provided by Miltenyi Biotec; all rights reserved.

The neuronal cell line **SH-SY5Y** (CRL-2266; ATCC) used in this research was maintained in DMEM /F12 supplemented with 10% fetal bovine serum (FBS) and 1% antibiotics (penicillin/streptomycin) at 37°C. Cells were initially differentiated using 10 µM retinoic acid (Thermo Scientific Chemicals) in both Neurobasal medium as well as DMEM/F12, after which DMEM/F12 was chosen for maintaining and differentiating cells in further experiments.

5.2. Virus

The human herpesvirus type 7 Ji strain was derived from the NIH HIV Reagent Program, Division of AIDS, NIAID (NIH: Human Herpesvirus 7 (HHV-7) Ji-infected Sup-T1 Cells, ARP-12184, contributed by Dr. Dharam Ablashi, HHV-6 Foundation)(Ablashi *et al*, 1995). HHV-7 was propagated in SupT1 cells.

5.3. Plasmids

Donor plasmids were constructed using the HiFi DNA assembly method (NEB). All donor plasmids consisted of a pcDNA3-mRFP1 backbone (gift from Doug Golenbock; Addgene plasmid number 13032). The gBlock contained part of the respective viral gene we wanted to mutate fused to a fluorophore and flanked by homology arms that match viral genes upstream and downstream of the targeted region. A protein linker was attached if the viral protein precedes mRFP, but not if it was located downstream of mRFP, as the C-terminus of mRFP1 could function as a linker. The mutants were modified so the necessary STOP- or START-codons were removed. The PAM sequence was also mutated to avoid cleavage of mutant virus DNA during CRISPR-mediated homology-directed repair (HDR). Two PCR fragments were generated by PCR of the gBblock and of the plasmid and was combined using Hifi DNA assembly.

5.4. CRISPR/Cas9-mediated homology-directed repair of the HHV-7 genome

This protocol is based on previous research where this method has been performed on another herpesvirus, the pseudorabies virus (Cleemput *et al*, 2021).

First, CRISPR lentiviruses bearing *Cas9* and a sgRNA against specific viral target proteins were produced by transfection of LentiCRISPRv2 plasmids (gift from Feng Zhang (Addgene plasmid # 52961 ; http://n2t.net/addgene:52961;RRID:Addgene_52961) and packaging plasmids psPAX2 (gift from Didier Trono (Addgene plasmid # 12260 ; http://n2t.net/addgene:12260 ; RRID:Addgene_12260)) and pMD2.G (gift from Didier Trono (Addgene plasmid # 12259 ; http://n2t.net/addgene:12259 ; RRID:Addgene_12259)) in Hek293T cells. HEK293T cells were pre-treated with chloroquine hydrochloride prior to transfection with plasmids using JETOptimus reagent as described by the manufacturer. Seventy-two hours later, supernatant was collected, filtered over 0.2 µM filters and concentrated via spin filtration. Next, fresh HEK293T cells were transduced by these lentiviruses via spinoculation. Puromycin was added for selection of puromycin resistance protein and thus Cas9/sgRNA expression. Cas9 expression was verified using ELISA (see below). LentiCRISPRv2-transduced HEK293T cells were then transfected with matching donor plasmids. After 24 h, cells were inoculated with 0.5 mL HHV-7 with a TCID50/mL ranging from $10^{6.54}$ to $10^{4.80}$. Cells were maintained in DMEM complete supplemented with 10 mM SCR7 and 10 mM RS-1 (Sigma-Aldrich) to inhibit non-homologous end joining and enhance homologous

recombination, respectively. Forty-eight hours post-inoculation, cells and supernatant were harvested, pooled, and stored at –80°C. Finally, progeny virus containing viral mutants was used to inoculate SupT1 cells to further infect HEK293T cells to purify the mutants using plaque purification, a described in 5.4.1.

With this method, we wanted to create mutated HHV-7 particles that contain fluorophore-tagged versions of our proteins of interest, which were used to infect different cell types in following experiments. Currently, CRISPR/Cas9 is one of the most effective and adaptable methods available for precise gene editing. It outperforms the conventional method for creating herpesvirus mutants, which entails slow and tedious homologous recombination of DNA fragments with the viral genome, frequently introduced as a BAC.

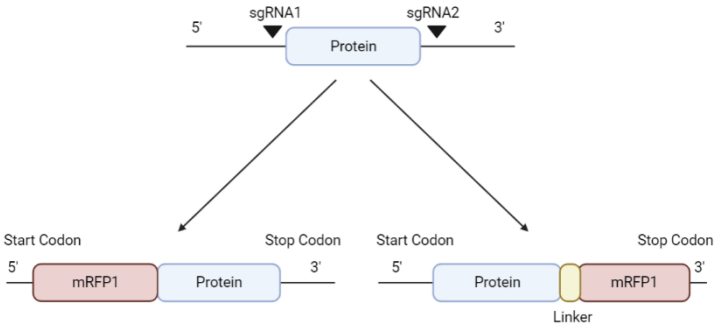

Figure 43. **CRISPR/Cas9-mediated mutagenesis of PRV through homology-directed recombineering of the HHV-7 genome.** Schematic of protein targeting and *mRFP1* incorporation made using Biorender.

We have considered the possibility that the tag could give the protein a different function. However, there are no alternatives to track protein localization inside the cell, since no antibodies directed at the selected viral proteins are available. In other experiments concerning beta-herpesviruses, including the beta-herpesvirus CMV, tegument and capsid proteins have already been successfully linked to mRFP (Coller *et al*, 2007; Chaudhuri *et al*, 2008; Tomtishen, 2012). This led us to expect that the tag would not inhibit the proteins activity or localization. Furthermore, we designed both N- and C-terminally tagged proteins for verification.

5.4.1. Viral plaque assay

To purify the mutant viruses, a viral plaque assay was performed. The assay involves adding the mutant viruses, either free or in infected SupT1 cells, to HEK293T cells and applying a semisolid overlay that limits the spread of infection to neighboring cells, while cell death leads to the formation of plaques. This overlay consists of 1% carboxymethylcellulose (C4888 Sigma), 1X RPMI + L-glutamine, 7.5% sodium bicarbonate (58761 sigma), 2% FBS, 20 mg/mL folic acid (F8758 Sigma), 7.5 mM HEPES and 1% Penicillin/streptomycin.

Plaques were subsequently picked using a 200 µL pipet and used to infect other HEK293T cells, until all observed plaques were fluorescent.

5.5. Western Blot & Elisa

5.5.1. SDS-PAGE Western Blot

First, a Western Blot was performed to confirm the presence of Cas9 in the transduced HEK293T cell cultures. Cell lysates were prepared by incubating 2 million cells with 500 µL ice-cold RIPA buffer with protease inhibitors and collecting the supernatant after incubating for 30 minutes.

A discontinuous SDS-PAGE gel was used with a 10% running gel (0.1% SDS, 375 mM Tris-HCl, pH 8.8) and 6% stacking gel (125 mM Tris-HCl, pH 6.8) for separating the proteins. The samples were loaded on the gel (25 µl) and the Novex Sharp™ prestained protein standard (10 µl) was used as a reference standard. After running the gel for 30min at 60V and 40min at 150V, a semi-dry Western Blot was performed. The proteins were transferred from the gel to a nitrocellulose membrane for the duration of 1 h at 300 mA. After the transfer, a Ponceau coloring was executed for examining the efficacy of the Western Blot and to check protein levels. The Ponceau coloring was washed away using TBS-T (20 nM Tris-HCl, pH 7.6, 137 mM NaCl, 0.1% Tween-20) and the membranes were blocked in a milk solution (5% milk in TBS-T) for 1 h.

The detection was done with the use of an anti-Cas9 mouse monoclonal antibody (10C11-A12; ThermoFisher Scientific) at a dilution of 1:1000 and incubated overnight at 4°C.

The next day, the membranes were washed with TBS-T (3 x) after which the secondary antibodies were added. These secondary antibodies were HRP-coupled goat antibodies (ThermoFisher Scientific) against mouse IgGs and used at a 1:10 000 dilution. After incubating the membranes at room temperature for one hour, they were washed with TBS-T (3x).

Proteins were visualized by chemiluminescence after incubation with Pierce™ ECL Western Blotting Substrate (ThermoFisher Scientific). This HRP-induced light was captured by the BioRad ChemiDoc™ Touch Imaging System at intervals of 15 seconds. This image was digitally created and interpreted.

5.5.2. ELISA

An ELISA was performed as an alternative to the Western Blot for the detection of Cas9, using a Cas9-CRISPR ELISA kit (PRB-5079; Cell Biolabs).

Samples were prepared identically to the samples in the Western Blot, and the supernatant in the RIPA buffer was used to perform the ELISA according to the protocol provided by Cell Biolabs™.

The sample was then diluted 100x to achieve optimal assay sensitivity and specificity.

A dilution series of Cas9 standards in the concentration range of 0 to 100 ng/mL was prepared into Assay Diluent for the preparation of the standard curve. A 96-well microtiter plate was coated with a capture antibody that specifically binds to the target protein or antibody of interest. To this plate, 100 µL of Cas9 unknown sample or standard was added in duplicate. The plate was incubated for 1h on an orbital shaker. The microwell strips were washed 3 times with 250 µL 1X Wash Buffer per well, with thorough aspiration between each wash. After this, 100 µL of the diluted Biotinylated Anti-Cas9 antibody was added to each well. The plate was incubated at room temperature for 1 h on an orbital shaker.

A detection antibody that specifically recognizes an epitope on the Cas9 target protein is added to the plate. The detection antibody is typically conjugated to an enzyme, such as horseradish peroxidase or alkaline phosphatase, that can produce a colorimetric or chemiluminescent signal. In the Cell Biolabs kit, the detection antibody was a streptavidin-enzyme conjugate, which was added to the wells at a volume of 100 µL. The plate was then incubated at room temperature for 1h on an orbital shaker. The wells were washed again 3 times with 250 µL 1X Wash Buffer per well, with thorough aspiration between each wash. To obtain a colorimetric reaction, 100 µL of substrate solution was added to each well, including the blank wells, after which the plate was incubated room temperature on an orbital shaker. The enzyme reaction was stopped 100 µL of stop solution into each well, including the blank wells. Results were obtained by reading the absorbance of each microwell on the Thermo FisherMultiskan spectrophotometer using 450 nm as the primary wavelength. The signal intensity is proportional to the amount of target protein or antibody present in the sample, and the concentration can be calculated using the standard curve generated from the known concentrations of the purified Cas9 protein.

5.6. Determination of the presence of (replication competent) HHV-7

5.6.1. ***qPCR***

A quantitative PCR (qPCR) was performed to determine the genome copies per mL for the HHV-7 virus in multiple experiments. An alternative for qPCR is digital PCR (dPCR), which was avoided due to budgetary reasons.

Viral DNA was purified from cell pellets using the Qiagen DNeasy blood & tissue kit (Qiagen, Hilden, Germany), while viral DNA from supernatants was isolated using the Qiagen QIAamp® Viral RNA Mini kit, both according to the manufacturer's protocol. The DNA concentration was determined using the NanoDrop™. Since HHV-7 is a DNA virus, no reverse transcription was needed, and the samples could be used immediately for qPCR.

Multiple primers were designed to anneal to a viral DNA sequence to obtain a quantification of the levels of viral DNA (Table 6).

The qPCR reaction was set up in 96-well plate, and each well contained 2,5 µL 2x LightCycler® 480 SYBR Green I Master Mix, 0,125 µL 10 µM forward primer, 0,125 µL 10 µM reverse primer, 0,25 µL H_2O and 2 µL of DNA concentrated at 2,5 ng/µL. The 96-well plate was spun down and a qPCR procedure was performed using the LightCycler®. A qPCR cycle consists of 95°C for 10 sec, 60 °C for 30 sec, 72 °C for 30 sec, and is repeated 45 times. The fluorescence data was analyzed using LightCycler® 480 software that calculated the threshold cycle (Cq) value, which is the cycle number at which the fluorescence signal crosses a predefined threshold. The Cq value is inversely proportional to the amount of target DNA or RNA in the sample and can be used to quantify the target concentration relative to a standard curve generated from known concentrations of the target. Melting curves were also determined using the LightCycler® 480 software to look for amplification of non-specific products.

Table 6. **Primer pairs used for qPCR**. Primers were directed against the gB, gH, gL, gO, and gQ genes, the U37 and U57 genes as taken from literature and primers designed against the 139515-139663 sequence using Benchling (HHV-7)

Primer	Forward	Reverse
gB	CGATTTGACAGGGAGGTTTCT	GAACGTGTGTGCTTCAATCTTT
gH	CAACAGAGAAGGCTGTGAAGA	CCGAAACATTTGCGAAGTAGAC
gL	GTTCACGGGCAACATCTTTG	GTGTGCGAGTCTCCTCATTT
gO	CGGTGTTACCAACTTCTCCTT	CGGAATTGCTGTAGGCTTAGTA
gQ	CCAGACGAAGCACAGGTTAT	GACTTCAGACAGCCCTTTACTC
U37	TTAGACATCTTACACGACAGC	CAGCTTTTCGAACTTGTCAC
U57	CGGAAGTCACTGGAGTAATGACAA	CCAATCCTTCCGAAACCGAT
HHV-7	TCCGTCTGCCTCCTCACCCTT	GTGTCGTCCCAGAAGCAGCCAC

*5.6.2. **Virus titration assay***

Since the qPCR technique is limited to quantification of DNA, we used the virus titration assay to determine whether infectious particles are produced in and released from the different infected cell types.

The titration experiment was performed in 96-well plates. A serial dilution (0, 10^{-1}, 10^{-2}, 10^{-3}, …, 10^{-7}) of the samples at a volume of 50 µl, was added to a 50 µL cell suspension of 50 000 SupT1 cells/well in a 96-well plate. After 7 days, the presence of a CPE was verified using light microscopy. The viral titer was derived from the respective presence or absence of a CPE at the different dilutions of the samples and calculated according to the formula of Reed-Müench.

Reed-Müench formula: $proportional\ distance = \frac{(\%mortality\ at\ next\ dilution\ above\ 50\%)-50\%)}{(\%mortality\ at\ next\ dilution\ above\ 50\%)-(\%mortality\ at\ next\ diulution\ below\ 50\%} . dilution$

5.7. Time course experiment of direct HHV-7 infection

For each cell type, being the SH-SY5Y cell line, the SupT1 cell line and the primary activated and non-activated $CD4^+$ cells, 500 000 cells were seeded in triplicate in a 24-well plate. Four rows were used to obtain samples for 4 different time points (1 day, 2 days, 4 days, and 7 days). These cells were inoculated with WT HHV-7 at a MOI of 0.1 for 2 h. Next, cells were spinoculated for 60 min 2300 rpm at 20°C. After spinoculation, the inoculum was removed, and the cells were incubated with 1 mL of fresh medium for their respective cell types. Cells were subsequently harvested at their respective time points and the supernatant was separated from the cell pellet by centrifugation to obtain information on the amount of extracellular and intracellular HHV-7, respectively. These samples were subsequently titrated on SupT1 cells as described above.

5.8. Time course experiment of indirect HHV-7 infection through cell-cell contact

SH-SY5Y cells and HEK293T cells were seeded at a density of 500 000 cells/ well in a 24-well plate in triplicate. Three rows were used to obtain samples for 4 different time points (1 day, 2 days and 7 days). These cells were inoculated with either HHV-7 infected SupT1 cells or free HHV-7 virus particles at a $TCID_{50}$/mL of $10^{5.05}$. Next, cells were spinoculated for 60 min 2300 rpm at 20°C. After spinoculation, the inoculum was removed, and the cells were incubated with 1 mL of fresh medium for their respective cell types. Cells were subsequently harvested at their respective time points and the supernatant was separated from the cell pellet to obtain information on the amount of extracellular and intracellular HHV-7, respectively. These samples were subsequently titrated on SupT1 cells as described above.

5.9. Inoculation of SupT1 cells and differentiated SH-SY5Y cells with mutant HHV-7

SH-SY5Y cells were differentiated using 10 µM RA at a density of 40 000 cells/well in a 96-well plate. Meanwhile, SupT1 cells were inoculated with U32-mRFP1 mutant HHV-7 isolated from a fluorescent plaque as obtained by 5.4.1. In parallel, 50 000 SupT1 cells/well were seeded in the same 96-well plate. Infected SupT1s were collected and added to half of the differentiated SH-Sy5Y cells and SupT1 cells. To the other half, free virus (obtained by freezing, thawing, and centrifuging at 2000 rpm for 5 min of the infected SupT1 cells) was added. Before adding the infected SupT1 cells to the other SupT1 cells, they were stained with anti-CD4 FITC antibodies diluted 1:100, to discern between the initially infected and non-infected SupT1s. Inoculation consisted of 1 h of spinoculation at 2300 rpm at 20°C, followed by 2 h of incubation for the SH-SY5Y cells. The inoculum was subsequently removed from the SH-SY5Y cells and replaced with 200 µL fresh complete DMEM/F12 + 10 µM RA.

Cells were analyzed with confocal microscopy 1 h post inoculation and on day 1, 2, 3 and 7. To visualize the nucleus and relative position of the mutated HHV-7 particles, DAPI was added to stain the nucleus.

5.10. Statistical analysis

Statistical analysis was performed using the SPSS Statistics 28 software. Data was first assessed for multiple assumptions, being normal distribution, independence of cases, and homogeneity of variance.

Normal distribution was assessed using the residuals and the Shapiro-Wilk test. This test's null hypothesis is that the population is normally distributed. The null hypothesis is disproven, and the tested data are not normally distributed, if the p value is smaller than the selected alpha level, in our case 0.05. On the other hand, the null hypothesis (that the data comes from a regularly distributed population) cannot be rejected if the p value is higher than the selected alpha level. If the residuals are not normally distributed, the data will be transformed either logarithmically or exponentially until normality is obtained.

The homogeneity of variances was assessed using the Levene's test. It evaluates the null hypothesis of homogeneity of variance, which states that population variances are equal. If the resulting p-value of Levene's test is less than a certain significance level, in our instance 0.001, the obtained differences in sample variances most likely did not occur based on random sampling from a population that has equal variances. Consequently, it is concluded that there is a difference between the population variances and that the null hypothesis of equal variances is untrue as a result.

The independence of different factors is measured by testing the between-subject effects. If there is interference between the variables (when $p<0.05$), the data was split based on the respective factor.

When the data adheres to all assumptions, an ANOVA was performed. This was done one-way or two-way depending on the amount of variables tested. In the case that there were 3 groups of more, the ANOVA was paired with a post-hoc Tukey test to find means that are significantly different from each other. If the data did not adhere to all assumptions, a non-parametric Kruskal Wallis test with independent samples and pairwise comparisons were performed. If $p<0.05$, the null hypothesis was rejected.

References

Ablashi D V., Berneman ZN, Kramarsky B, Whitman J, Asano Y & Pearson GR (1995) Human herpesvirus-7 (HHV-7): current status. Clin Diagn Virol 4: 1–13

Ablashi D V., Handy M, Bernbaum J, Chatlynne LG, Lapps W, Kramarsky B, Berneman ZN, Komaroff AL & Whitman JE (1998) Propagation and characterization of human herpesvirus-7 (HHV-7) isolates in a continuous T-lymphoblastoid cell line (SupT1). J Virol Methods 73: 123–140

Aburakawa Y, Katayama T, Saito T, Sawada J, Suzutani T, Aizawa H & Hasebe N (2017a) Limbic Encephalitis Associated with Human Herpesvirus-7 (HHV-7) in an Immunocompetent Adult: The First Reported Case in Japan. Internal Medicine 56: 1919

Aburakawa Y, Katayama T, Saito T, Sawada J, Suzutani T, Aizawa H & Hasebe N (2017b) Limbic Encephalitis Associated with Human Herpesvirus-7 (HHV-7) in an Immunocompetent Adult: The First Reported Case in Japan. Internal Medicine 56: 1919

Agol VI (2012) Cytopathic effects: virus-modulated manifestations of innate immunity? Trends Microbiol 20: 570–576

Agut H, Bonnafous P & Gautheret-Dejean A (2016) Human Herpesviruses 6A, 6B, and 7. Microbiol Spectr 4

Agut H, Dupin N, Aubin JT & Calvez V (1996) Novel human herpesviruses (human herpesviruses 6, 7 and 8). Clinical Microbiology and Infection 2: 159–167

Ahlqvist J, Fotheringham J, Akhyani N, Yao K, Fogdell-Hahn A & Jacobson S (2005) Differential tropism of human herpesvirus 6 (HHV-6) variants and induction of latency by HHV-6A in oligodendrocytes. J Neurovirol 11: 384

Albright A V., Lavi E, Black JB, Goldberg S, O'Connor MJ & González-Scarano F (1998) The effect of human herpesvirus-6 (HHV-6) on cultured human neural cells: oligodendrocytes and microglia. J Neurovirol 4: 486–494

Ansari A, Li S, Abzug MJ & Weinberg A (2004) Human Herpesviruses 6 and 7 and Central Nervous System Infection in Children1. Emerg Infect Dis 10: 1450

Aoshima T, Komura J & Ofuji S (1981) Virus-Like Particles in the Herald Patch of Pityriasis rosea. Dermatology 162: 64–65

Asano Y, Yoshikawa T, Suga S, Yazaki T, Hata T, Nagai T, Kajita Y, Ozaki T & Yoshida S (1989) Viremia and neutralizing antibody response in infants with exanthem subitum. J Pediatr 114: 535–539

Bahramian E, Furr M, Wu JT & Ceballos RM (2022) Differential Impacts of HHV-6A versus HHV-6B Infection in Differentiated Human Neural Stem Cells. Front Immunol 13

Benchling (2023) https://benchling.com

Van Den Berg JSP, Van Zeijl JH, Rotteveel JJ, Melchers WJG, Gabreëls FJM & Galama JMD (1999) Neuroinvasion by human herpesvirus type 7 in a case of exanthem subitum with severe neurologic manifestations. Neurology 52: 1077–1079

Black JB, Schwarz TF, Patton JL, Kite-Powell K, Pellett PE, Wiersbitzky S, Bruns R, Müller C, Jäger G & Stewart JA (1996) Evaluation of immunoassays for detection of antibodies to human herpesvirus 7. Clin Diagn Lab Immunol 3: 79

Boeck K, Mempel M, Schmidt T & Abeck D (1998) Gianotti-Crosti syndrome: clinical, serologic, and therapeutic data from nine children. Cutis 62: 271–4; quiz 286

Borza CM & Hutt-Fletcher LM (2002) Alternate replication in B cells and epithelial cells switches tropism of Epstein–Barr virus. Nature Medicine 2002 8:6 8: 594–599

Brennan DC, Storch GA, Singer GG, Lee L, Rueda J & Schnitzler MA (2000) The Prevalence of Human Herpesvirus—7 in Renal Transplant Recipients Is Unaffected by Oral or Intravenous Ganciclovir. J Infect Dis 181: 1557–1561

Broccolo F, Drago F, Careddu AM, Foglieni C, Turbino L, Cocuzza CE, Gelmetti C, Lusso P, Rebora AE & Malnati MS (2005) Additional evidence that pityriasis rosea is associated with reactivation of human herpesvirus-6 and -7. J Invest Dermatol 124: 1234–1240

Browning JC (2009) An update on pityriasis rosea and other similar childhood exanthems. Curr Opin Pediatr 21: 481–485

Cacheaux LP, Ivens S, David Y, Lakhter AJ, Bar-Klein G, Shapira M, Heinemann U, Friedman A & Kaufer D (2009) Transcriptome Profiling Reveals TGF-β Signaling Involvement in Epileptogenesis. Journal of Neuroscience 29: 8927–8935

Caputo R, Gelmetti C, Ermacora E, Gianni E & Silvestri A (1992) Gianotti-Crosti syndrome: A retrospective analysis of 308 cases. J Am Acad Dermatol 26: 207–210

Carmichael JC, Yokota H, Craven RC, Schmitt A & Wills JW (2018) The HSV-1 mechanisms of cell-to-cell spread and fusion are critically dependent on host PTP1B. PLoS Pathog 14

Caserta MT (2018) Human Herpesviruses 6 and 7 (Roseola, Exanthem Subitum). Principles and Practice of Pediatric Infectious Diseases: 1081-1088.e4

Cermelli C, Pietrosemoli P, Meacci M, Pecorari M, Sabbatini AMT, Colombari B & Portolani M (1997) SupT-1: a cell system suitable for an efficient propagation of both HHV-7 and HHV-6 variants A and B. New Microbiol 20: 187–196

Chan PKS, Chik KW, To KF, Li CK, Shing MMK, Ng KC, Yuen PMP & Cheng AF (2002) Case report: human herpesvirus 7 associated fatal encephalitis in a peripheral blood stem cell transplant recipient. J Med Virol 66: 493–496

Chan PKS, Peiris JSM, Yuen KY, Liang RHS, Lau YL, Chen FE, Lo SKF, Cheung CY, Chan TK & Ng MH (1997) Human Herpesvirus-6 and Human Herpesvirus-7 Infections in Bone Marrow Transplant Recipients. J Med Virol 53: 295–305

Chanas A, Tomik A & Werner B (2021) Recurrent HHV-7 myocarditis in a 16-year-old boy. Pediatria i Medycyna Rodzinna 17: 67–71

Chapenko S, Roga S, Skuja S, Rasa S, Cistjakovs M, Svirskis S, Zaserska Z, Groma V & Murovska M (2016) Detection frequency of human herpesviruses-6A, -6B, and -7 genomic sequences in central nervous system DNA samples from post-mortem individuals with unspecified encephalopathy. J Neurovirol 22: 488–497

Charpentier JC & King PD (2021) Mechanisms and functions of endocytosis in T cells. Cell Communication and Signaling 19: 92

Chaudhuri V, Sommer M, Rajamani J, Zerboni L & Arvin AM (2008) Functions of Varicella-Zoster Virus ORF23 Capsid Protein in Viral Replication and the Pathogenesis of Skin Infection. J Virol 82: 10231

Chen HL, Chang JK & Tang R Bin (2015) Current recommendations for the Japanese encephalitis vaccine. Journal of the Chinese Medical Association 78: 271–275

Chin K-C & Cresswell P (2001) Viperin (cig5), an IFN-inducible antiviral protein directly induced by human cytomegalovirus. Proceedings of the National Academy of Sciences 98: 15125–15130

Christou E, Mastrogianni S, Bourousis E, Bachou T, Tsikrikas T, Mouskou S, Voudris K & Delis D (2022) A case of seronegative autoimmune encephalitis associated with human herpesvirus-7 (HHV-7). J Med Virol 94: 795–798

Chuh AAT, Chan HHL, Chiu SSS, Ng HY & Peiris JSM (2002) A Prospective Case Control Study of the Association of Gianotti–Crosti Syndrome with Human Herpesvirus 6 and Human Herpesvirus 7 Infections. Pediatr Dermatol 19: 492–497

Clark AA, Emery CC & Griffiths DD (2003) Cytomegalovirus, human herpesvirus-6, and human herpesvirus-7 in hematological patients. Semin Hematol 40: 154–162

Clark DA (2002) Human herpesvirus 6 and human herpesvirus 7: emerging pathogens in transplant patients. Int J Hematol 76 Suppl 2: 246–252

Clark DA, Freeland JML, Mackie PLK, Jarrett RF & Onions DE (1993) Prevalence of Antibody to Human Herpesvirus 7 by Age. J Infect Dis 168: 251–252

Clark DA & Griffiths PD (2003) Human herpesvirus 6: relevance of infection in the immunocompromised host. Br J Haematol 120: 384–395

Clark DA, Michael Kidd I, Collingham KE, Tarlow M, Ayeni T, Riordan A, Griffiths PD, Emery VC & Pillay D (1997) Diagnosis of primary human herpesvirus 6 and 7 infections in febrile infants by polymerase chain reaction. Arch Dis Child 77: 42

Cleemput J Van, Koyuncu OO, Laval K, Engel EA & Enquist LW (2021) CRISPR/Cas9-Constructed Pseudorabies Virus Mutants Reveal the Importance of UL13 in Alphaherpesvirus Escape from Genome Silencing. J Virol 95

De Clercq E, Naesens L, De Bolle L, Schols D, Zhang Y & Neyts J (2001) Antiviral agents active against human herpesviruses HHV-6, HHV-7 and HHV-8. Rev Med Virol 11: 381–395

Cohen JI (2015) Human Herpesvirus Types 6 and 7 (Exanthem Subitum). Mandell, Douglas, and Bennett's Principles and Practice of Infectious Diseases 2: 1772-1776.e1

Cohen JI (2020) Herpesvirus latency. J Clin Invest 130: 3361

Coller KE, Lee JI-H, Ueda A & Smith GA (2007) The Capsid and Tegument of the Alphaherpesviruses Are Linked by an Interaction between the UL25 and VP1/2 Proteins. J Virol 81: 11790

Corral Í, Sainz de la Maza S, Rodríguez M, Kawiorski MM, López-Martínez MJ & Galán JC (2018) Molecular detection of human herpesvirus 7 DNA in cerebrospinal fluid from adult patients with neurological disorders. J Neurovirol 24: 333–338

Coserta MT, Breese Hall C, Schnabel K, Long CE & D'Heron N (1998) Primary human herpesvirus 7 infection: a comparison of human herpesvirus 7 and human herpesvirus 6 infections in children. J Pediatr 133: 386–389

Davison AJ (2007) Comparative analysis of the genomes. Human Herpesviruses: Biology, Therapy, and Immunoprophylaxis: 10–26

Desai J & Mitchell WG (2012) Acute Cerebellar Ataxia, Acute Cerebellitis, and Opsoclonus-Myoclonus Syndrome. J Child Neurol

Donati D, Akhyani N, Fogdell-Hahn A, Cermelli C, Cassiani-Ingoni R, Vortmeyer A, Heiss JD, Cogen P, Gaillard WD, Sato S, et al (2003) Detection of human herpesvirus-6 in mesial temporal lobe epilepsy surgical brain resections. Neurology 61: 1405

Drago F, Broccolo F & Rebora A (2009) Pityriasis rosea: an update with a critical appraisal of its possible herpesviral etiology. J Am Acad Dermatol 61: 303–318

Drago F, Ranieri E, Malaguti F, Battifoglio ML, Losi E & Reborn A (1997) Human herpesvirus 7 in patients with pityriasis rosea. Electron microscopy investigations and polymerase chain reaction in mononuclear cells, plasma and skin. Dermatology 195: 374–378

Eisman S & Sinclair R (2015) Pityriasis rosea. BMJ 351

Emery VC & Clark DA (2007) HHV-6A, 6B, and 7: persistence in the population, epidemiology and transmission. Human Herpesviruses: Biology, Therapy, and Immunoprophylaxis: 875–882

Epstein LG, Shinnar S, Hesdorffer DC, Nordli DR, Hamidullah A, Benn EKT, Pellock JM, Frank LM, Lewis D V., Moshe SL, et al (2012) Human herpesvirus 6 and 7 in febrile status epilepticus: the FEBSTAT study. Epilepsia 53: 1481–1488

Fay AJ, Noetzel MJ & Mar SS (2015) Pediatric Hemorrhagic Brainstem Encephalitis Associated With HHV-7 Infection. Pediatr Neurol 53: 523–526

Flamand L, Lautenschlager I, Krueger GRF & Ablashi D V. (2014) Human Herpesviruses HHV-6A, HHV-6B, and HHV-7, Third Edition. Human Herpesviruses HHV-6A, HHV-6B, and HHV-7, Third Edition: 1–341

Flamand Louis (2014) Human Herpesviruses HHV-6A, HHV-6B & HHV-7: diagnosis and clinical management. 362

Foiadelli T, Rossi V, Paolucci S, Rovida F, Novazzi F, Orsini A, Brambilla I, Marseglia GL, Baldanti F & Savasta S (2022) Human Herpes Virus 7-related encephalopathy in children. Acta Biomed 92

Fotheringham J, Donati D, Akhyani N, Fogdell-Hahn A, Vortmeyer A, Heiss JD, Williams E, Weinstein S, Bruce DA, Gaillard WD, et al (2007) Association of human herpesvirus-6B with mesial temporal lobe epilepsy. PLoS Med 4: 0848–0857

Frenkel N, Schirmer EC, Wyatt LS, Katsafanas G, Roffman E, Danovich RM & June CH (1990) Isolation of a new herpesvirus from human CD4+ T cells. Proc Natl Acad Sci U S A 87: 748–752

Fujisaki H, Tanaka-Taya K, Tanabe H, Hara T, Miyoshi H, Okada S & Yamanishi K (1998) Detection of Human Herpesvirus 7 (HHV-7) DNA in Breast Milk by Polymerase Chain Reaction and Prevalence of HHV-7 Antibody in Breast-Fed and Bottle-Fed Children. J Med Virol 56: 275–279

Galarraga MC, Gomez E, De Oña M, Rodriguez A, Laures A, Boga JA & Melon S (2005) Influence of ganciclovir prophylaxis on citomegalovirus, human herpesvirus 6, and human herpesvirus 7 viremia in renal transplant recipients. Transplant Proc 37: 2124–2126

GASTAUT H, POIRIER F, PAYAN H, SALAMON G, TOGA M & VIGOUROUX M (1959) H. H. E. Syndrome Hemiconvulsions, Hemiplegia, Epilepsy. Epilepsia 1: 418–447

Gautheret-Dejean A, Agut H, Nicolas JC & Beaugerie L (2003) Roseolovirus DNA in the colonic mucosa of HIV-seropositive patients with diarrhea . Clinical Infectious Diseases 36: 1348–1349

Giese S, Pelchen-Matthews A & Marsh M (2016) HIV – The Cell Biology of Virus Infection and Replication. In Encyclopedia of Cell Biology pp 828–838. Elsevier

Gompels UA (2014) Human Herpesviruses 6A, 6B and 7 (Herpesviridae). Reference Module in Biomedical Sciences

Grose C (2022) Metagenomic sequencing of cerebrospinal fluid from children with meningitis. EBioMedicine 84

Guo J, Wang W, Yu D & Wu Y (2011) Spinoculation Triggers Dynamic Actin and Cofilin Activity That Facilitates HIV-1 Infection of Transformed and Resting CD4 T Cells. J Virol 85: 9824

Hacohen Y, Niotakis G, Aujla A, Siddiqui A, McCormick D, Bassi S, Clarke A & Lim M (2011) Acute life threatening cerebellitis presenting with no apparent cerebellar signs. Clin Neurol Neurosurg 113: 928–930

Haki M, Tsuchida M, Kotsuji M, Lijima S, Tamura K, Koike K, Izumi I, Tanaka M & Hirano T (1997) Gianotti–Crosti syndrome associated with cytomegalovirus antigenemia after bone marrow transplantation. Bone Marrow Transplantation 1997 20:8 20: 691–693

Hall CB, Caserta MT, Schnabel KC, Boettrich C, McDermott MP, Lofthus GK, Carnahan JA & Dewhurst S (2004) Congenital infections with human herpesvirus 6 (HHV6) and human herpesvirus 7 (HHV7). J Pediatr 145: 472–477

Hall CB, Caserta MT, Schnabel KC, McDermott MP, Lofthus GK, Carnahan JA, Gilbert LM & Dewhurst S (2006) Characteristics and Acquisition of Human Herpesvirus (HHV)–7 Infections in Relation to Infection with HHV-6. J Infect Dis 193: 1063–1069

Harr T & French LE (2010) Toxic epidermal necrolysis and Stevens-Johnson syndrome. Orphanet J Rare Dis 5

Heaton NS (2017) Revisiting the concept of a cytopathic viral infection. PLoS Pathog 13

Heckenberg SGB, Brouwer MC & Van de Beek D (2014) Bacterial meningitis. Handb Clin Neurol 121: 1361–1375

Helmke BM, Deichmann M & Otto HF (2001) Prevalence and distribution of human herpesvirus 6 variants A and B in adult human brain. J Med Virol 64: 42–46

Holden SR & Vas AL (2007) Severe encephalitis in a haematopoietic stem cell transplant recipient caused by reactivation of human herpesvirus 6 and 7. Journal of Clinical Virology 40: 245–247

Houshmandi MM, Moayedi A, Rahmati MB, Nazemi A, Fakhrai D & Zare S (2015) Human Herpes Virus Type 6 and Febrile Convulsion. Iran J Child Neurol 9: 10

Hudnall SD, Stanberry LR & Griffiths PD (2011) Human Herpesvirus Infections. Tropical Infectious Diseases: Principles, Pathogens and Practice: 355–368

Ihira M, Yoshikawa T, Ishii J, Nomura M, Hishida H, Ohashi M, Enomoto Y, Suga S, Iida K, Saito Y, et al (2002) Serological examination of human herpesvirus 6 and 7 in patients with coronary artery Disease. J Med Virol 67: 534–537

Imamura S, Yanase K, Taniguchi S, Ofuji S & Mangaoil L (1980) Erythema multiforme: demonstration of immune complexes in the sera and skin lesions. Br J Dermatol 102: 161–166

Kato Z, Kozawa R, Teramoto T, Hashimoto K, Shinoda S & Kondo N (2003) Acute cerebellitis in primary human herpesvirus-6 infection. Eur J Pediatr 162: 801–803

Kawada JI, Kimura H, Yoshikawa T, Ihira M, Okumura A, Morishima T & Hayakawa F (2004) Hemiconvulsion–hemiplegia syndrome and primary human herpesvirus 7 infection. Brain Dev 26: 412–414

Kennedy PGE (2004) Viral Encephalitis: Causes, Differential Diagnosis, and Management. J Neurol Neurosurg Psychiatry 75: i10–i15

Kent WJ, Sugnet CW, Furey TS, Roskin KM, Pringle TH, Zahler AM & Haussler and D (2002) The Human Genome Browser at UCSC. Genome Res 12: 996–1006

Kerur N, Veettil MV, Sharma-Walia N, Sadagopan S, Bottero V, Paul AG & Chandran B (2010) Characterization of entry and infection of monocytic THP-1 cells by Kaposi's sarcoma associated herpesvirus (KSHV): Role of heparan sulfate, DC-SIGN, integrins and signaling. Virology 406: 103–116

Kim Y, Jang G, Lee D, Kim N, Seon JW, Kim Y hoan & Lee C (2022) Trypsin enhances SARS-CoV-2 infection by facilitating viral entry. Arch Virol 167: 441

King MW & Munger J (2019) Editing the human cytomegalovirus genome with the CRISPR/Cas9 system. Virology 529: 186–194

Klussmann JP, Krueger E, Sloots T, Berneman Z, Arnold G & Krueger GRF (1997a) Ultrastructural study of human herpesvirus-7 replication in tissue culture. Virchows Arch 430: 417–426

Klussmann JP, Krueger E, Sloots T, Berneman Z, Arnold G & Krueger GRF (1997b) Ultrastructural study of human herpesvirus-7 replication in tissue culture. Virchows Arch 430: 417–426

Koike H, Chiba A & Katsuno M (2021) Emerging Infection, Vaccination, and Guillain–Barré Syndrome: A Review. Neurol Ther 10: 523–537

Koike H & Katsuno M (2021) The role of macrophages in Guillain-Barré syndrome and chronic inflammatory demyelinating polyneuropathy. Neurol Clin Neurosci 9: 203–210

Kondo K & Yamanishi K (2007) HHV-6A, 6B, and 7: molecular basis of latency and reactivation. Human Herpesviruses: Biology, Therapy, and Immunoprophylaxis: 843–849

Kovalevich J & Langford D (2013) Considerations for the Use of SH-SY5Y Neuroblastoma Cells in Neurobiology. Methods Mol Biol 1078: 9

Laurent-Crawford AG, Krust B, Muller S, Rivière Y, Rey-Cuillé MA, Béchet JM, Montagnier L & Hovanessian AG (1991) The cytopathic effect of hiv is associated with apoptosis. Virology 185: 829–839

Lee BE & Davies HD (2007) Aseptic meningitis. Curr Opin Infect Dis 20: 272–277

LI C, GOODRICH JM & YANG X (2003) Interferon-gamma (IFN-γ) regulates production of IL-10 and IL-12 in human herpesvirus-6 (HHV-6)-infected monocyte/macrophage lineage. Clin Exp Immunol 109: 421–425

Li JM, Huang C, Yan B, Wang W, Zhou Q, Sander JW & Zhou D (2014) HHV-7 in adults with drug-resistant epilepsy: A pathological role in hippocampal sclerosis? Journal of Clinical Virology 61: 387–392

Li Y, Qu T, Li D, Jing J, Deng Q & Wan X (2022) Human herpesvirus 7 encephalitis in an immunocompetent adult and a literature review. Virol J 19: 1–5

Li Y, Wan Z, Zuo L, Li S, Liu H, Ma Y, Zhou L, Jin X, Li Y & Zhang C (2021) A Novel 2-dimensional Multiplex qPCR Assay for Single-Tube Detection of Nine Human Herpesviruses. Virol Sin 36: 746–754

Ljungman P (2002) Beta-herpesvirus challenges in the transplant recipient. J Infect Dis 186 Suppl 1

Loddenkemper T (2014) Febrile Status Epilepticus: Time Is of the Essence. Epilepsy Curr 14: 345

Lusso P, Secchiero P, Crowley RW, Garzino-Demo A, Berneman ZN & Gallo RC (1994) CD4 is a critical component of the receptor for human herpesvirus 7: interference with human immunodeficiency virus. Proc Natl Acad Sci U S A 91: 3872

Maldonado YA (2011) Less Common Viral Infections. Infectious Diseases of the Fetus and Newborn Infant: 905–916

Maltsev D (2022) A comparative study of valaciclovir, valganciclovir, and artesunate efficacy in reactivated HHV-6 and HHV-7 infections associated with chronic fatigue syndrome/myalgic encephalomyelitis. Microbiol Immunol 66: 193–199

Mangeot PE, Risson V, Fusil F, Marnef A, Laurent E, Blin J, Mournetas V, Massouridès E, Sohier TJM, Corbin A, et al (2019) Genome editing in primary cells and in vivo using viral-derived Nanoblades loaded with Cas9-sgRNA ribonucleoproteins. Nature Communications 2019 10:1 10: 1–15

Marcelo Miranda C, Juan Pablo Torres T, Carmen Larrañaga L & Guillermo Acuña L (2011) Meningomyelitis associated with infection by human herpes virus 7: report of two cases. Rev Med Chil 139: 1588–1591

Markham NR & Zuker M (2008) UNAFold. In pp 3–31.

McGeoch DJ, Cook S, Dolan A, Jamieson FE & Telford EA (1995) Molecular phylogeny and evolutionary timescale for the family of mammalian herpesviruses. J Mol Biol 247: 443–58

Mendez JC, Dockrell DH, Espy MJ, Smith TF, Wilson JA, Harmsen WS, Ilstrup D & Paya C V. (2001) Human β-Herpesvirus Interactions in Solid Organ Transplant Recipients. J Infect Dis 183: 179–184

Mori Y & Yamanishi K (2007) HHV-6A, 6B, and 7: pathogenesis, host response, and clinical disease. Human Herpesviruses: Biology, Therapy, and Immunoprophylaxis 9780521827140: 833–842

Mtiri A, Bouslama G, Messouad NS Ben, Abidi I, Youssef S Ben & Sriha B (2021) Erythema Multiforme Attributable to Herpes Simplex Virus: Clinical Aspects and Treatment. Case Rep Dent 2021

Murata S, Okasora K, Tanabe T, Ogino M, Yamazaki S, Oba C, Syabana K, Nomura S, Shirasu A, Inoue K, et al (2018) Acetaminophen and Febrile Seizure Recurrences During the Same Fever Episode. Pediatrics 142

Notomi T, Okayama H, Masubuchi H, Yonekawa T, Watanabe K, Amino N & Hase T (2000) Loop-mediated isothermal amplification of DNA. Nucleic Acids Res 28: e63

O'Doherty U, Swiggard WJ & Malim MH (2000) Human Immunodeficiency Virus Type 1 Spinoculation Enhances Infection through Virus Binding. J Virol 74: 10074

Okuno T, Oishi H, Hayashi K, Nonogaki M, Tanaka K & Yamanishi K (1995) Human herpesviruses 6 and 7 in cervixes of pregnant women. J Clin Microbiol 33: 1968–1970

Opsahl ML & Kennedy PGE (2005) Early and late HHV-6 gene transcripts in multiple sclerosis lesions and normal appearing white matter. Brain 128: 516–527

Özkara Ç & Aronica E (2012) Hippocampal sclerosis. Handb Clin Neurol 108: 621–639

Parra M, Alcala A, Amoros C, Baeza A, Galiana A, Tarragó D, García-Quesada MÁ & Sánchez-Hellín V (2017) Encephalitis associated with human herpesvirus-7 infection in an immunocompetent adult. Virol J 14

Pass RF (2004) HHV6 and HHV7: Persistence and vertical transmission. Journal of Pediatrics 145: 432–435

Patel SJ, Zhao G, Penna VR, Park E, Lauron EJ, Harvey IB, Beatty WL, Plougastel-Douglas B, Poursine-Laurent J, Fremont DH, et al (2017) A Murine Herpesvirus Closely Related to Ubiquitous Human Herpesviruses Causes T-Cell Depletion. J Virol 91

Payne S (2017) Immunity and Resistance to Viruses. In Viruses pp 61–71. Elsevier

Dela Paz NG, Melchior B, Shayo FY & Frangos JA (2014) Heparan Sulfates Mediate the Interaction between Platelet Endothelial Cell Adhesion Molecule-1 (PECAM-1) and the Gαq/11 Subunits of Heterotrimeric G Proteins. J Biol Chem 289: 7413

Pellett Madan R & Hand J (2019) Human herpesvirus 6, 7, and 8 in solid organ transplantation: Guidelines from the American Society of Transplantation Infectious Diseases Community of Practice. Clin Transplant 33

Piña-Garza JE & James KC (2019) Hemiplegia. Fenichel's Clinical Pediatric Neurology: 238–254

Pohl-Koppe A, Blay M, Jäger G & Weiss M (2001) Human herpes virus type 7 DNA in the cerebrospinal fluid of children with central nervous system diseases. Eur J Pediatr 160: 351–358

Prayson RA (2018) Pathology of Epilepsy. Practical Surgical Neuropathology: A Diagnostic Approach A Volume in the Pattern Recognition Series: 617–632

Putz K, Hayani K & Zar FA (2013) Meningitis. Primary Care - Clinics in Office Practice 40: 707–726

Rangel MA, Moreira D, Vila Real M & Santos F (2017) Meningoradiculopathy Associated with Human Herpesvirus 7 - A Virus with Potential to Cause Severe Neurologic Disease with Sequelae. Pediatric Infectious Disease Journal 36: 427–429

Raposo JV, Sarmento DJDS, Pinto RBDS, Lopes AO, Gallottini M, Tozetto-Mendoza TR, Braz-Silva PH & de Paula VS (2020a) Longitudinal study on oral shedding of human betaherpesviruses 6 and 7 in renal transplant recipients reveals active replication. https://doi.org/101080/2000229720201785801 12

Raposo JV, Sarmento DJDS, Pinto RBDS, Lopes AO, Gallottini M, Tozetto-Mendoza TR, Braz-Silva PH & de Paula VS (2020b) Longitudinal study on oral shedding of human betaherpesviruses 6 and 7 in renal transplant recipients reveals active replication. J Oral Microbiol 12: 1785801

Razonable RR & Paya C V. (2002) The impact of human herpesvirus-6 and -7 infection on the outcome of liver transplantation. Liver Transplantation 8: 651–658

Reed LJ & Müench H (1938) A simple method of estimating fifty per cent endpoints. Am J Epidemiol 27: 493–497

Relhan V, Sinha S, Garg VK & Khurana N (2013) Pityriasis Rosea with Erythema Multiforme – Like Lesions: An Observational Analysis. Indian J Dermatol 58: 242

de Risi-Pugliese T, Sbidian E, Ingen-Housz-Oro S & Le Cleach L (2019) Erythema Multiforme: Recognition and Management. Am Fam Physician 100: 82–88

Riva N, Franconi I, Meschiari M, Franceschini E, Puzzolante C, Cuomo G, Bianchi A, Cavalleri F, Genovese M & Mussini C (2017) Acute human herpes virus 7 (HHV-7) encephalitis in an immunocompetent adult patient: a case report and review of literature. Infection 45: 385–388

Robert A Schwartz, Camila K Janniger & Richard Lichenstein (2022) Pityriasis Rosea: Practice Essentials, Pathophysiology, Etiology. Medscape

Roos KL (1999) Encephalitis. Neurol Clin 17: 813–833

Ruiz-Villalba A, Ruijter JM & van den Hoff MJB (2021) Use and Misuse of Cq in qPCR Data Analysis and Reporting. Life 11: 496

Sakurada S, Katano H, Sata T, Ohkuni H, Watanabe T & Mori S (2001) Effective Human Herpesvirus 8 Infection of Human Umbilical Vein Endothelial Cells by Cell-Mediated Transmission. J Virol 75: 7717

Sampaio KL, Cavignac Y, Stierhof Y-D & Sinzger C (2005) Human Cytomegalovirus Labeled with Green Fluorescent Protein for Live Analysis of Intracellular Particle Movements. J Virol 79: 2754

Sanchez V, Dong JJ, Battley J, Jackson KN & Dykes BC (2012) Human cytomegalovirus infection of THP-1 derived macrophages reveals strain-specific regulation of actin dynamics. Virology 433: 64–72

Schwartz KL, Richardson SE, Ward KN, Donaldson C, MacGregor D, Banwell B, Mahant S & Bitnun A (2014) Delayed Primary HHV-7 Infection and Neurologic Disease. Pediatrics 133: e1541–e1547

Schwartz RA, McDonough PH & Lee BW (2013) Toxic epidermal necrolysis: Part I. Introduction, history, classification, clinical features, systemic manifestations, etiology, and immunopathogenesis. J Am Acad Dermatol 69: 173.e1-173.e13

Secchiero P, Flamand L, Gibellini D, Falcieri E, Robuffo I, Capitani S, Gallo RC & Zauli G (1997a) Human herpesvirus 7 induces CD4+T-cell death by two distinct mechanisms: Necrotic lysis in productively infected cells and apoptosis in uninfected or nonproductively infected cells. Blood 90: 4502–4512

Secchiero P, Sun D, De Vico AL, Crowley RW, Reitz MS, Zauli G, Lusso P & Gallo RC (1997b) Role of the extracellular domain of human herpesvirus 7 glycoprotein B in virus binding to cell surface heparan sulfate proteoglycans. J Virol 71: 4571

Seishima M, Yamanaka S, Fujisawa T, Tohyama M & Hashimoto K (2006) Reactivation of human herpesvirus (HHV) family members other than HHV-6 in drug-induced hypersensitivity syndrome. British Journal of Dermatology 155: 344–349

Shahrizaila N, Lehmann HC & Kuwabara S (2021) Guillain-Barré syndrome. The Lancet 397: 1214–1228

Shang P, Zhu M, Baker M, Feng J, Zhou C & Zhang HL (2020) Mechanical ventilation in Guillain–Barré syndrome. Expert Rev Clin Immunol 16: 1053–1064

Shen MH, Liu MT, Chung WH & Lu CW (2020) Toxic epidermal necrolysis induced by human herpesvirus 7 treated with a tumor necrosis factor-α inhibitor. Journal of Dermatology 47: 1179–1181

Shiohara T, Inaoka M & Kano Y (2006) Drug-induced Hypersensitivity Syndrome(DIHS): A Reaction Induced by a Complex Interplay among Herpesviruses and Antiviral and Antidrug Immune Responses. Allergology International 55: 1–8

Shipley MM, Mangold CA & Szpara ML (2016) Differentiation of the SH-SY5Y Human Neuroblastoma Cell Line. J Vis Exp 2016: 53193

Simonetti FR, Dewar R & Maldarelli F (2015) Diagnosis of Human Immunodeficiency Virus Infection. In Mandell, Douglas, and Bennett's Principles and Practice of Infectious Diseases pp 1503-1525.e7. Elsevier

Skuja S, Svirskis S & Murovska M (2021) Human Herpesvirus-6 and -7 in the Brain Microenvironment of Persons with Neurological Pathology and Healthy People. Int J Mol Sci 22: 1–19

Staheli JP, Dyen MR, Deutsch GH, Basom RS, Fitzgibbon MP, Lewis P & Barcy S (2016) Complete Unique Genome Sequence, Expression Profile, and Salivary Gland Tissue Tropism of the Herpesvirus 7 Homolog in Pigtailed Macaques. J Virol 90: 6657

Stone RC, Micali GA & Schwartz RA (2014) Roseola infantum and its causal human herpesviruses. Int J Dermatol 53: 397–403

Sullivan BM & Coscoy L (2010) The U24 Protein from Human Herpesvirus 6 and 7 Affects Endocytic Recycling. J Virol 84: 1265

Swanson D (2015) Meningitis. Pediatr Rev 36: 514–526

Tognarelli EI, Reyes A, Corrales N, Carreño LJ, Bueno SM, Kalergis AM & González PA (2021) Modulation of Endosome Function, Vesicle Trafficking and Autophagy by Human Herpesviruses. Cells 10: 542

Tomtishen J (2012) Human cytomegalovirus tegument proteins (pp65, pp71, pp150, pp28). Virol J 9: 22

Tong CY, Bakran A, Williams H, Cheung CY & Peiris JS (2000) Association of human herpesvirus 7 with cytomegalovirus disease in renal transplant recipients. Transplantation 70: 213–6

Torigoe S, Koide W, Yamada M, Miyashiro E, Tanaka-Taya K & Yamanishi K (1996) Human herpesvirus 7 infection associated with central nervous system manifestations. J Pediatr 129: 301–305

Le Tortorec A, Willey S & Neil SJD (2011) Antiviral Inhibition of Enveloped Virus Release by Tetherin/BST-2: Action and Counteraction. Viruses 3: 520–540

Tuck RR & McLeod JG (1981) Autonomic dysfunction in Guillain-Barré syndrome. J Neurol Neurosurg Psychiatry 44: 983–990

Vasques Raposo J, José De Santana Sarmento D, Barbosa Da Silva Pinto R, Oliveira Lopes A, Gallottini M, Regina Tozetto-Mendoza T, Henrique Braz-Silva P & Salete de Paula V (1785) Longitudinal study on oral shedding of human betaherpesviruses 6 and 7 in renal transplant recipients reveals active replication. J Oral Microbiol 12

Venkatesan A & Murphy OC (2018) Viral Encephalitis. Neurol Clin 36: 705–724

Venkatesan A, Tunkel AR, Bloch KC, Lauring AS, Sejvar J, Bitnun A, Stahl JP, Mailles A, Drebot M, Rupprecht CE, et al (2013) Case Definitions, Diagnostic Algorithms, and Priorities in Encephalitis: Consensus Statement of the International Encephalitis Consortium. Clinical Infectious Diseases 57: 1114–1128

De Vries HJC, Van Marle J, Teunissen MBM, Picavet D, Zorgdrager F, Bos JD, Weel J & Cornelissen M (2006) Lichen planus is associated with human herpesvirus type 7 replication and infiltration of plasmacytoid dendritic cells. Br J Dermatol 154: 361–364

Wada K, Mizoguchi S, Ito Y, Kawada JI, Yamauchi Y, Morishima T, Nishiyama Y & Kimura H (2009) Multiplex real-time PCR for the simultaneous detection of herpes simplex virus, human herpesvirus 6, and human herpesvirus 7. Microbiol Immunol 53: 22–29

Wang B, Saito Y, Nishimura M, Ren Z, Tjan LH, Refaat A, Iida-Norita R, Tsukamoto R, Komatsu M, Itoh T, et al (2020) An Animal Model That Mimics Human Herpesvirus 6B Pathogenesis. J Virol 94

Wang FZ & Pellett PE (2007) HHV-6A, 6B, and 7: immunobiology and host response. Human Herpesviruses: Biology, Therapy, and Immunoprophylaxis: 850–874

Ward KN, Andrews NJ, Verity CM, Miller E & Ross EM (2005) Human herpesviruses-6 and -7 each cause significant neurological morbidity in Britain and Ireland. Arch Dis Child 90: 619–623

Ward KN, Kalima P, MacLeod KM & Riordan T (2002a) Neuroinvasion during delayed primary HHV-7 infection in an immunocompetent adult with encephalitis and flaccid paralysis. J Med Virol 67: 538–541

Ward KN, Leong HN, Nacheva EP, Howard J, Atkinson CE, Davies NWS, Griffiths PD & Clark DA (2006) Human Herpesvirus 6 Chromosomal Integration in Immunocompetent Patients Results in High Levels of Viral DNA in Blood, Sera, and Hair Follicles. J Clin Microbiol 44: 1571–1574

Ward KN, Turner DJ, Couto Parada X & Thiruchelvam AD (2001a) Use of immunoglobulin G antibody avidity for differentiation of primary human herpesvirus 6 and 7 infections. J Clin Microbiol 39: 959–963

Ward KN, Turner DJ, Parada XC & Thiruchelvam AD (2001b) Use of Immunoglobulin G Antibody Avidity for Differentiation of Primary Human Herpesvirus 6 and 7 Infections. J Clin Microbiol 39: 959–963

Ward KN, White RP, Mackinnon S & Hanna M (2002b) Human herpesvirus-7 infection of the CNS with acute myelitis in an adult bone marrow recipient. Bone Marrow Transplantation 2002 30:12 30: 983–985

Watanabe T, Kawamura T, Jacob SE, Aquilino EA, Orenstein JM, Black JB & Blauvelt A (2002) Pityriasis rosea is associated with systemic active infection with both human herpesvirus-7 and human herpesvirus-6. J Invest Dermatol 119: 793–797

Whitley RJ (2010) Viral Encephalitis. N Engl J Med 323: 242–250

Whitley RJ & Gnann JW (2002) Viral encephalitis: familiar infections and emerging pathogens. The Lancet 359: 507–513

Wijdicks EFM & Klein CJ (2017) Guillain-Barré Syndrome. Mayo Clin Proc 92: 467–479

Wolz MM, Sciallis GF & Pittelkow MR (2012) Human Herpesviruses 6, 7, and 8 From a Dermatologic Perspective. Mayo Clin Proc 87: 1004

Yagami A, Yoshikawa T, Asano Y, Koie S, Shiohara T & Matsunaga K (2006) Drug-induced hypersensitivity syndrome due to mexiletine hydrochloride associated with reactivation of human herpesvirus 7. Dermatology 213: 341–344

Yamanishi K, Shiraki K, Kondo T, Okuno T, Takahashi M, Asano Y & Kurata T (1988) Identification of human herpesvirus-6 as a causal agent for exanthem subitum. Lancet 1: 1065–1067

Yang J, Wu P, Liu X, Xia H & Lai Z (2022) Autoimmune Encephalitis With Multiple Auto-Antibodies With Concomitant Human Herpesvirus-7 and Ovarian Teratoma: A Case Report. Front Med (Lausanne) 8: 3118

Yao K, Crawford JR, Komaroff AL, Ablashi D V. & Jacobson S (2010) Review Part 2: Human Herpesvirus-6 in Central Nervous System Diseases. J Med Virol 82: 1669

Yao K, Honarmand S, Espinosa A, Akhyani N, Glaser C & Jacobson S (2009) Detection Of Human Herpesvirus-6 In Cerebrospinal Fluid Of Patients With Encephalitis. Ann Neurol 65: 257

Yasukawa M, Inoue Y, Ohminami H, Sada E, Miyake K, Tohyama T, Shimada T & Fujita S (1997) Human herpesvirus 7 infection of lymphoid and myeloid cell lines transduced with an adenovirus vector containing the CD4 gene. J Virol 71: 1708–1712

Yildirim M, Aridogan BC, Baysal V & Inaloz HS (2004) The role of human herpes virus 6 and 7 in the pathogenesis of pityriasis rosea. Int J Clin Pract 58: 119–121

Yoshikawa T, Ihira M, Akimoto S, Usui C, Miyake F, Suga S, Enomoto Y, Suzuki R, Nishiyama Y & Asano Y (2004) Detection of Human Herpesvirus 7 DNA by Loop-Mediated Isothermal Amplification. J Clin Microbiol 42: 1348

Yoshikawa T, Suga S, Asano Y, Yazaki T, Kodama H & Ozaki T (1989) Distribution of antibodies to a causative agent of exanthem subitum (human herpesvirus-6) in healthy individuals. Pediatrics 84: 675–677

Yoshikawa T, Yoshida J, Hamaguchi M, Kubota T, Akimoto S, Ihira M, Nishiyama Y & Asano Y (2003) Human herpesvirus 7-associated meningitis and optic neuritis in a patient after allogeneic stem cell transplantation. J Med Virol 70: 440–443

Zhang Y, Bolle L de, Aquaro S, Lommel A van, Clercq E De & Schols D (2001) Productive Infection of Primary Macrophages with Human Herpesvirus 7. J Virol 75: 10511

Zhang Y, Schols D & De Clercq E (1999) Selective activity of various antiviral compounds against HHV-7 infection. Antiviral Res 43: 23–35

Zheng Y, Zhao Y, Wang Y & Rao J (2021) A multiplex real-time PCR quantitation of human herpesvirus-6, 7, 8 viruses: application in blood transfusions. Virol J 18: 38

Attachments

Protocols can be found at:

https://ugentbe-my.sharepoint.com/personal/rianne_verbeek_ugent_be/_layouts/15/onedrive.aspx?id=%2Fpersonal%2Frianne%5Fverbeek%5Fugent%5Fbe%2FDocuments%2FProtocols%20%2D%20kopie&ga=1

Plasmids can be found at:

https://ugentbe-my.sharepoint.com/:f:/g/personal/rianne_verbeek_ugent_be/Es4HA9OoEKJHpXp3jgiredEBAxpaNWu8o9AVM7e61iUKww?e=rKqomZ

Confocal microscopy photos can be found at:

https://ugentbe-my.sharepoint.com/:f:/g/personal/rianne_verbeek_ugent_be/Evf6PAaEBX1AgXgHYBJ0McsB4A8CjeFSfNtcjE0bqMDQ-A?e=vS60CF